The 4th Aquaphotomics International Conference

March 20 - 22, 2021

Kobe University Centennial Hall (Rokko Hall), Japan

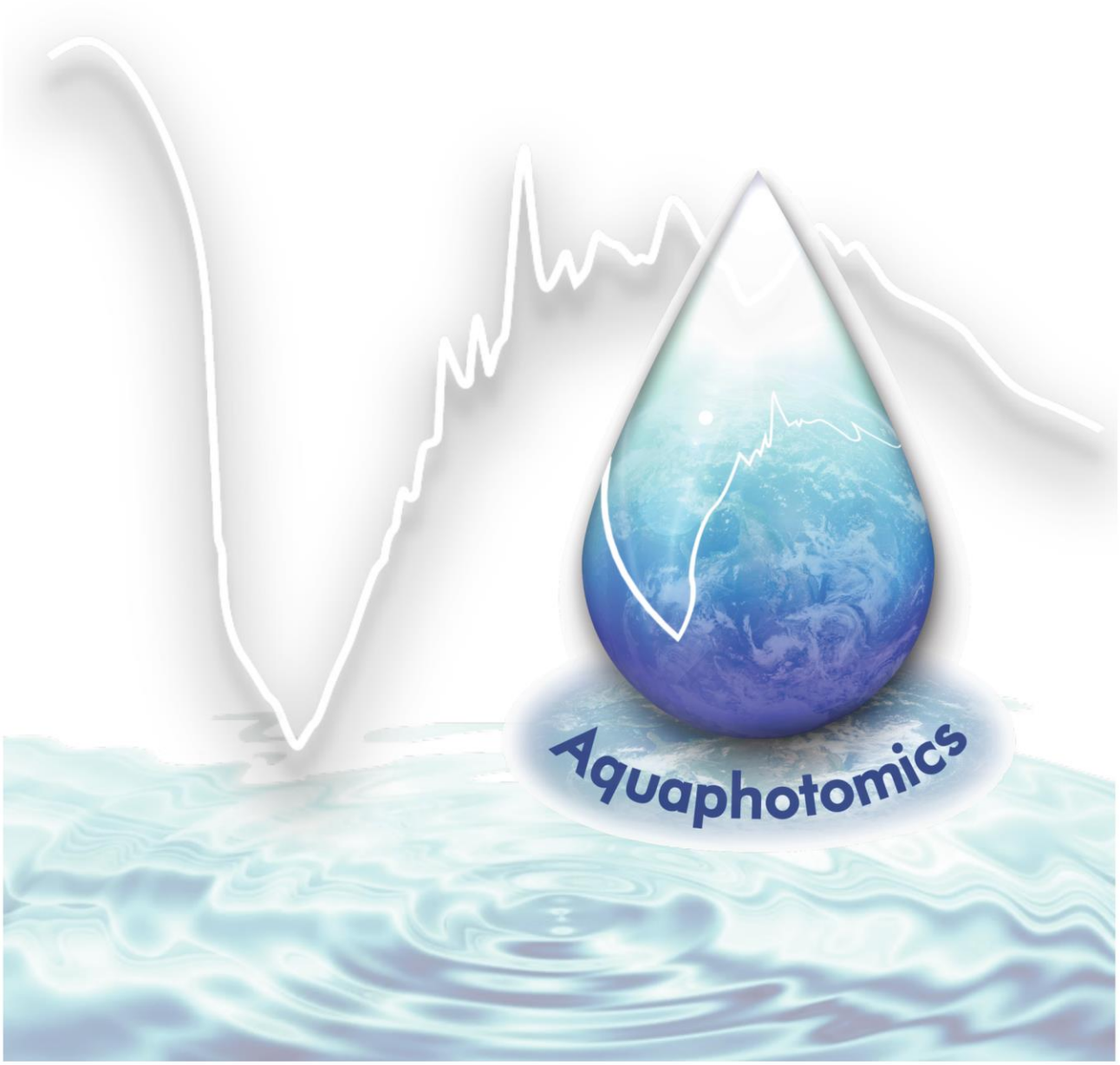

Aquaphotomics.com

The 4th Aquaphotomics International Conference

March 20 – 22, 2021
Hybrid Event - Kobe University, Centennial Hall (Rokko Hall)

Organized by
Aquaphotomics International Society
Biomeasurement Technology Laboratory, Graduate School of Agricultural Science, Kobe University

Conference Chairperson: Professor Dr Roumiana Tsenkova

Biomeasurement Technology Laboratory, Graduate School of Agricultural Science, Kobe University

1-1 Rokkodaicho, Nada, Kobe, Hyogo, Japan

Tel. & Fax. 078-803-5911

Email: conference@aquaphotomics.com

Website: www.aquaphotomics.com/conference

PROCEEDING OF

The 4th Aquaphotomics International Conference

EDITED BY

Roumiana Tsenkova

Masoto Yasui

Zoltan Kovacs

Jelena Muncan

Organizing Committee Members

Honorable Chairperson

Mutsuo IWAMOTO (Kagoshima-Osumi Food Technology Center, Japan)

Chairperson

Roumiana TSENKOVA (Kobe University)

Vice Chairperson

Masato YASUI (Keio University)

Vice Chairperson

Christian HUCK (University of Innsbruck)

International Advisor

Yukihiro OZAKI (Kwansei Gakuin University)

Local Organizing Committee Members

Lawrence WONG

Ayako SEKO

Tomoko MIYAGAWA

Sukritta ANANTAWITTAYANON

Masamichi IWAI

Makoto SAKAI

Preface

It has been sixteen years since the announcement of this delightful journey in 2005. At that time, Aquaphotomics was proposed as a new discipline guided by the vision to explore the biological world and the aqueous systems using light-water interaction. In the past, the water was seen as a passive element, an inert molecule, hindering the useful spectral signals. A radical new approach in spectroscopy – to use the water-light interaction opened a new door for the world of science. The role of water as an active factor, one which builds miscellaneous structures leading to various functionalities has been recognized and it is slowly becoming a new interdisciplinary scientific platform connecting sciences and technology.

The mission of Aquaphotomics, our mission, is to understand the role of water, the simple but sophisticated molecule that connects everything with its rhythm and ability for self-organization. All spectroscopy techniques are crucially important for Aquaphotomics, whether they cover visible light, Infrared (IR), Near-Infrared (NIR), ultra-violet (UV), Raman, or Terahertz frequencies. The water spectra of the systems under various perturbations make a large ocean of data. Thanks to the advancement of computer science, data analysis, and new measurement technologies, in recent years, the spectral studies of water are expanding in a wide variety of disciplines. Now is the perfect moment.

In October 2014, the 1st Aquaphotomics International Symposium was organized as a part of the Kobe University Symposium held at its European Office in Brussels, Belgium. Researchers from 11 countries came to exchange knowledge in various fields, including biology, nanotechnology, spectroscopy, and food science. Since then, Aquaphotomics-related joint research projects and endeavors resulted in many successful collaborations and co-authored publications.

In 2021, after 7 short years, 2 more international symposia, several regional chapters in Japan, Europe and China we are now reaching a new page. It is time for the 4th Aquaphotomics International Conference. This Conference and the Proceeding is the joint co-creation of all contributors to this memorable event. As a Chairperson of the Organizing committee, it is an honor and a privilege to be a witness of this incredible development, something I never could have imagined, when an initial thought of aquaphotomics occurred to me.

I would like to express my sincere appreciation to all the authors in this Proceeding, for the contributions to this Conference and the Aquaphotomics society and to all the people who made this possible.

This Conference could not have happened without the support from all of our sponsors. My most sincere appreciation and heartfelt gratitude goes to all of you for your dedication and continuous, kind support to the development of aquaphotomics, stimulation of scientific discussions and our expansion.

Expectantly, the 4th Aquaphotomics International Conference will greatly contribute to all of us, to science and technological developments and ultimately to our well-being and quality of life. We hope that, during this unprecedented pandemic time, learning about water will make connections and motivate many people to know more about life and the surrounding world, a paradigm shift that will change our attitude towards nature.

Roumiana Tsenkova, Chairperson
The 4th International Aquaphotomics Conference
20-22 March, Kobe, Japan

Program

The 4th Aquaphotomics International Conference

Kobe University, Centennial Hall (Rokko Hall)

March 20 - 22, 2021

SATURDAY March 20, 2021

On site & On line (English & Japanese real-time interpretation)

AQUAPHOTOMICS WORKSHOP

Chairperson: Roumiana Tsenkova

9:30	10:30	A closer look at preprocessing with focus on aquaphotomics	Federico Marini
10:30	12:00	Aquaphotomics tutorial - from experiment to interpretetation	Jelena Muncan
12:00	13:00	∽ Lunch break	

AQUAPHOTOMICS OPEN LECTURE

Chairperson: Masato Yasui

13:00	14:30	From non-invasive disease diagnostics to aquaphotomics	Roumiana Tsenkova
14:30	15:00	∽ Coffee break	

LEADING EDGE OF SCIENCE

Chairperson: Christian Huck

15:00	15:40	Encounter with peculiarity in physical properties of water and expectation for definite developments of aquaphotomics	Mutsuo Iwamoto
15:40	16:20	Molecular spectroscopy studies of water from Far-ultraviolet to Far-infrared/Terahertz and Raman spectroscopy	Yukihiro Ozaki
16:20	16:50	Water biology and medicine - roles of aquaporins in biological system	Masato Yasui
16:50	17:20	∽ Coffee break	

FURTHER DEVELOPMENTS

Chairperson: Zoltan Kovacs

17:20	17:50	Modern tools of NIR spectroscopy in water-related analysis. Miniaturized spectrometers, quantum chemistry and neural networks	Christian Huck※1
17:50	18:20	Aquaphotomics Laboratory in Yunosato	Shogo Shigeoka
18:20	18:50	Aquaphotomics science - looking at nature through water spectral patterns	Jelena Muncan
19:00		∽ Recess	

※1 The invitation is supported by Naito Foundation

SUNDAY March 21, 2021

FROM WATER STRUCTURE AND SPECTRAL PATTERNS TO DIAGNOSTICS

Chairperson: Jelena Muncan

9:00	9:30	Analyzing the water in chemical changes by Temperature-Dependent Near-Infrared Spectroscopy	Xuengang Shao
9:30	9:50	Aquaphotomics profiling of blood serum vs. plasma offers complementary modes of discriminating *Manheimia heamolytica* infection in dairy calves	Carry Vance
9:50	10:10	Aquaphotomics profile of near Infrared spectral signatures from four Anastomosis groups of the fungi *Rhizoctonia solani*	Mariana Santos Rivera
10:10	10:30	ꕥ Coffee break	

QUANTUM BRAIN DYNAMICS - ROLE OF WATER

Chairperson: Hiroshi Murakami

10:30	11:00	Modelling the measured microtubule conductivity and capacitance as a function of ionic concentrations	Jack Tuzsynski
11:00	11:20	Non-equilibrium quantum brain dynamics in 3+1 dimension with water dipoles and photons	Akihiro Nishiyama

WATER AS A PART OF BIOLOGICAL PROCESSES

Chairperson: Sae Tanaka

11:20	11:40	Studies on cryopreservation mechanism using Trehalose-transporter expressing cells	Tsutomu Uchida
11:40	12:00	Assessment of biological functions and metabolic activity during embryogenesis by water analysis using near-infrared spectroscopy	Mika Ishigaki
12:00	13:00	ꕥ Lunch break	

HYDRATION & INTERFACIAL WATER

Chairperson: Shigeaki Morita

13:00	13:30	Role of interfacial water in determining the interaction of proteins and cells with hydrated materials	Masaru Tanaka
13:30	13:50	Investigation on the reaction mechanism for dehydration of $Mg(OH)_2$ and hydration of MgO by NIR spectroscopy	Masato Takeuchi
13:50	14:10	Water at biointerfaces: what makes surfaces bioinert?	Tomohiro Hayashi
14:10	14:30	Investigation of the electronic states of water in hydrate-melt	Yusuke Morisawa
14:30	15:00	ꕥ Coffee break	

AQUAPHOTOMICS FOR FOOD QUALITY CONTROL

Chairperson: Mika Ishigaki

15:00	15:30	Food quality and process investigated through water absorption variations in NIR range	Tiziana M.P. Cattaneo
15:30	15:50	Dairy products analysis – near-infrared spectroscopy and aquaphotomics approach	Stefka Atanassova
15:50	16:10	Recent applications of aquaphotomics in the field of food science	Zoltan Kovacs
16:10	16:30	Can aquaphotomics improve quality prediction of intact fruit?	Harpreet Kaur
16:30	16:45	ꕥ Coffee break	

WATER STRUCTURE - NEW INSIGHTS & IMPLICATIONS

Chairperson: Krzysztof Bec

16:45	17:15	Extending the spectrum: NIR spectroscopy of crystalline H_2O-ices	Christina Tonauer
17:15	17:35	Water structure and water mirror effect in NIR region. A perspective from the quantum chemical simulations.	Justyna Grabska
17:35	17:55	Detection of dissolved salts using the water spectrum	Herman Offerhaus
17:55	18:15	Near Infrared and aquaphotomic analysis of water absorption in lactate containing media	Nystha Baishya
18:15	19:00	**AQUAPHOTOMICS INTERNATIONAL ASSEMBLY**	
19:00	19:45	**POSTER SESSION I**	
19:45		ꕥ Recess	

MONDAY March 22, 2021

WATER & OTHER BIOMOLECULES

Chairperson: Xuegang Shao

9:00	9:30	The role of water activity in the thermodynamic response of lipid interphases	E. Anibal Disalvo
9:30	9:50	Near infrared spectroscopy and multivariate analysis for the study of water in lipidic membranes	Jorge J. Wenz
9:50	10:10	Understanding hyaluronic acid induced variation of water structure by near-infrared spectroscopy	Hengang Zhang
10:10	10:30	Details of glucose solution near-infrared band assignment revealed using deuterium oxide and glucose isotopes	Sae Tanaka
10:30	10:40	ꕥ Coffee break	

WATER STRUCTURE & HYDRATION

Chairperson: Masato Takeuchi

10:40	11:00	Recent and future X-ray measurements of pure water	Craig Schwartz
11:00	11:20	Concentration-dependent near-infrared spectra of water-aprotic organic solvents binary systems	Shigeaki Morita
11:20	11:40	Highly precise characterization of the hydration state upon thermal denaturation of globular protein	Keichiro Shiraga
11:40	12:00	Study on the dynamic state of free, hydrogen-bonded water with wood by near-infrared hyperspectral imaging	Te Ma
12:00	13:00	ꕥ Lunch break	

POSTER SPECIALS

Chairperson: Jelena Muncan

13:00	13:15	NIR Spectroscopy and aquaphotomics in Carambola B10 Averrhoa	Siti Anis Dalila Muhammad Zahir
13:15	13:25	Water Changes Spectral Patterns When Perturbed by Sound Frequencies	Ryo Takagi
13:25	13:35	Understanding of Yogurt Bio-Functional Water	Alexander Stoilov
13:30	13:45	**SPONSORS**	
13:45	14:30	**POSTER SESSION II**	
14:30	15:00	**Post-worskhop discussion / Questions&Answers**	Jelena Muncan

FORCES SHAPING THE WATER - BEYOND SENSING TO BIOMODULATION

Chairperson: Justyna Grabska

15:00	15:30	Microwaves and nanosecond electric pulses for analysis and influencing of microtubule systems	Michal Cifra
15:30	16:00	Heretics or pioneers: Viktor Schauberger and Wilhelm Reich - a fresh look	Pierre Madl
16:00	16:20	ꕥ Coffee break	

SPECTRAL PATTERN OF BIOMATERIAL - WATER INTERACTION

Chairperson: Masaru Tanaka

16:20	16:50	Spectral imaging and spectroscopic methods for characterizing and monitoring biomaterial/water interactions	Aoife Gowen
16:50	17:10	Aquaphotomics for revealing the interaction between water molecular and surface: Potential applications to predict cell response and biofilm formation	Junli Xu
17:10	17:20	ꕥ Coffee break	

SPECTRAL PREPROCESSING FOR AQUAPHOTOMICS

Chairperson: Federico Marini

17:20	17:50	New trends in the pre-processing of near-infrared spectra	Jean Michelle Roger
17:50	18:10	Non-linear regression and artificial neural networks in NIR spectroscopy: insights into fundamental phenomena and impact on practical applications in water-related scenarios	Krzysztof Bec
18:10	18:30	The effects of water on scattering: taking into account path-length modifications	Alexander Mallet
18:30	19:00	**POSTER AWARD CEREMONY & CLOSING SPEECH**	Roumiana Tsenkova
19:00		ꕥ Goodbye	

Until we meet again!

AQUAPHOTOMICS WORKSHOP

A closer look at preprocessing with focus on aquaphotomics

Federico Marini [1,*]

[1] Department of Chemistry, University of Rome La Sapienza, P.le Aldo Moro 5, I-00185 Rome, Italy;
***** Presenting author and Correspondence: Federico.marini@uniroma1.it

The workshop will illustrate the main chemometric strategies for data preprocessing with particular focus on predictive model building in the context of aquaphotomics. First of all, the rationale for data preprocessing will be presented and the main family of techniques will be discussed. In detail, methods for smoothing, scatter correction, spectral differentiation, normalization and baselining/detrending will be presented. Moreover, some recently proposed approaches, such as Variable Sorting for Normalization, which allow a preliminary weighting of the variables will also be introduced. Lastly, strategies for boosting model performances based on the fusion of different preprocessing approaches will also be presented.

Keywords: Pre-processing, derivation, scatter correction, data fusion

Introduction

Spectroscopic data (or, more in general, experimental data) may be affected by several sources of variability, not all of interest for the specific task the data are collected for. On the other hand, when chemometric tools are applied to the data, very often model building is based on extracting components accounting for a relevant share of the variance in the predictor space, so that all the sources of data variability (wanted or unwanted) will be included in the model: accordingly, if spurious/unwanted variance is still present in the data, it can have a detrimental effect on the resulting model. To, at least partially, reduce or eliminate the effect of such unwanted variability, chemometric model building usually includes one or more pre-processing steps [1]. However, the choice of the best pretreatment or combination of pretreatments to be applied to the data is not always obvious and, in general, a trial and error procedure is followed. Aim of the present workshop will be to illustrate the main chemometric strategies for data preprocessing, by presenting their theoretical background and discussing the impact of varying their metaparameters, if any. All the techniques will be illustrated by means of worked examples in Matlab and functions will be made available to the participants upon request.

Content of the workshop

As anticipated, data may be affected by many different sources of spurious variation and the aim of data pre-processing is to remove as much as possible the impact of such sources on the spectroscopic signal. Since the attention will be mainly focused on NIR data, the techniques which will be illustrated in greater detail are the ones which are most frequently used when dealing with such profiles. A relevant role in this context is played by scatter correction techniques, such as the standard normal variate transform (SNV) [2] and multiplicative scatter correction (MSC) [3], together with its extended version (EMSC) [4], which has proved to be particularly effective in aquaphotomics studies. Together with this "well-established" approaches, a recently proposed algorithm, named Variable sorting for normalization (VSN) [5], which allows to weight the predictors in a hypothesis-free way prior to the calculation of the correction parameters will also be discussed.

Lastly, some recent trends in the pre-processing of spectroscopic data based on the use of data fusion approaches will also be presented. Indeed, one of the main problems when dealing with data pre-processing is to select what the best individual technique or combination of techniques could be and, in the latter case, to define the order according to which the different techniques should be applied. Recently, the possibility of exploiting the advantages of multi-block data analysis to overcome the problems related to the limitations illustrated above was presented in the literature. In particular, it was noted how, by applying different pre-processings to the same data, the resulting matrices constitute a multi-block set, which can be processed by specifically designed data fusion approaches. In this framework, the possibility of using sequential and orthogonal approaches for multi-

block modeling may represent an advantage, as they allow to evaluate the relevance of the individual pre-processings, the possible redundancies and the incremental contribution to the model. Accordingly, the combination of sequential and orthogonalized partial least squares modeling (SO-PLS) with the use of multiple pre-processing techniques to build a multi-block set is exploited by the recently proposed strategy called SPORT (Sequential Preprocessing through ORThogonalization) [6]. The theory and the practical use of this technique will also be illustrated during the workshop.

References

1. Roger J-M, Boulet J-C, Zeaiter M, Rutledge DN (2020) Preprocessing methods. In: Brown, SD, Tauler R, Walczak B (eds) Comprehensive chemometrics 2nd ed. Elsevier, Oxford, UK, vol.3 pp. 1-73.
2. Barnes RJ, Dhanoa MS, Lister SJ (1989) Standard Normal Variate Transformation and De-Trending of Near-Infrared Diffuse Reflectance Spectra. Appl Spectrosc 43:772-777.
3. Geladi P, McDougall D, Martens H (1985) Linearization and scatter-correction for near-infrared reflectance spectra of meat. Appl Spectrosc 39:491-500.
4. Martens H, Stark E (1991) Extended multiplicative signal correction and spectral interference subtraction: New preprocessing methods for near infrared spectroscopy. J Pharm Biomed Anal 9:625–635.
5. Rabatel G, Marini F, Walczak B, Roger J-M (2020) Variable sorting for normalization. J Chemometr 34:e3164.
6. Roger J-M, Biancolillo A, Marini F (2020) Sequential preprocessing through ORThogonalization (SPORT) and its application to near infrared spectroscopy. Chemometr Intell Lab Syst 199:103975.

Aquaphotomics tutorial – from experiment to interpretation

Jelena Muncan[1*]

[1] Biomeasurement Technology Laboratory, Graduate School of Agricultural Science, Kobe University, Rokkodai-cho 1-1, Nada-ku, Kobe, 657-8501, Hyogo, Japan
***** Presenting author and Correspondence: jmuncan@people.kobe-u.ac.jp; jln.muncan@gmail.com

Keywords: aquaphotomics, spectroscopy, experimental design, preprocessing, analysis

"If you want to find the secrets of the universe, think in terms of energy, frequency and vibration."
Nikola Tesla

Introduction

There are many articles, webpages, and book chapters written about what aquaphotomics is, what exciting new discovery it made, for what purposes it can be used and how it can be applied. It sounds exciting and as if it can really bring better understanding! Until…you acquire spectra, you look at them. And you see nothing!
You go over material and methods of the scientific papers, if you are lucky enough you understand the half of the new preprocessing and data analysis methods, you repeat the experiment, try this and that analysis. You create nice aquagrams. And yet the spectra stubbornly refuse to cooperate. You feel stuck trying to understand what BIG words like WAMACS, WASP or WABS mean. And I do not even want to mention the words which are so commonly used, like moisture content, water content, bulk water, bound water which despite their simplicity remain elusive.

I know that in the beginning of my aquaphotomics experience the water did not look like mirror to me, and the spectra looked like a bunch of similar looking lines. Many of us have been there. I have spent almost 2 years at "that place", where aquaphotomics seemed like a closed world I did not have access to. This workshop will show you how to find your way through.

Aquaphotomics – a survivial guide

At the beginning of my aquaphotomics journey, I spent one month in the Bio measurement Technology Lab at Kobe University, Japan , doing the standard "beginner`s experiment" – measurement of near infrared spectra of several tap, spring and commercial mineral waters. My objective was to use the spectra to identify each water. After 5 days of morning and afternoon measurements of 10 different waters, I had enough data to analyze. I learned few things, how to subtract the spectra, create aquagrams and make a lot of nice-looking graphs. However, I was far from reaching my objective and I understood nothing.

Looking back to this experience, even though at that time I was not aware of it, I left the Lab of prof. Tsenkova equipped with only 3 things:

1) Good data! I knew how the water spectra should look like. And this is the most important step. It depends on the instrument, measurement technique and acquisition software. Not all instruments are designed with the precision needed for aquaphotomics analysis, nor they provide the spectra in the form which can usually be seen in the papers. But if you know how the spectra should look like, it is enough. In the visible near-infrared range the spectra must be smooth across the entire 400 – 2500 nm region, with clearly recognizable 4 peaks (Fig.1). Whichever part you zoom in, like presented in the Fig. 1, even when you subtract the average spectrum or pure water spectrum, the spectra still must look smooth enough. This is important step to learn to recognize what is noise and what is spectral response, which in the case of water is very subtle. There will be occasions when good signal is not possible to achieve in the whole region, but in that case look for any usable parts.
2) The second thing I had was a corner-stone paper "Aquaphotomics – Dynamic spectroscopy of aqueous systems describes peculiarities of water" [1]. This paper is aquaphotomics in a nutshell, a perfect

introduction to the basics of water structure, different water species, conformations and their functionality in different systems. It also contains the fundamental table with the 12 best known water absorbance bands in the area of 1st overtone of water (1300 – 1600 nm).

3) Lastly, I had one more paper "Prion protein governed by metal binding" [2], written by prof. Tsenkova back in pre-aquaphotomics era. This paper tends to be overshadowed by later publications, but it is one of the best written papers from which I have learned how to "read" the graphs and do basic analysis like Principal Components Analysis and SIMCA, and I always recommend it as a great paper for beginners.

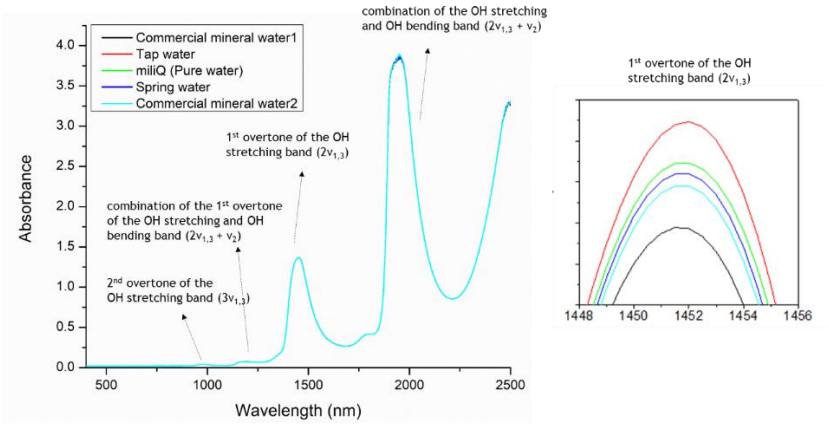

Figure 1. Visible-near infrared spectra of several types of water

These three simple things provided me in the following years with much more than I initially intended. And now I often feel overwhelmed by how many lovely interesting things can be seen from only one dataset!
With so many on-line materials now available like open access papers, free software and programming tools, YouTube video instructions, it is easy to build on the knowledge after laying down the good foundation. Starting from scratch, can sometimes be difficult, especially when it comes to performing the experiment. Materials & methods sections of the papers do not provide sufficient enough details because they are often considered unimportant or trivial. This is the reason why we specifically wrote "Essentials of aquaphotomics and its chemometric approaches" [3] in which we addressed many of such issues.

What will be learned

Aquaphotomics is still an uncharted territory, and what may seem as an obstacle in the analysis will in most cases reveal something new which builds your experience, a valuable contribution that can be shared with other aquaphotomics researchers. Each step matters. The workshop will present all the steps needed for successful performance of experiment and analysis. A variety of different scenarios, working with different samples and measurement techniques will be presented and explained in an easy to understand manner. You will be guided how to find solutions for obstacles and difficult cases which might happen when you are doing the preprocessing and/or analysis. Lastly, in the interpretation part you will learn how to read the story the water mirror is telling you using WAMACs as letters and WASPs as words.

References

1. Tsenkova R (2009) Aquaphotomics: Dynamic spectroscopy of aqueous and biological systems describes peculiarities of water. J Near Infrared Spectrosc 17:303–313.
2. Tsenkova, RN, Iordanova IK, Toyoda K, Brown DR. (2004) Prion protein fate governed by metal binding. BBRC 325.3: 1005-1012
3. Tsenkova R, Muncan J, Pollner B, Kovacs Z (2018) Essentials of aquaphotomics and its chemometric approaches. Front Chem 6:363

AQUAPHOTOMICS OPEN LECTURE

From Non-invasive Diagnostics to Aquaphotomics

Roumiana Tsenkova[1*]

[1] Biomeasurement Technology Laboratory, Kobe University, Japan
***** Presenting author and Correspondence: rtsen@kobe-u.ac.jp

Near-infrared spectral data of body fluid, milk, have been used for non-invasive disease diagnostics (mammary gland inflammation) in dairy cows [1], for the first time in science, in 1985, collaborative study was done in Bulgaria and Russia. Later on, in 2013, in-vivo diagnostics of the same disease has been achieved at Kobe University in Japan using the spectra of mammary gland tissue[2] acquired by the Japanese Fantec NIR instrument in the range of 600– 1100nm. Our Laboratory of Bio measurement Technology at Kobe University, Japan has been the leader in this field using Near-infrared spectra for diagnostics of many other diseases like prion disease in mouse, mosaic virus in soybean, HIV in humans, oxidative stress etc., for pathogen identification and other physiological studies like diagnosis of estrus in animals, real time amyloidogenic nucleation monitoring, UV-induced DNA cyclobutane pyrimidine dimers etc. In 1996, thanks to the Japanese scientific grant for 5 years, 5 teams (Japanese National Institutes of Animal Welfare and Food Science and 3 universities: Hokkaido University, Kwansei University, and Kobe University, have been working on NIR spectroscopy for Bio measurements [3]. One of the main achievements was the discovery that mammary gland inflammation could be diagnosed not only by the spectra of milk or udder tissue. Similar accuracy has been achieved when using other respective biofluids of the same animal, for example blood or urine spectra. High correlation has been observed between the components of one bio fluid and the spectra of another biofluid, too. The main difference in the spectra of healthy and diseased animals has been found in water's spectral pattern in the biofluids or tissue. These findings lead to discovering that vast information is hidden in the long time neglected and avoided water absorbance regions in the NIR spectra.

In 2005, at the International Conference on NIRS in New Zealand, for the first time, a new scientific discipline called Aquaphotomics, Figure. 1, has been proposed as life science' "– omics discipline". The word "Aquaphotomics" means all about water–light interaction. Light represents the energy at various frequencies over the entire electromagnetic spectrum. NIRS Aquaphotomics is the most suitable method for in-vivo non-destructive spectral monitoring, a source of immense information extracted after multivariate analysis of the real-time spectral data. The main concept of Aquaphtomics is the "water mirror approach", which proves that light describes as a spectral pattern reflecting how the water molecular system is structured under the influence of all internal and external factors like a mirror image of the surrounding matter and energy. Water spectral pattern is a new integrative multidimensional biomarker directly related to system functionality. Unlike other reductionist "–omics" sciences, Aquaphotomics is interdisciplinary and integrative.

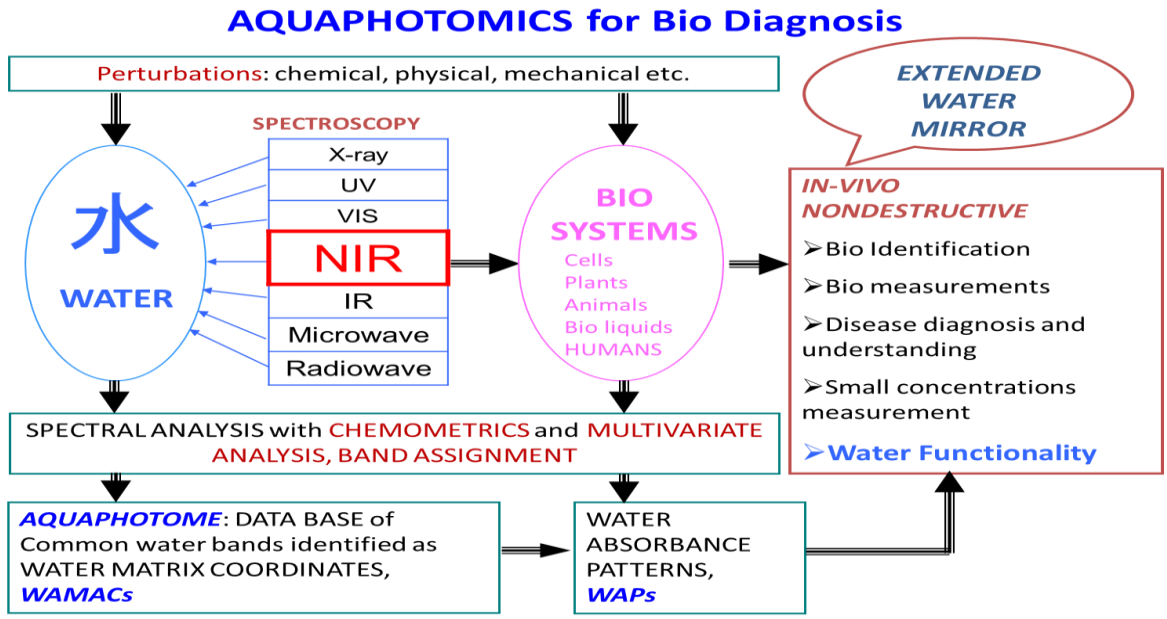

Figure 1. Aquaphotomics outline

References

1. Kirilin, N., Tsenkova, R.: Определение Субклинического Мастита У Коров Путем Ик-Спектроскопии (Near Infrared Spectroscopy for Diagnosis of Cow's Mastitis), Mechanizatsiya I Electrifikatsiya Sel'skogo Khozyastva, 2: 59-60, 1985, Russia.
2. Morita, H., Kuroki, S., Ikuta, K., Tsenkova, R.: Real time near infrared spectral monitoring of mammary gland for inflammation diagnosis in dairy cows, Journal of Near Infrared Spectroscopy, Vol. 21, 5, 427-434, 2013.
3. Tsenkova, R.: Near infrared spectroscopy: A uniform measuring technology for sustainable dairy production system, Journal of Near Infrared Spectroscopy, 6: A45-A51, 1998.
4. Tsenkova, R., Atanassova, S., Toyoda, K.: Near infrared spectroscopy for diagnosis: Influence of mammary gland inflammation on cow's milk composition measurement, Near Infrared Analysis, 2: 59-66, 2001.
5. Tsenkova, R.: Aquaphotomics: dynamic spectroscopy of aqueous and biological systems
6. describes peculiarities of water, Journal of Near Infrared Spectroscopy 17 (6): 303-314, 2009.

LEADING EDGE OF SCIENCE

Encounter with Peculiarity in Physical Properties of Water and Expectation for Aquaphotomics

Mutsuo Iwamoto
Former Director General, Kagoshima Food Technology Development Research Center
mutsuo-iwamoto@nifty.com

Introduction

As a food technologist, my concerns with water content in foods and also the state of water in food which are closely related to their physicochemical properties. A great deal of evidence on the state of water in foods have been reported in use of various instrumental methods such as nuclear magnetic resonance (NMR), differential thermal analysis (DTA), thermogravimetric analysis (TGA) and so on. Water activity (Aw) is also useful for a convenient indication of an intrinsic parameter in relation to a water vapor sorption isotherm of foods.

Meanwhile, more than five decades have passed since near infrared spectroscopy (NIRS) was brought to the public notice since NIRS for nondestructive evaluation techniques of foods and agricultural products. I had a great experience to learn the technology under Karl Norris in USDA Beltsville Agricultural Research Center (BARC) for a year during 1978 and 1979. It is not necessary to say that he had been highly respected as "The Farther of NIRS" and a pioneer who had quickened the technology evaluated as less worthy for a long period.

One day in measuring a spectrum of water itself as one of compositions in foods, I got well known three major bands due to water around 1150, 1450 and 1940 in the wavelength between 1200 nm and 2700 nm (Fig.1). Additionally, in the second derivative spectra, I happened to find an evidence that each absorption must be consisted of three components of spectra. Since that time I always think of "what the bands mean" in my carrier.

I was very happy to commence research on NIRS in the home institute, National Food Research Institute, with imported NIRS instrument of Neotec 6350 which was firstly designed as a fully computerized one modified by "Norris Machine" which was home-made instrument. Additionally, it is also happy to meet a book named "Mizu to Yoeki" (Water and Solution) by Professor Dr. Keizo Suzuki of Ritsumeikan University [1]. The book edited by reviewing more than 300 papers has a chapter mentioning about fundaments of peculiarity in physicochemical properties of water as well as instrumentation for measuring them, including NIRS as related to a part of vibrating spectroscopy technology.

Glance at water molecule

The water molecule is consisted of one oxygen atom and the two hydrogen atoms which are bonded together by two covalent bonds, forming the angle between O-H bonds is approximately 104.5^0, depending on environmental conditions around the molecule. Consequently, the water molecule has a spherical geometry as small as about 3.5Åin diameter. As compared to other substances, water molecule is very simple in terms of molecular weight, for example. However, it has much peculiarity of physicochemical properties.

In addition, it is important to know that one of special features of water molecule has two lone- pairs of electrons in the oxygen atom, being caused by so higher electronegativity character of the oxygen atom as compared with that of hydrogen atom in the covalent bond. As results, one water molecule has a potential to form two proton donor type of hydrogen bonds O-H···O and two proton acceptor type of hydrogen bonds H···O-H between neighboring water molecules, and then totally four hydrogen bonds per one water molecule are formed to create so-called cluster structure that was proposed by Nemethy and Scheraga in 1962 [2] (Fig.2).

As far as the cluster is concerned, there are many hypotheses which have been proposed on the basis of theoretical and experimental approaches to explain the structure of cluster. However, since one of difficulties in this kind of study is that the cluster maintains its configuration for only a short time less than picosecond

because the water molecule perturbs to make and break hydrogen bonds in the cluster, we need an instrumentation which allows us to observe such high speed motion of the water molecule in the cluster.

Fig.3 [3] shows the methods for observing the perturbation of water molecules as a function of time-scale of perturbation period. For example, an instantaneous perturbation of water molecule corresponding to so-called I-structure has the time-scale of perturbation period is less than 10^{-14} sec. Due to the perturbation period is too short, there is no available instrumentation to observe the perturbation directly. A newly development technique in use of super-computer simulation for dynamics of water/ice molecules is a powerful way to visualize and understand the I-structure at the present time.

On the contrary, most of instrumentations for thermal parameters for example reflect only a diffused structure of so-called D-structure which gives an information related to molecular perturbation averaged in the time length longer than around 10^{-6} sec. In addition, the structure having a time-scale of perturbation period between D-structure and I-structure is defined as V-structure. It is noted that both IR and Raman in the vibrational spectroscopy, for example, can observe the state of water with a perturbation period time length nearly close to I-structure. On the other hand, presently improved NMR makes it enable to observe much shorter perturbation period as compared to one in several decades ago.

As far as NIRS is concerned, it is very important to note that it has great advantages for understanding the state of hydrogen bonds in water as compared to IR and Raman for the reasons as follows [1];

(a) Characteristics that molecular absorption coefficient of NIRS is small as much as 10^{-3} in comparison to MID-IR is absolutely fatal for a spectroscopic technology. However, in other words, much more amount of water sample of cm-order in thickness can be used in NIRS to enable us to measure transmittance measurement of spectra more easily.

(b) NIR spectra tend to show a larger shift in the wavelength at the peak band that was influenced by surrounding condition such as temperature and solutes, for example. Particularly, NIR spectra are more sensitive to hydrogen bond than MID-IR.

(c) No influence from Fermi resonance appears in NIR spectra.

Mixture model of water molecule

The structure of water molecule has been one of research subjects that are attractive to scientist. Several structural models had been proposed in order to explain the peculiarity in physicochemical properties of water. A mixture model reported by Buijs-Choppin (1963) [4] is that water spectrum in around 1200 nm consists of mixture of three components and peak bands of the component appear at 1160 nm, 1200 nm and 1250 nm, respectively. He assigned respective band in terms of number of hydrogen bond in the water molecule. Namely band at 1160 nm is assigned to free water (S0) with no hydrogen bond, band at 1200 nm with one hydrogen bond (S1) and band at 1250nm with two hydrogen bonds (S2), respectively. Also, Fornes-Chaussidon (1978) [5] made similar observation of absorption band at 2000nm for water and ice in the temperature range of -50－50^{o}C. Using the spectrum decomposition method, he classified the spectra into three components to appeal the mixture model.

Assuming that the mixture model of water molecule is correct, it is possible to decompose the water spectrum very easily into each component in use of the second derivative spectrum. For example, it is noted that second derivative spectrum due to water at 1240nm shows that the spectrum consists of 1156nm (S0), 1202nm (S1) and 1244nm (S2), band at 1450nm does 1412nm (S0), 1466nm (S1) and 1510nm (S2) and also band at 1940nm does 1900nm and 1974nm. The band at 1950nm is complicated but 1900nm will be assigned to (S0). It is important to understand that the band at 1450nm was convenient for qualitative analysis of water structure because the band is assigned simply as combination of symmetrical valence vibration (ν_1) and unsymmetrical valence vibration (ν_3) by Bonner and Woolsey (1968) [6].

As results of investigation regarding the spectra at 1450nm region at different temperature in the range of 30－60^{0}C, the original spectra show (1) the spectra show an apparent isosbestic point at 1422nm and (2) the peak

bands shift to the shorter wavelength as temperature increases with a decrease of absorption at a higher wavelength as well as ones reported by Fornes and Chaussidon in 1978. On the other hand, the second derivative spectra at 1400 nm (S0) increase in intensity as temperature increases and bands at 1466 nm (S1) and 1510 nm (S2) show an inverse tendency. However, temperature shows no influence on a shift of bands in the second derivative spectra (Fig4). The same tendency as obtained in the second derivative spectra at 1450 nm region can be seen at 1150 nm region, but only a little difference at 1930 nm [6].

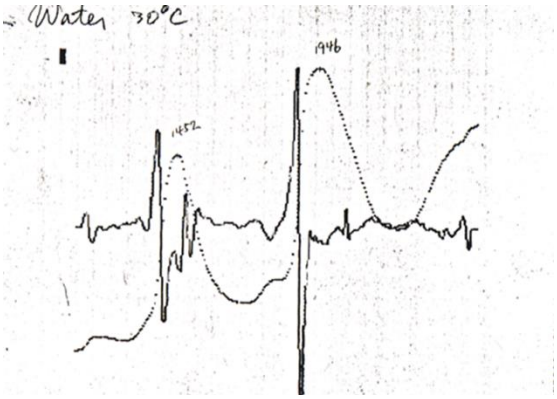

Figure 1. NIR spectrum of water measured by "Norris machine" in 1978.

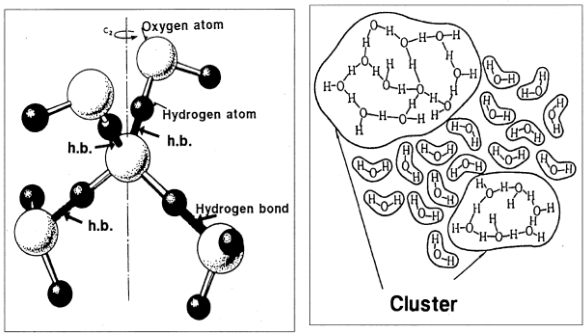

Figure 2. Formation of hydrogen bonds between neighboring water molecules (left) and Cluster structure of water (right).

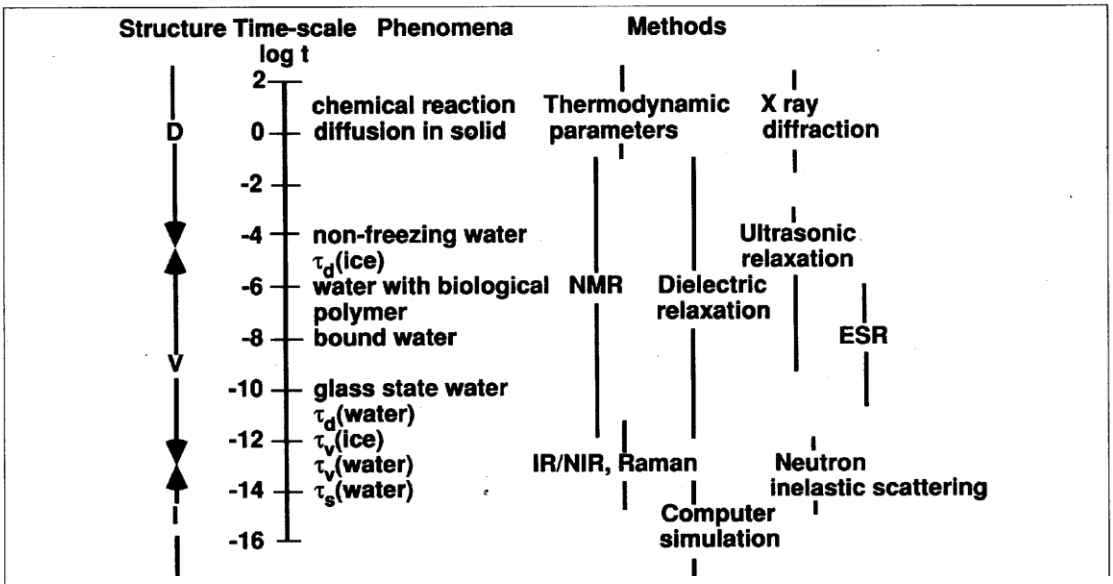

Figure 3. Instrumental methods for observing perturbation of water molecules as a function of time-scale of perturbation period.

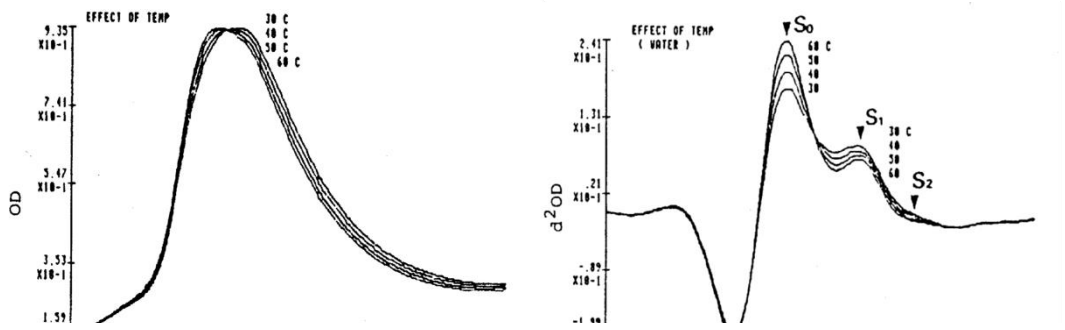

Figure 4. Changes of NIRS spectra of water as affected by temperature. Original spectra (left) and 2nd derivative spectra (right).

Effect of solutes on water molecule

Regarding effect of solutes, major effects of the interaction in the spectra can be observed as a shift of peak absorption bands and also a change of their intensity as well as an increase of half width of the band. Summary of observation of solution are as follows: (1) A shift of bands in the second derivative spectrum is strengthen in solutions depending appreciably on the sort of solutes, (2) The shift is appreciable only at the bands which can be associated with molecular fractions of (S0) and (S1) species, (3) The shift seems to be related to the hydration potential of respective solute, (4) In most cases, the absorption intensity at 1150nm and 1450 regions decreases in the solution, (5) The absorption intensity at 1930nm region changes complicatedly. In most cases, the band at 1974nm observed in pure water shifts to nearly 1990nm and increases in the intensity. This band may be associated with (S1) species, (6)MgCl2 show the most appreciable influence on the bands, and NaF did an inverse tendency [6].

Together with results of investigation conducted later in use of a home-made apparatus which is installed a temperature-controlled sample cell in the ranges of -140－80^{0}C, interesting spectra obtained obviously will be reported. In conclusion, NIRS with the second derivative procedure of spectra have a great advantage in a direct observation way of various phenomena of foods and biological objects as well as other materials in terms of interaction between compositions as solutes with the water molecule in general [7].

NIRS applied for analyzing characteristics super-heated steam

We applied NIRS to investigate physical properties of super-heated steam by mean of home-made apparatus which enable to control the temperature and pressure up to 500^{0}C and 0.5 MPa, respectively. Spectra of steam inside the vessel are measured by a NIRS system using a fiber optic connected to the spectrophotometer. The bands at 1950nm which is one of bands assigned to water molecule. It is interesting to note that super-heated steam is consisted of 1838nm, 1872nm 1916nm and 1920nm. It is clear that band below 1900nm is supposed to be assigned to the third overtone of O-H deformation or rotation.

In addition, it is very interesting to find that super-heated steam has reducing power. The phenomena is verified simply by reducing red rust (hematite) to black one (magnetite) of nails under the condition exposed by the steam. It is reasonable to suppose that most of water molecule in the steam under slightly lower in pressure at certain temperature condition than that of saturated steam are consisted of water molecule S0 mainly and this phenomena is produced by the two lone-pair electrons in oxygen atom in the steam.

Applications of peculiarity in properties of water molecule

Together with interests in fundamental researches on physicochemical properties, a great potential of applications in use of their properties for industrial technology and medical diagnostic technology. For these, “Aquaphotomics” should play an important role through interdisciplinary collaborations.

References

1. Suzuki, K., “Mizu to Yoeki” (in Japanese) , Kyoritu Zensho (235) (1980)
2. Nemthy G., et al, J. Chem. Phys. **36**, 3382 (1962)
3. Iwamoto, M. *NIR* news, **6,** 10 (1995)
4. Buijs, K., et al, J. Chem. Phys., **39**, 2035 (1963)
5. Fornes, V. et al, J. Chem. Phys., **68**, 4667 (1978)
6. Iwamoto, M., et al, Proc. of Int. NIR/NIT Conference, Budapest, Hungary (1986)
7. Abe, H., et al, J. Spectroscopical Soc. Japan, **44,** 247 (1995)

Molecular Spectroscopy Studies of Water from Far-ultraviolet to Far-infrared/Terahertz and Raman Spectroscopy

Yukihiro Ozaki[1,2,3]*

[1]School of Science and Technology, Kwansei Gakuin University, Sanda, Hyogo 669-1337, Japan.
[2]Research Center for Molecular Photoscience Research Center, Kobe University, Nada-ku, Kobe, Hyogo 657-8501, Japan
[3]Development of Far-Infrared Region, University of Fukui, Fukui 910-8507, Japan,
*Presenting author and Correspondence: yukiz89016@gmail.com

This article overviews molecular spectroscopy studies of water from far-ultraviolet (FUV) to far-infrared (FIR)/Terahertz (THz) and Raman spectroscopy. In our studies FUV, NIR, IR, FIR, THz, and Raman spectroscopy including imaging techniques have been used to investigate the water structure. We compared various spectroscopic methods and elucidate their characteristics and advantages in investigating water, water adsorption, water diffusion, and water interactions. Not only pure water but also aqueous solutions, water in polymers and water in biological tissues were studied.

Keywords: water structure, molecular spectroscopy, hydrogen bonds, vibrational spectroscopy, electronic spectroscopy

Introduction

I started water research about 40 years ago. I investigated the aging and cataractgenesis of rat lenses using Raman spectroscopy. [1] I found the water content in the lenses decreases with aging and increases with cataractgenesis by measuring Raman spectra of lenses in situ. Since that time I have been interested in nondestructive analysis of water in biological tissues. In this review article. I report FUV, IR, Raman and NIR studies of water, water interactions and water diffusion.

Electronic and vibrational spectra of water

Figure 1 shows an electronic and vibrational spectrum of water in the regions from vaccume-ultraviolet (VUV) to FIR. From the VUV to FUV region one can observe an electronic spectrum of water and from the NIR to FIR region its vibrational spectrum can be observed.

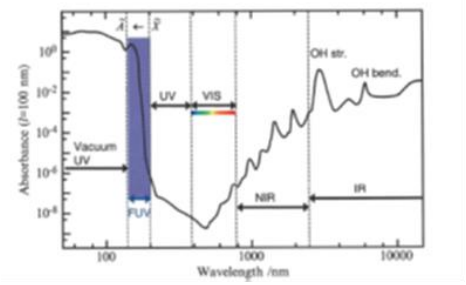

Figure 1. An electronic and vibrational spectrum of water.

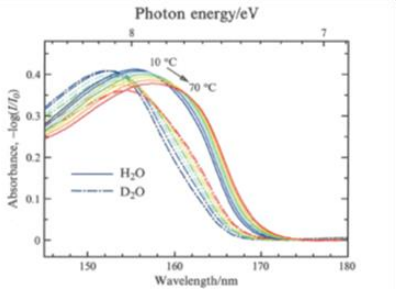

Figure 2. ATR-FUV spectra of H_2O and D_2O

ATR-FUV spectrum of water

Figure 2 shows temperature-dependent ATR-FUV spectra of H_2O and D_2O in the 145-180 nm region. [2] The 150 nm band is assigned to the n-σ* or n-3s-Rydberg transition. This band reflects the hydrogen bonds of

water. We investigated the effects of inons on this band. We also studied structure of water adsorbed on an aluminum surface by variable angle-ATR-FUV technique.

Raman and IR studies of changes in water structure and interactions among water, CH2, and COO- groups during water absorption in acrylic acid-based super absorbnet polymers (SAP)

Figures 3 and 4 show temperature-dependent variations of Raman and IR spectra and their second derivatives of water.[3] (The spectra were normalized by the intensity at 3400 cm^{-1}). Bands at around 3600, 3400, and 3200 cm^{-1} are ascribed to dangling water, weakly-hydrogen bonded water, and strongly hydrogen-bonded water, respectively. Figure 5 displays temperature-dependent spectral changes of Raman spectra of SAP with the water content of 60%. [3] Comparison of the spectra in Figure 5 with those in Figure 3 reveals that the relative intensity of the 3200 cm^{-1} band decreases in the spectra in Figure 5. The intensity decrease of this band becomes larger with the decrease in the water content in SAP. This band shows a higher wavenumber shift with temperature decreases in the cases of water content of 60 and 50 %, but in the case of water content of 40% the shift is small.

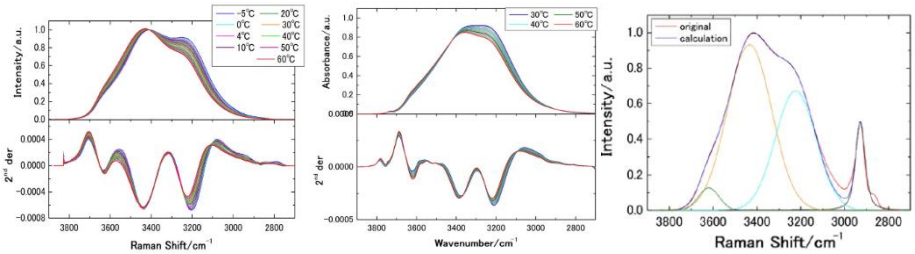

Figures 3 and 4 (left and middle). Temperature-dependent variations of Raman and IR spectra and their second derivatives of water. [3] **Figure 5** (right). Temperature-dependent spectral changes of Raman spectra of SAP with the water content of 60%. [3]

Water diffusion in a tablet monitored by NIR spectroscopy

Figure 6 displays changes in the peak-hight ratio-based image of tablet dissolution developed using the second derivative intensities at 1361 and 1354 nm due to ascorbic acid and water, respectively. [4] NIR spectroscopy is very useful for water dispersion in tablets, polymers and other materials.

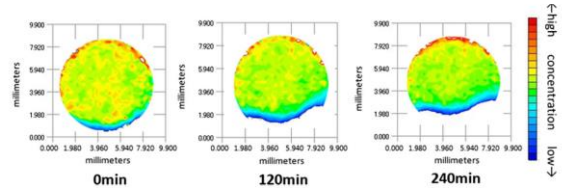

Figure 6. Time-dependent changes in the peak-hight ratio-based image of tablet dissolution developed using the second derivative intensities at 1361 and 1354 nm due to ascorbic acid and water, respectively.[4]

References

1. Y. Ozaki, Appl. Spectrosc. Rev. 24, 259 (1988).
2. A. Ikehata, Y. Ozaki, N. Higashi, J. Chem. Phys.,129, 234510 (2008).
3. T. Nasu, Y. Ozaki, H. Sato, Spectrochim. Acta, A. 250, 119305 (2021).
4. D. Ishikawa, K. Murayama, K. Awa, T. Genkawa, M. Komiyama, S. Kazarian, Y. Ozaki, Anal. Bioanal. Chem. 405, 9401 (2013),

Water Biology and Medicine; roles of aquaporins in biological system

Masato Yasui* [1,2]

[1] Affiliation 1; Department of Pharmacology, Keio University School of Medicine
[2] Affiliation 2; Center for Water Biology & Medicine, Keio University Global Research Institute
***** Presenting author and Correspondence: myasui@keio.jp

Keywords: aquaporin, glymphatic system.

Water constitutes roughly 70% of the mass of our body. Water balance is one of the most important homeostatic functions. There is a dynamic and precise regulation for water balance in our body; secretion such as tears or saliva and absorption in digestive tracts or kidney. Disturbance in water balance can be seen in many clinical disorders from dry syndromes to brain edema. The discovery of the water channel, aquaporin (AQP) greatly expanded our understanding of the regulation of the water permeability of biological membranes.

We have introduced a couple of new technologies in order to understand water dynamics and biological relevance of AQP in the living system. A nonlinear optical microscopy technique, the coherent anti-stokes Raman scattering (CARS) imaging, has been applied to directly and quantitatively imaging water transport through cell membranes. We introduce “Aquaphotomics” approach to access water dynamics of the cells as well as AQP functions. Molecular dynamics simulation is also used to evaluate our experimental findings regarding to the water permeability through AQP.

Interestingly, it’s been accumulating evidence that AQP4 may be involved in the brain lymphatic pathway and its dysfunction may lead to the neurodegenerative disorders such as Alzheimer’s disease and amyotrophic lateral sclerosis (ALS). I will also discuss about this issue with some recent experimental data.

Taken together, we try to understand life science better by focusing on water molecule behaviors at a microscopic level.

FURTHER DEVELOPMENTS

Modern tools of NIR spectroscopy in water-related analysis. Miniaturized spectrometers, quantum chemistry and neural networks.

Christian W. Huck[1*], Krzysztof B. Bec[1], and Justyna Grabska[1]

[1] University of Innsbruck, Institute of Analytical Chemistry and Radiochemistry, Innrain 80-82, 6020 Innsbruck, Austria

***** Presenting author and Correspondence: Christian.W.Huck@uibk.ac.at

Keywords: near-infrared spectroscopy, miniaturized (handheld) spectrometers, water content analysis, NIR spectra simulation, non-linear regression, Artificial Neural Network (ANN)

During the last four decades, near-infrared (NIR) spectroscopy (800–2500 nm; 12,500–4000 cm−1) has become one of the most attractive and used methods for analysis for the following reasons: it represents a non-destructive analytical tool allowing a fast and simultaneous qualitative and quantitative characterization of a wide variety of samples [1]. The last decade marked a rapid acceleration in the continuing trend of the miniaturization of NIR spectrometers (Fig. 1). These devices remarkably increase the flexibility of analysis; however, attention needs to be paid to the various factors affecting their performance in different scenarios [2]. Currently, it is a focused and very active research direction to perform systematical evaluation studies of the analytical accuracy and reliability of various miniaturized spectrometers available at the market [2].

NIR spectroscopy a particularly potent tool for analyzing natural products and their constituents [3]. Water is an important substance from the point of view of NIR spectroscopy of natural products and in various bio-related applications. As the result of relatively high index of absorption, water is a strong contributor to NIR spectra of such samples. Furthermore, moisture content is often a critical factor affecting the quality and suitability of a product. Therefore, the applicability and analytical performance of miniaturized NIR spectrometers in the analysis of water content, or an independent property of the sample, in which water is present, is a factor of critical importance.

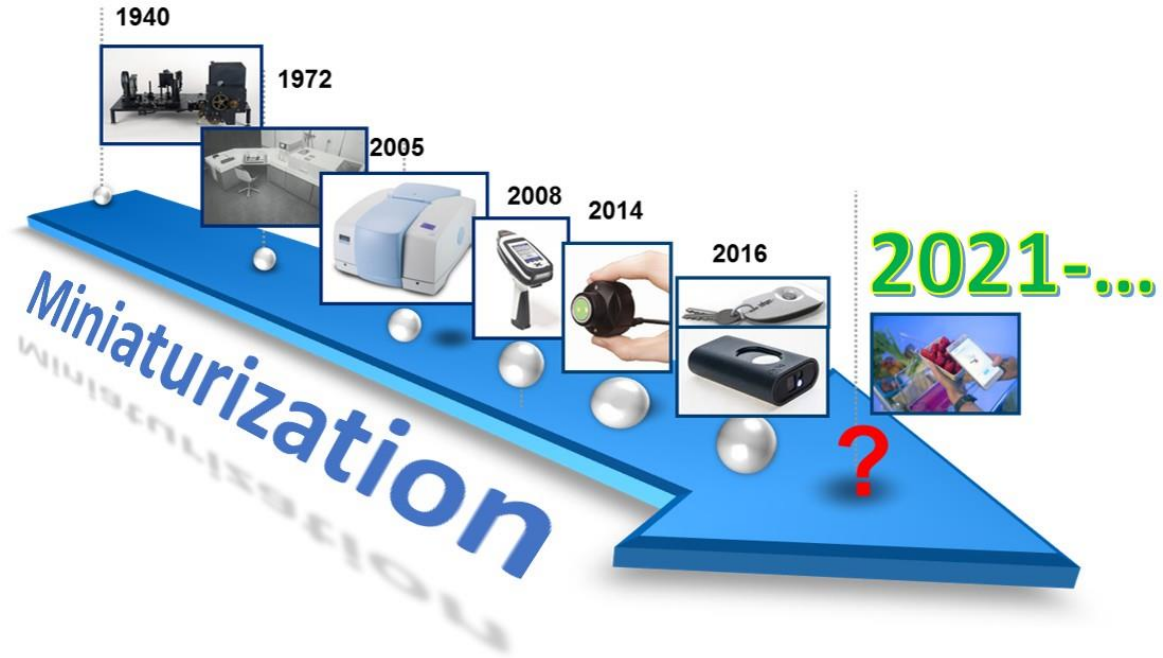

Figure 1. The accelerating trend in the miniaturization of NIR spectrometers with visible recent breakthroughs in the flexibility and deployability factors.

This presentation focuses on a variety of scenarios, in which water plays important role either as the target analyte, or by forming the matrix and interfering with the outcome of the analysis. Overviewed are the research directions at this wide-horizon of investigation, currently advanced by the Institute of Analytical Chemistry and Radiochemistry, University of Innsbruck (Austria). The importance of using combined tools, integrated into NIR analytical method, which improve its accuracy, reliability and applicability, is discussed (Fig. 2). Advanced methods of calibration (e.g. Artificial Neural Networks) directly improve the performance of miniaturized instruments in analyzing moisture, equalizing the accuracy of these instruments with benchtop spectrometers. Two-dimensional correlation spectroscopy (2D-COS) yields insights into the relative sensitivity observed between different instruments towards specific NIR bands. Quantum mechanical simulation of NIR spectra unveils the role that the interaction of the targeted analyte with the surrounding water molecules play in enhancing the information acquired from NIR spectra. The simulation also enables interpreting the instrumental difference observed between different handheld sensors in light of the chemical information on a given constituent, and to predict the performance level of a spectrometer in similar analysis. This suite of methods enables intelligent design of future NIRS analysis, which is particularly important for moist samples with complex matrix [3].

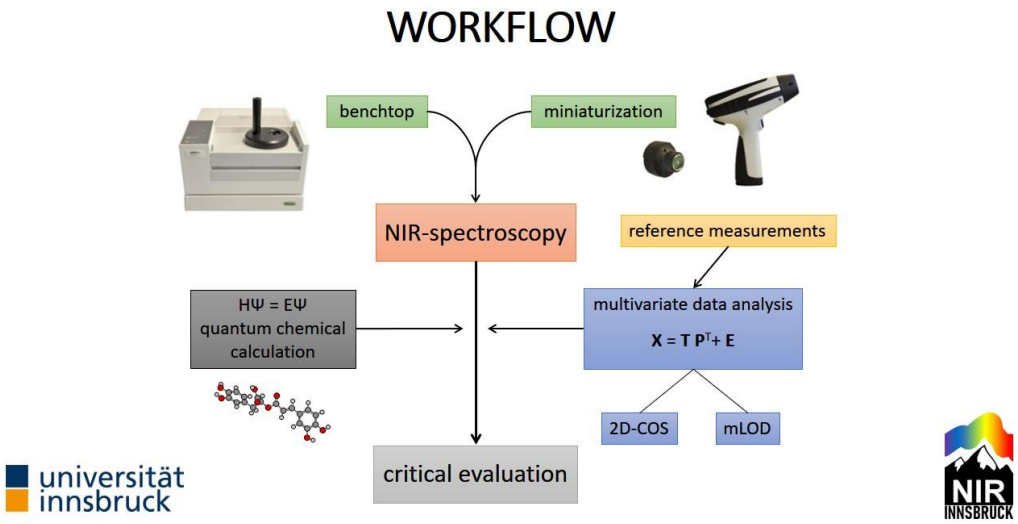

Figure 2. The scheme of multi-planar methodology used for increasing the accuracy, flexibility and applicability of modern NIR spectroscopy.

References

1. Huck, CW, Beć, KB, Grabska, J (2020) Near infrared spectroscopy in natural product research. In: Encyclopedia of analytical chemistry: applications, theory and instrumentation, Meyers, RA, (Ed) John Wiley & Sons.
2. Beć, KB, Grabska, J, Huck, CW (2021) Principles and applications of miniaturized near-infrared (NIR) spectrometers, Chemistry - A European Journal 27:1514-1532.
3. Beć, KB, Grabska, J, Huck, CW (2020) NIR spectral analysis of natural medicines supported by novel instrumentation, methods of data analysis and interpretation, JPBA 193:113686.

This work was supported by Austrian Science Fund (FWF): P32004-N28.

Aquaphotomics Laboratory in Yunosato

Shogo Shigeoka[1,2,*]

[1] Shigeoka Co. Ltd., President
[2] Yunosato Aquaphotomics Lab, 1075 Konono, Hashimoto city, Wakayama 648-0086, Japan
***** Presenting author and Correspondence: s.shigeoka@spa-yunosato.com

Keywords: near-infrared spectroscopy, aquaphotomics, applied aquaphotomics, bio-functional water, Yunosato, yogurt, water monitoring

Yunosato is an all-encompassing hot spring and hotel facility, including restaurants supplied by their own organic farm, offering dressings, jams, and yogurts made at their designated Taeko's Kitchen (Fig. 1). All services and products, such as mineral water and cosmetics are produced with their well water. It is located in Konono, Wakayama Prefecture, at the base of the historic World Heritage Site, Koyasan. Kukai, a Buddhist monk who founded the esoteric Shingon school of Buddhism in Koyasan, prophesized that the land of Konono would later supply water that would help the people.

Three types of water are found at Yunosato, named as Gold Water, Silver Water, and Bronze Water. All three are unique in their own respective ways. Since their grand opening in 1987, many customers and employees alike have voiced inexplicable improvements to their health utilizing these waters in various forms. Searching for explanations, minerals and substances within the water were investigated. However, no approach could capture the nuanced phenomena of these waters, until they were introduced to Aquaphotomics – a fast and non-invasive method of looking at water using light – the water-mirror approach.

Figure 1. Facilities of Yunosato

This presentation focuses on a variety of ways Yunsoato has been involved with aquaphotomics. Meeting Professor Roumiana Tsenkova inspired new hope and collaborative research with Kobe University promptly began. Now, 10 years later, a new aquaphotomics lab has been developed on the Yunosato property.

Earlier studies investigated the characteristics of the Yunosato waters and how they correlate with temperature, humidity, and the moon cycle. Since then, Yunosato has acquired over 50,000 spectra and still continue to use near infra-red spectroscopy (NIRS) to monitor the quality of the water offered to the guests in various forms [1]. Aquaphotomics enabled Yunosato to better understand their waters and the change in their characteristics when blended with one another or with other various liquids and organic products at different ratios. Furthermore, utilizing NIRS to analyze the water spectral patterns of probiotics [2] and their mixtures with various strains and waters enabled the development and production of Yunosato's signature soy yogurt, "Sasho Yogurt."

Lastly, this presentation shares one of its latest and on-going projects, where organic products are placed in a vacuum chamber with pressure as low as -98kPa at 35°C temperature using a vacuum drying unit. The evaporated water is then filtered and called bio-functional water, while the remaining solids are collected separately. The extracted samples and their blends with chosen liquids and solids are then analyzed and evaluated using aquaphotomics method to develop functionally designed products. Yunosato hopes to continue facilitating and encouraging the use of aquaphotomics in product development.

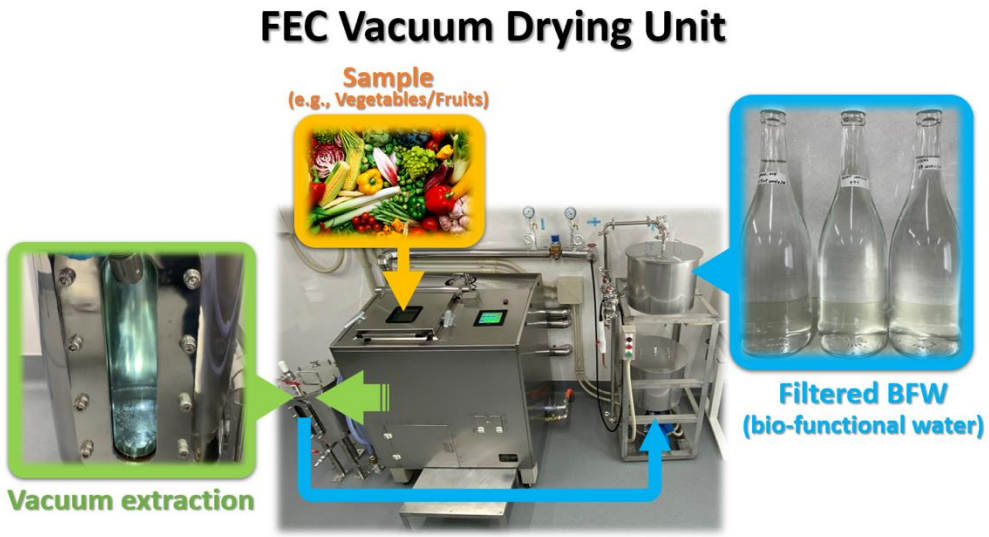

Figure 2. Overview of extracting bio-functional water using FEC vacuum drying unit

References

1. Kovacs, Zoltan & Bázár, György & Oshima, Mitsue & Shigeoka, Shogo & Tanaka, Mariko & Furukawa, Akane & Nagai, Airi & Osawa, Manami & Itakura, Yukari & Tsenkova, Roumiana. (2015). Water spectral pattern as holistic marker for water quality monitoring. Talanta. 147. 10.1016/j.talanta.2015.10.024.
2. Slavchev, Aleksandar & Kovacs, Zoltan & Koshiba, Haruki & Nagai, Airi & Bázár, György & Krastanov, Albert & Kubota, Yousuke & Tsenkova, Roumiana. (2015). Monitoring of Water Spectral Pattern Reveals Differences in Probiotics Growth When Used for Rapid Bacteria Selection. PLoS ONE. 10. 10.1371/journal.pone.0130698.

Aquaphotomics science – looking at nature through water spectral patterns

Jelena Muncan[1*]

[1] Biomeasurement Technology Laboratory, Graduate School of Agricultural Science, Kobe University, Rokkodai-cho 1-1, Nada-ku, Kobe, 657-8501, Hyogo, Japan
***** Presenting author and Correspondence: jmuncan@people.kobe-u.ac.jp ; jln.muncan@gmail.com

Keywords: aquaphotomics, water spectral patterns, WAMACS, WASPs, functionality

"It was six men of Indostan
To learning much inclined,
Who went to see the Elephant
(Though all of them were blind),
That each by observation
Might satisfy his mind"
...
"And so these men of Indostan
Disputed loud and long
Each of his own opinion
Exceeding stiff and strong
Though each was partly in the right,
And all were in the wrong"

The Blind Men and the Elephant by John Godfrey Saxe (1816-1887)

Why Aquaphotomics?

In answer to this question in 2009 paper "Aquaphotomics: dynamic spectroscopy of aqueous and biological systems describes peculiarities of water" [1] there is a phrase summing up nicely the goal of Life science – it is simply a " Complete understanding of life". The Science, which is today an enormous enterprise has been developed with the sole purpose of answering questions present in the mind of *Homo Sapiens* probably from the first moments of its awareness such as "What am I? What is life?" and even more mundane questions, like "How can I stop this pain?", "How can I make this food last?", "How can I know if this plant will kill me or heal me?". Initially, the Science started simply as a "Phillosophy" or love for knowledge, a desire to get to the "truth of the matter" when stories told in myths, legends and superstions were no longer enough. So the ancient, wise people started chopping all the big questions into smaller ones that were easier to answer and then all that unfolded into what we now know as different scientific disciplines. The Nature was divided into different realms, light into visible and invisible, living systems into plants, animals, humans, microorganisms, the organisms into organs, tissues, cells. What was once "WHOLE" was repeatedly divided into smaller and smaller components and studied in more and more details by individual scientific disciplines, each one stimulating the development of specific scientific methods, measurement techniques and analytical tools.

However, this practice of dividing seems to be in stark contrast with the works of Nature. The things we call "isolated system", "ideal gas", "pure water" or "free water molecule" do not really exist. Apparently, the Nature loves networks, creating bonds and organizing into the complex patterns, using some rules which we don't understand and so we call them "chaos" if we absolutely can't predict how the things are going to turn out, or "deterministic chaos" – when we do (amazingly, science became capable of that). This is where aquaphotomics comes into the picture with its aim to integrate, bring together, connect (Fig.1).

It allows observation of Nature and all living processes, dynamically, through the water molecular network, a highly sophisticated, sensitive network of hydrogen bonds connecting all the components of any aqueous or biological system into a functional unit, that can not be isolated from the influences of its "environement". That said, even this division "system-environment" is blury, the Nature doesn't really make disctinction and borders.

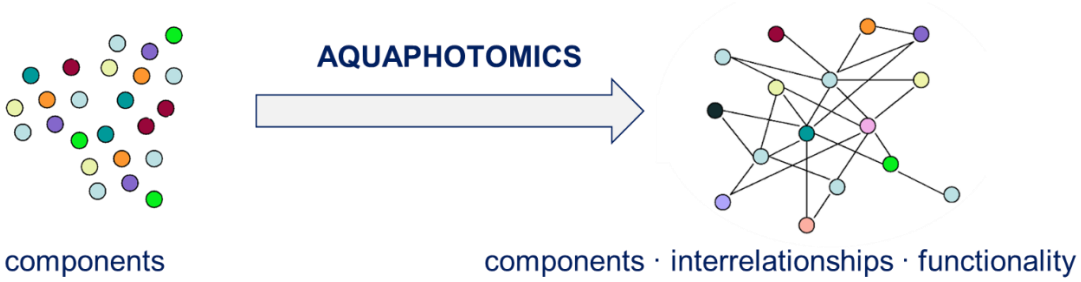

Figure 1. Disintegrative approach separates systems into components, which brings better understanding of components at the price of losing the function of the system. Integrative approach places focus on studying the system as a whole with the primary objective to understand its functionality arising as a direct result of the complex interrelationship of components.

The Language of Nature

Networking is one of the fundamental principles of Nature governing the function of Life as we know it. That's why aquaphotomics – to use all the "senses" of spectroscopy like ultraviolet, visible, near infrared, infrared, Raman, Terahertz, X ray to work together on observation and making sense of it.

The aquaphotomics research is showing clearly that "Everything is connected". We studied fatty acids in milk, and find out something new about the protonated water. Then we would study perfluorinated compounds (surfactants, similar to detergents) and the same water species would appear, telling us something about how they combine into micellar forms. The micelles would lead us to what we call "hydration water". The same hydration water which was repeatedly found in connection with misshaped proteins. Or also with deposited proteins on the surfaces of worn contact lenses. The new contact lenses would show importance of strongly hydrogen bonded water. The same water found to be important for detection of damage on surface of mushrooms. Then, from the mushroom study, in connection to damage what we now call "trapped water" can be seen and further connected to the membrane damage and ion disbalans. This would be connected to dehydration and stress in plants leaves. And sugar-water interaction. Then speaking of salts we would encounter what we call solvation water, and that would be a guide to water vapour. The sugar-water interaction to phase transition. Water vapour would make connection between mealiness of apples, mobility of protons and water activity, which then leads further to phenomena of preservation, adsorption, wettability, moisture content and surface tension…The list is endless. Different phenomena could be described and connected to a pattern of different water species, absorbing at different frequencies. These freqeuncies in aquaphotomics we call WAMACS or letters, and their combinations we call spectral pattern or WASPs - words. And we are looking at Life through water spectral patterns reading the language of Nature which expresses itself in the "terms of energy, frequency and vibation".

Reference

1. Tsenkova R (2009) Aquaphotomics: Dynamic spectroscopy of aqueous and biological systems describes peculiarities of water. J Near Infrared Spectrosc 17:303–313.

FROM WATER STRUCTURE AND SPECTRAL PATTERNS TO DIAGNOSTICS

Analyzing the Water in Chemical Changes by Temperature-Dependent Near-Infrared Spectroscopy

Xueguang Shao*, Wensheng Cai

Research Center for Analytical Sciences, College of Chemistry, Nankai University, Tianjin 300071, China

Temperature-dependent near-infrared (NIR) spectroscopy has been developed for quantitative and structural analysis. The technique has shown its potential in analyzing the water structures in chemical processes. Due to the complexity of the structure of water and the NIR spectra, chemometric methods were adopted for analyzing the spectral data. Continuous wavelet transform (CWT) was employed for removing the variant background and enhancing the resolution. 2D correlation NIR spectroscopy and Gaussian fitting with GA optimization were employed to analyze the spectral components of water. High order chemometric methods were employed for dealing with the high-dimensional spectral data. The function of water during the gelation of ovalbumin (OVA) and the aggregation of poly (N, N-dimethylaminoethyl methacrylate) (PDMAEMA) in aqueous solution were studied in our recent studies. The results show that all the water species change obviously with temperature and the structural change of the protein, but the water molecule with two hydrogen bonds (S_2) plays an important role in the gelation. The aggregation of the polymer may happen directly from the dehydrated chains to the micelle in high concentration solution, but a two-stage conformation change was observed in the phase transition in low concentration solution. S_2 water was also found to play an important in the transition. Therefore, temperature-dependent NIR spectroscopy combined with chemometric methods may be a powerful tool and water may be a probe for studying the structural changes in chemical processes.

Aquaphotomics profiling of blood serum vs. plasma offers complementary modes of discriminating *Manheimia heamolytica* infection in dairy calves

Mariana Santos-Rivera[1], Amelia Woolums[2], Merrilee Thoresen[2], Ellianna Blair[1], Victoria Jefferson[1], Florencia Meyer[1], and Carrie K. Vance[1]*

[1] Department of Biochemistry, Molecular Biology, Entomology and Plant Pathology, Mississippi State University, Mississippi State, MS 39762
[2] College of Veterinary Medicine, Pathobiology & Population Medicine, Mississippi State University, Mississippi State, MS 39762
* Presenting author
Correspondence e-mail: ckv7@msstate.edu

Keywords: bacteria, controlled challenge, blood plasma, blood serum, Aquaphotomics

Introduction

Bovine respiratory disease (BRD) associated with *Mannheimia haemolytica* is the principal cause of pneumonia in cattle[1]. Diagnosis of BRD traditionally relies on visual assessment and more rapid and accurate diagnostic tests are needed[2]. Near Infrared Spectroscopy (NIRS) in combination with chemometrics allows fast, noninvasive assessment of biofluids, whereby the biochemical profile is described by the intensity and structure of sample transmittance spectra in the NIR band (780 to 2500 nm)[3]. Currently, blood plasma and blood serum are used to detect BRD with techniques such as PCR, NMR, and GC – MS. Serum is the supernatant of blood after coagulation, while blood plasma is the supernatant including coagulation factors that remains when the cellular componants are pelleted. [4]. Both plasma and serum are aqueous solutions (≥95% water) considered to be very similar and to produce similar results in clinical and biological studies[4]. Here we characterized the NIR spectral profile of blood plasma and blood serum from dairy calves infected in a controlled challenge with *M. haemolytica* by Aquaphotomics to map the molecular organization of the aqueous phase of these biofluids as complementary modes of discriminating this bacterial infection.

Materials and Methods

In the controlled challenge an infectious agent is introduced to the calves, procedurally carried out in accordance with the MSU-Institutional Animal Care and Use Committee (IACUC-19-037). The bacterial M. haemolytica isolate D153 was administered via bronchoalveolar lavage (BAL) catheter to five Holstein steers housed at Mississippi State University (MSU). Blood samples were collected via jugular venipuncture into two commercial blood collection tubes, one of them containing the anticoagulant EDTA. Samples were collected and processed to obtain plasma and serum pre- and post-challenge during four baseline days, 11 days immediately after challenge, and then every other day until Day 23 post-infection. NIR spectra was collected using a portable spectrophotometer ASD FieldSpec®3 +Indico®Pro (Malvern Panalytical, Boulder, CO. USA). Principal Component Analysis (PCA) was performed using Unscrambler® X v.10.5 (CAMO Analytics, Oslo, Norway) on the first overtone region of the near-infrared spectrum in the vibrational combination band between 1300 - 1600 nm. Aquaphotomic profiles, including barcodes based on WAMACS and aquagrams, were created following published procedures[5–7].

Results

Aquaphotomic and Chemometric analyses displayed a different spectral pattern in the wavelength range 1300 - 1600 nm for the evaluated biofluids. The first three Principal Components (PCs) explained the variance of the databases in 66.7% for blood plasma and 72.7% for the blood serum. No outliers were found in the Hotelling's T^2 influence plots obtained in the PCA. Barcodes for each biofluid showed shifts in specific WAMACS after *M. haemolytica* infection, as seen in Figure 1a. The Aquagrams displaying the normalized averaged spectra

showed different WASPs for both biofluids in addition to the highest points of the spectra located in specific coordinates for the samples collected during the Baseline and Infected periods of the challenge (Figure 1b, 1c).

Overall, these blood biofluids are composed of proteins and peptides, carbohydrates, lipids, amino acids, electrolytes, organic wastes, and a variety of other small organic molecules dissolved in them[8]. However, plasma and serum contain some different biochemical components and metabolites, therefore offering different views of the animal condition. The main difference is that plasma retains solubilized blood clotting factors and fibrinogen, which are primarily composed of glycoproteins. The presence of these proteins alters the fluidity of the plasma as they are highly soluble and are surrounded by dynamic solvation shells in the water matrix. By contrast, significant portions of the protein composition are removed from serum in the clotting process, thus concentrations of proteins, and proteins of different molecular weight are present, such that the water matrix is less structured. These differences may suggest that the proteins in the plasma and serum between baseline and infected stages are influencing the patterns observed in the Aquaphotomics analysis, opening the possibility of using them as complementary modes of discriminating this bacterial infection and ultimately allowing to map the infection by *M. haemolytica*.

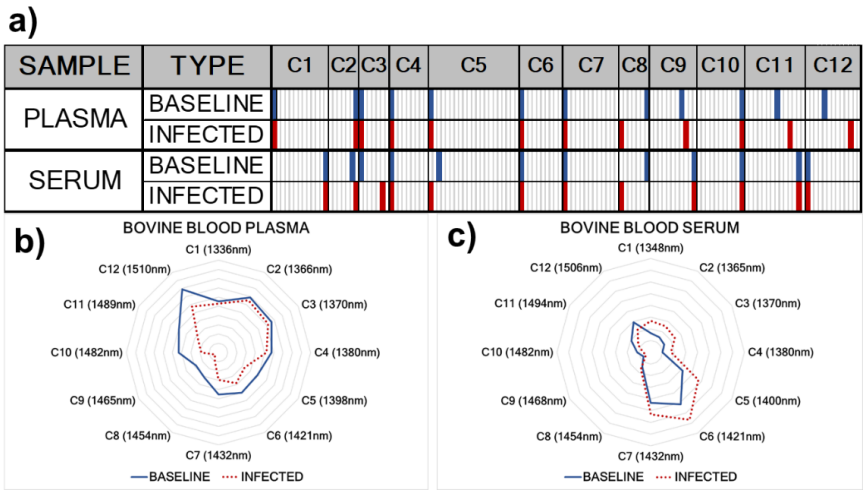

Figure 1. Aquaphotomics. (a) Barcode based on the WAMACS, for the bovine blood plasma peak shifts can be seen in the coordinates C8, C9, C11, and C12. For the serum shifts were observed in the coordinates C2, C3, C5 and C8. (b) Aquagram displaying the normalized averaged spectra for the bovine blood plasma showing different WASPs and the highest points of absorbance at 1366 and 1510 nm for the Infected and Baseline plasma, respectively. (c) Aquagram displaying the normalized averaged spectra for the blood serum showing the highest peaks for the Infected and Baseline samples at 1421 nm.

Conclusions

1. NIR spectral signatures revealed distinct biochemical patterns and WASPs in the blood plasma and blood serum with potential to be use as complementary modes of discriminating M. haemolytica infection in dairy calves.
2. NIR Spectroscopy in combination with Chemometrics and Aquaphotomics has potential as a rapid in-line test for BRD detection using biofluids.

This project was supported by the Mississippi Agricultural and Forestry Experiment Station, the National Institute of Food and Agriculture, U.S. Department of Agriculture, Hatch project under accession number W3173, and the USDA-ARS 58-6402-018 Biophotonics Initiative, Grant # G00003581.

References

1. Griffin D, Chengappa MM, Kuszak J, McVey DS (2010) Bacterial pathogens of the bovine respiratory disease complex. Vet Clin North Am - Food Anim Pract 26:381–394. https://doi.org/10.1016/j.cvfa.2010.04.004
2. Wolfger B, Timsit E, White BJ, Orsel K (2015) A Systematic Review of Bovine Respiratory Disease Diagnosis Focused on Diagnostic Confirmation, Early Detection, and Prediction of Unfavorable Outcomes in Feedlot Cattle. Vet Clin North Am - Food Anim Pract 31:351–365. https://doi.org/10.1016/j.cvfa.2015.05.005
3. Pasquini C (2003) Near infrared spectroscopy: Fundamentals, practical aspects and analytical applications. J Braz Chem Soc 14:198–219. https://doi.org/10.1590/S0103-50532003000200006
4. Suarez-Diez M, Adam J, Adamski J, et al (2017) Plasma and Serum Metabolite Association Networks: Comparability within and between Studies Using NMR and MS Profiling. J Proteome Res 16:2547–2559. https://doi.org/10.1021/acs.jproteome.7b00106
5. Tsenkova R, Munćan J, Pollner B, Kovacs Z (2018) Essentials of Aquaphotomics and Its Chemometrics Approaches. Front Chem 6:1–25. https://doi.org/10.3389/fchem.2018.00363
6. Muncan J, Tsenkova R (2019) Aquaphotomics-From Innovative Knowledge to Integrative Platform in Science and Technology. Molecules 24:. https://doi.org/10.3390/molecules24152742
7. Santos-Rivera M, Woolums A, Thoresen M, et al (2021) Profiling Mannheimia haemolytica infection in dairy calves using near infrared spectroscopy (NIRS) and multivariate analysis (MVA). Sci Rep 1–13. https://doi.org/10.1038/s41598-021-81032-x
8. Psychogios N, Hau DD, Peng J, et al (2011) The human serum metabolome. PLoS One 6:. https://doi.org/10.1371/journal.pone.0016957

Aquaphotomic profile of Near Infrared spectral signatures from four Anastomosis Groups of the fungi *Rhizoctonia solani*

Mariana Santos-Rivera[1]*, Matt Harjes[1], Richard Baird[1,2], and Carrie K. Vance[1]

[1] Department of Biochemistry, Molecular Biology, Entomology and Plant Pathology, Mississippi State University, Mississippi State, MS 39762
[2] Department of Kinesiology, Mississippi State University, Mississippi State, MS 39762
* Presenting author
Correspondence e-mail: ckv7@msstate.edu

Keywords: Liquid cultures, fungi, Anastomosis, Near-Infrared Spectroscopy, Aquaphotomics

Introduction

Rhizoctonia spp. are soil-borne pathogens causing seedling disease affecting economically important crops and plants worldwide, such as cereals, field crops, ornamentals, and fruit trees. In Rhizoctonia fungi, cellular extentions called hyphae are the main mode of vegetative growth. Diagnostic classification of a new isolate or Anastomosis Group (AG) is traditionally based on its hyphae compatibility with reference Rhizoctonia solani isolates, of which 14 AGs are currently defined. The AGs: 1, 2, 3, and 4 are associated with the most destructive Rhizoctonia diseases worldwide, whereas the others are regarded as less destructive, making group identification critical for accurate treatment selection before economic losses occur[1, 2]. Although the anastomosis classification method is accurate, it is time-consuming, and in some cases it is not possible to determine which AG an isolate belongs to. Several molecular techniques like rDNA-ITS (ribosomal DNA internal transcribed spacer) have been found to simplify and/or more accurately classify isolates from R. solani[3]. However, genetic analyses are labor-intensive, costly, and require special handling to avoid DNA contamination and degradation. Here we proposed the use of Near Infrared Spectroscopy (NIRS) and Aquaphotomics to create a growth profile for four multinucleate AGs (AG-2, AG-4, AG-7, and AG-13) inoculated in basal liquid media and evaluated over time as the basis for the development of a rapid laboratory tool to differentiate infection by R. solani AGs.

Materials and Methods

Basal media containing glucose, amino acids, minerals, and vitamins, was prepared with the aim of providing a chemically defined medium to allow rapid growth of R. solani isolates for their further discrimination. Four R. solani isolates: AG-2 and AG-4 (destructive), AG-7 and AG-13 (less destructive) from the culture collection of tester Anastomosis Groups available in the Plant Pathology Unit at Mississippi State University, were inoculated in petri dishes containing solid basal media and incubated at 21°C for 8 days. Then, AGs were sub-cultured in basal liquid media, and NIR spectra was collected using a portable spectrophotometer ASD FieldSpec®3 +Indico®Pro (Malvern Panalytical, Boulder, CO. USA) 1, 3, 7, and 15 days post-inoculation (d.p.i) to test the potential to detect and discriminate these AGs at an early stage of growth. Aquaphotomic profiles, including barcodes based on WAMACS and aquagrams, were created following published procedures[4, 5]. Additional chemometric analyses were performed to all the AGs simultaneously using Unscrambler® X v.10.5 (CAMO Analytics, Oslo, Norway) on the first overtone region of the near-infrared spectrum in the vibrational combination band between 1300 - 1600 nm and included Principal Component Analysis (PCA) and Discriminant Analysis (PCA-LDA).

Results

The mycelium, which is a mass of hyphae formed due to fungal growth based on energy metabolism in the basal media, was evident for all the AGs as soon as 1-day post inoculation. Aquaphotomic and Chemometric analyses (PCA) displayed a different spectral pattern in the wavelength range 1300 - 1600 nm for the liquid cultures containing the R. solani AGs, suggesting the biochemical changes on energy substrates, products, and key metabolites observed between each of the AG, over time, can be detected with NIRS and may be related to

different contributions from two metabolic pathways (PPP pentose phosphate pathway and TCA tricarboxylic acid cycle) involved in the formation of the mycelium. Barcodes show shifts between the four AGs in specific WAMACS after each d.p.i, as seen in Figure 1.

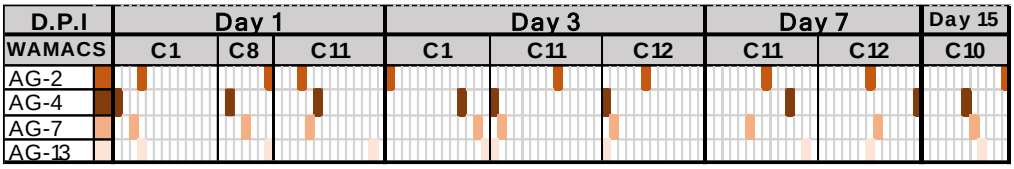

Figure 1. Aquaphotomics Barcode based on the WAMACS. Peak shifts can be observed for the evaluated AGs in specific coordinates after each d.p.i.

The first three Principal Components (PCs) from each d.p.i explained 70.8% ± 5.1 of the database variations. No outliers were found in the Hotelling's T^2 influence plots obtained in the PCA. The additional PCA-LDA models (Table 1) for the simultaneous discrimination of these *R. solani* AGs can identify NIR spectra from liquid cultures after each d.p.i with an accuracy >90 % in the calibration and validation processes and a specificity of 100%, meaning the control (basal media) simultaneously incubated with the samples was never classified as an AG.

Table 1. PCA - LDA spectra classification and quality parameters expressed as Mean ± SD for liquid cultures containing four *R. solani* AGs after each time post-inoculation. Cal=Calibration, Val=Validation

Quality	Day 1		Day 3		Day 7		Day 15	
	Cal 80%	Val 20%	Cal 80%	Val 20%	Cal 80%	Val 20%	Cal 80%	Val 20%
%Accuracy	99.2±0.4	96.7±0.4	97.5±0.9	96.7±0.4	91.7±2.3	93.3±0.5	98.3±0.5	90.0±1.3
% Specificity	100.0	100.0	100.0	100.0	100.0	100.0	100.0	100.0

Conclusions

1. We detected and discriminated four multinucleate *R. solani* AGs inoculated in basal liquid cultures using NIRS, chemometrics and aquaphotomics. Biochemical changes related to differences in metabolic growth generated distinct patterns in the WAMACs and WASPs based on dominant peaks in the wavelength range 1300-1600nm where OH, CH, and NH bonds interact with NIR light.
2. Our data indicates NIRS in combination with Chemometrics and Aquaphotomics has potential as a rapid laboratory assay for *R. solani* AGs detection and discrimination as soon as 1-day post-inoculation using liquid cultures, in comparison with the 8 days required with the traditional classification method. This will be useful to reduce the current detection time and the selection of an accurate treatment for a most or less destructive AGs before economic losses occur in the crops.

References

1. Ferrucho RL, Cifuentes JM, Ceresini P, García-domínguez C (2012) Rhizoctonia solani AG-3PT is the major pathogen associated with potato stem canker and black scurf in Colombia Rhizoctonia solani GA-3PT es el principal patógeno asociado con el. Agron Colomb 30:204–213
2. Carling DE, Baird RE, Gitaitis RD, et al (2002) Characterization of AG-13, a newly reported anastomosis group of Rhizoctonia solani. Phytopathology 92:893–899. https://doi.org/10.1094/PHYTO.2002.92.8.893
3. Sharon M, Kuninaga S, Hyakumachi M, Sneh B (2006) The advancing identification and classification of Rhizoctonia spp. using molecular and biotechnological methods compared with the classical anastomosis grouping. Mycoscience 47:299–316. https://doi.org/10.1007/s10267-006-0320-x
4. Tsenkova R, Munćan J, Pollner B, Kovacs Z (2018) Essentials of Aquaphotomics and Its Chemometrics Approaches. Front Chem 6:1–25. https://doi.org/10.3389/fchem.2018.00363
5. Muncan J, Tsenkova R (2019) Aquaphotomics-From Innovative Knowledge to Integrative Platform in Science and Technology. Molecules 24:. https://doi.org/10.3390/molecules24152742

This project was supported by the Mississippi Agricultural and Forestry Experiment Station, the National Institute of Food and Agriculture, U.S. Department of Agriculture, Hatch project under accession number W3173, and the USDA-ARS 58-6402-018 Biophotonics Initiative, Grant # G00003581.

QUANTUM BRAIN DYNAMICS - ROLE OF WATER

Modelling the measured microtubule conductivity and capacitance as a function of ionic concentrations

Boden B. Eakins1, Sahil D. Patel1, Aarat P. Kalra2, Vahid Rezania3, Karthik Shankar1 and Jack A. Tuszynski2,*

[1]Department of Electrical and Computer Engineering, Faculty of Engineering, University of Alberta, Edmonton, Canada
[2]Department of Physics, Faculty of Science, University of Alberta, Edmonton, Canada
3 Department of Physical Sciences, MacEwan University, Edmonton, Canada
*****Presenting author and Correspondence: jackt@ualberta.ca

Keywords: tubulin, microtubules, conductivity, electrostatics, capacitance, ionic solutions

Introduction

Microtubules are highly negatively charged proteins which have been shown to behave as bio-nanowires capable of conducting ionic currents. The electrical characteristics of microtubules are highly complicated and have been the subject of previous work under varying conditions of pH and ionic concentrations [1-4]. However, the impact of the ionic concentration of the buffer solution on microtubule electrical properties has often been overlooked and never fully explored in a quantitative way.

Materials and Methods

In this work we use the non-linear Poisson-Boltzmann equation, modified to account for a variable permittivity and a Stern Layer, to calculate counterion concentration profiles as a function of the ionic concentration of the buffer. We solve these equations using a combination of software packages, namely: (1) for molecular modeling of the tubulin dimer - MOE software (Molecular Operating Environment; Chemical Computing Group, Montréal, Quebéc, Canada, and (2) for solving Poisson-Boltzmann equations - COMSOL Multiphysics software (COMSOL Inc, Burlington, Massachusetts).

Results

We find that for low-concentration buffers ([KCl] from 10 μM to 10 mM) the counterion concentration is largely independent of the buffer's ionic concentration, but for physiological-concentration buffers ([KCl] from 100 mM to 500 mM) the counterion concentration varies dramatically with changes in the buffer's ionic concentration. We have calculated the conductivity of microtubule-counterion complexes, which are found to be more conductive than the buffer when the buffer's ionic concentrations is less than ≈ 100 mM and less conductive otherwise. These results demonstrate the importance of accounting for the ionic concentration of the buffer when analyzing microtubule electrical properties both under laboratory and physiological conditions.

Conclusions

The results in this work illustrate the influence of the buffer on the electrical properties of MTs. Counterionic condensation around MTs is strongly dependent on the buffer ionic concentration, which can be divided into two distinct regimes: the low concentration regime (10μM to 10mM), and the physiological concentration regime (100 mM to 500 mM). MTs in these regimes have marked differences in local and far-field counterionic condensation parameters which have been explored here in depth and should be considered in future biological and nano-device research. There is also important consequence of this work on the physiological properties of the cytoskeleton in neurons where electrical signaling can be seen to be very strongly dependent on the ionic composition of the cell. We conclude by calculating the basic electrical parameters of microtubules over a range of ionic buffer concentrations applicable to nanodevice and medical applications.

References

1. Kalra, Aarat P., et al. (2020) Investigation of the electrical properties of microtubule ensembles under cell-like conditions. Nanomaterials 10.2: 265.
2. Santelices, Iara B., et al. (2017) Response to alternating electric fields of tubulin dimers and microtubule ensembles in electrolytic solutions. Scientific reports 7.1: 1-11.
3. Kalra, Aarat P., et al. (2020) All Wired Up: An Exploration of the Electrical Properties of Microtubules and Tubulin. ACS nano 14.12: 16301-16320.
4. Kalra, Aarat P., et al. (2021) Revealing and Attenuating the Electrostatic Properties of Tubulin and Its Polymers. Small 17.1: 2003560.

Non-equilibrium Quantum Brain Dynamics in $3+1$ dimensions with Water Dipoles and Photons

Akihiro Nishiyama[1*], Shigenori Tanaka[1] and Jack A. Tuszynski[2, 3, 4]

[1]Graduate School of System Informatics, Kobe University, 1-1 Rokkodai, Nada-ku, Kobe, 657-8501, Japan
[2]Department of Oncology, University of Alberta, Cross Cancer Institute, Edmonton, Alberta, Canada T6G 1Z2
[3]Department of Physics, University of Alberta, Edmonton, Alberta, Canada T6G 2J1
[4]DIMEAS, Corso Duca degli Abruzzi, 24, Politecnico di Torino, Turin, TO, 10129, Italy
***** email: anishiyama@people.kobe-u.ac.jp

Quantum Brain Dynamics (QBD) with water dipoles and photon degrees of freedom is one of the hypotheses of memory in the brain. We aim to show non-equilibrium properties of QBD for memory formations. We start with the Lagrangian density of QBD in $3+1$ dimensions. We show time evolution equations, namely Schr"odinger-like equations for coherent electric dipole fields, the Klein–Gordon equations for coherent electric fields and the Kadanoff–Baym equations for incoherent dipoles and photons. We can describe non-equilibrium processes involving entropy production, super-radiance phenomena and the Higgs mechanism in this theory. We can apply non-equilibrium QBD to memory formation processes.

Keywords: Quantum Brain Dynamics, Kadanoff–Baym equation, Entropy Production

Introduction

Quantum Brain Dynamics (QBD) is one of the hypotheses expected to describe memory in the brain [1, 2, 3, 4, 5]. The concrete degrees of freedom in QBD are water electric dipoles and photons. Memory in QBD is represented by ordered patterns of dipoles and photons where water dipoles are aligned in the same direction (spontaneous breakdown of symmetry). The aim of this work is to show non-equilibrium properties in QBD using the Schro¨dinger-like equations, the Klein–Gordon equations and the Kadanoff–Baym equations. We find several aspects in non-equilibrium QBD, that is entropy production, super-radiance, and the Higgs mechanism, from our single Lagrangian [6]. Our results can be applied to the description of memory formations in QBD.

Methods

We adopt the Lagrangian density in Quantum Brain Dynamics (QBD) in $3+1$ dimensions based on the preceding work [4]. We adopt two-energy-level approximation of dipole fields for the 1st excited states ψ_α with $\alpha = 0, \pm 1$ and those for the ground state ψ_s in Fig. 1.

Results

We can derive the Schro¨dinger-like equations for coherent dipole fields $\overline{\psi}_s$ and $\overline{\psi}_\alpha$ ($\alpha = 0, \pm 1$) with the bar representing the expectation values, the Klein–Gordon equations for coherent electric fields $\boldsymbol{E}$ and the Kadanoff–Baym equations for incoherent dipoles and photons.

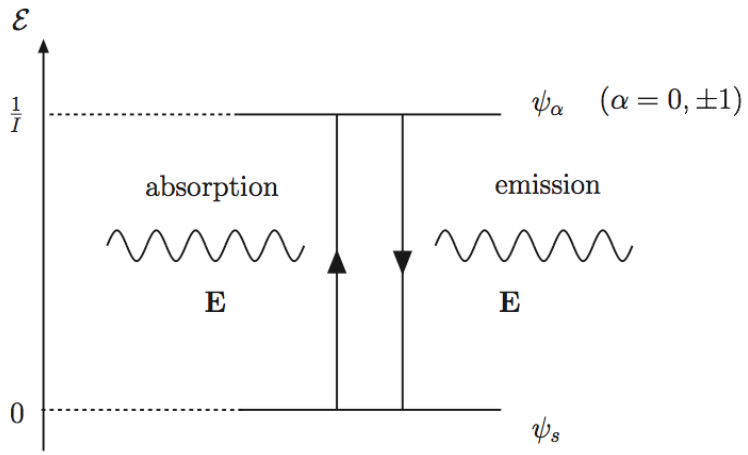

Figure 1. Two energy levels for electric dipole fields. The energy difference is $1/I = 4$ meV.

First, we find that the Kadanoff–Baym equations for incoherent dipoles and photons describe entropy producing dynamics, corresponding to the H-theorem which represents the 2nd law in thermodynamics in an isolated system. Next, we show the aspect of the super-radiance, the solution of flash light for quantum information transfer in memories diffused in the brain's neocortex. Finally, we show the Higgs mechanism, where the mass term emerges for the shielding effect of fields, namely the Meissner effect.

Conclusions

Starting with the Lagrangian density in QBD in 3+1 dimensions with water dipoles and photons, we have derived the Schro¨dinger-like equations for coherent dipole fields, the Klein–Gordon equations for coherent electric fields, and the Kadanoff–Baym equations for incoherent dipoles and photons. We can show entropy production with the H-theorem, super-radiance for quantum information transfer and the Higgs mechanism. Our theory can be applied to non-equilibrium phenomena in QBD, especially memory formations.

References

1. Luigi Maria Ricciardi and Horoomi Umezawa. Brain and physics of many-body problems. Kybernetik, 4(2):44–48, 1967.
2. C.I.J.M. Stuart, Y. Takahashi, and H. Umezawa. On the stability and non-local properties of memory. Journal of theoretical biology, 71(4):605–618, 1978.
3. C.I.J.M. Stuart, Y. Takahashi, and H. Umezawa. Mixed-system brain dynamics: neural memory as a macroscopic ordered state. Foundations of Physics, 9(3-4):301–327, 1979.
4. Emilio Del Giudice, Giuliano Preparata, and Giuseppe Vitiello. Water as a free electric dipole laser. Physical review letters, 61(9):1085, 1988.
5. Mari Jibu and Kunio Yasue. Quantum brain dynamics and consciousness. John Benjamins, 1995.
6. Akihiro Nishiyama, Shigenori Tanaka, and Jack A. Tuszynski. Non-equilibrium quantum brain dynamics ii: Formulation in 3+1 dimensions. Physica A: Statistical Mechanics and its Applications, 567:125706, 2021.

WATER AS A PART OF BIOLOGICAL PROCESSES

Studies on cryopreservation mechanism using Trehalose-transporter expressing cells

Tsutomu Uchida[1,*], Maho Furukawa[2], Takahiro Kikawada[3,4], Kenji Yamazaki[1] and Kazutoshi Gohara[1]

[1] Faculty of Engineering, Hokkaido University;
[2] Graduate School of Engineering, Hokkaido University;
[3] Institute of Agrobiological Sciences, National Agriculture and Food Research Organization;
[4] Graduate School of Frontier Sciences, The University of Tokyo
***** Presenting author and Correspondence: t-uchida@eng.hokudai.ac.jp

Cryopreservation of living cells is a technology used in the industries, and is the only way to stop the time of life. However, the mechanism has not been fully revealed scientifically. We are studying the cryopreservation mechanism using trehalose, which is expected as a natural cryoprotectant but is impermeable of cell membrane. Using the trehalose-transporter expressing cells, we found that the cryopreservation effect is significantly improved when trehalose was transported into cells. Various experiments were conducted to reveal this mechanism, and they suggested that the effect of dehydration was relatively small, although it has been regarded as important for a cell cryopreservation.

Keywords: freeze–thaw viability, trehalose uptake, dehydration, cryoprotect mechanism

Introduction

At present, the cryopreservation technology is used mainly for germ cells in the fisheries and livestock industries, and in the project of scarce-species preservation. It is also the only technology that can stop the time of lives. However, the mechanism of cryopreservation has not been fully revealed scientifically yet. Thus, the safe preservation techniques have not been established for cells in high demand, such as nerve cells and cardiomyocytes. Since a lot of water is included in a cell, the cryopreservation comes to the problem of how to control the freezing of intra- and extra-cellular water. It requires to control mainly the appropriate freezing rates, and to control the freezing processes by adding cryoprotective agents (CPAs). In the slow freezing method used industrial, the extracellular water is preferentially frozen which leads to dehydrate the intracellular water, and inhibit the intracellular freezing. However, the CPA used at this method is glycerin or DMSO, which are reported to have cytotoxicity. Therefore, it is desired to develop the alternative CPAs for a safer cryopreservation. On the other hand, rapid freezing method used for cryopreservation of small amounts of cells is a technique of adding high-concentration vitrifying agents to suppress the formation of ice crystals.

We are developing a safe cryopreservation method using trehalose, which is expected as a natural CPA but is impermeable of the cell membrane, and are revealing the cryopreservation mechanism of slow-freezing. This report shows our recent researches using the unique experimental system with cells expressing trehalose-transporter (TRET1), which allows to take up trehalose into cells.1)2) This system allows us to obtain the clear results on the significant improvement of the cryoprotective effect by the intracellular trehalose and to reveal the mechanism of cryoprotection effect of trehalose.

Materials and Methods

The cells used in the study were Chinese hamster oocytes expressing TRET1 on the membrane (CHO-TRET1 cells).3) TRET1 can selectively transport trehalose in both directions (depending on the trehalose-concentration difference between inside and outside of the cell) at high speed and in large quantities.3) By conducting experiments with cells with suppressed expression (CHO-vector cells), we can compare the state with and without intracellular trehalose under the same cells and under the same conditions.
Trehalose (donated by Hayashibara) was added to the culture medium at a concentration of 0~1 M to prepare the frozen solution. CHO cells were dispersed in 1 mL of the frozen solution at 105~106 cells/mL and stored in a CO2 incubator to uptake trehalose into the cells or to dehydrate. Then, the samples were put into the cooling container controlled at -20~-196 °C to freeze at various rates. The sample was thawed rapidly at 37 °C, and

replaced with a culture medium quickly. Then the cells were stained by calcein-AM and propidium iodide (Dojindo) to measure their viabilities by observing with an epifluorescence microscope (Olympus, IX-71). To confirm the proliferative ability of the viable cells, the thawed cells were cultured for a week.

Results and Discussion

Figure 1 shows the viability of CHO-vector cells and CHO-TRET1 cells at -80 °C depending on the trehalose concentrations in the frozen solution.1) Most of vector cells were dead at all concentrations, but TRET1 cells showed high viabilities, especially at concentrations of 400-500 mM. In experiments with different freezing temperatures, the significance of viabilities of TRET1 cells compared to vector cells was found at temperatures higher than -100 °C, but not at temperatures lower than -100 °C. From these results, the cryopreservation of cells was found to be significantly improved by transporting trehalose into the cells.

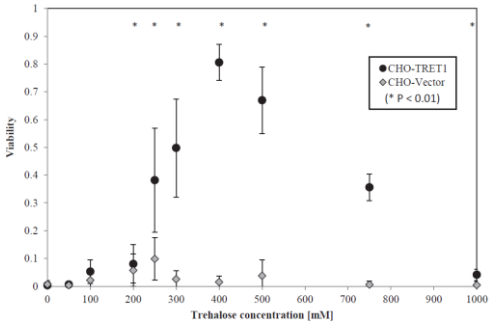

Figure 1. Viabilities of cryopreserved CHO-vector cells (gray diamonds) and CHO-TRET1 cells (solid circles) at various extracellular trehalose concentrations. Each viability is the mean ± SD of microscopic measurements. The asterisks mark cases with significant difference of viabilities between CHO-vector cells and CHO-TRET1 cells at the same conditions ($p < 0.01$). 1)

To clarify these phenomena, we evaluated the effect of trehalose on cells during the pre-freezing incubation and measured the amount of trehalose uptake into CHO-TRET1 cells.2) As a result, we found the upper limit (about 80 pg/cell) for the uptake amount of trehalose. The saturated intracellular solution is isotonic with the extracellular solution of about 400 mM trehalose, which maximizes the cryopreservation effect. Based on these results, we investigated which process, the intracellular trehalose transport process or the extracellular dehydration process is important for the cryopreservation effect. The model investigation suggested that, at concentrations smaller than 400 mM, trehalose was transported into the cell until being isotonic state, and the viability improved according to the amount of intracellular trehalose. However, the cells were considered to be damaged before freezing due to the dehydration stress at higher trehalose concentrations. That is, the presence of intracellular trehalose was found to be more important than dehydration from cells. In the future, we plan to use the aquaphotomic approaches using Raman or IR spectroscopies to understand the state of both intra- and extra-cellular water. We will also plan to examine the cryopreservation condition of the cells expressing aquaporins to clarify the cell dehydration effect on the slow cryopreservation mechanism.

References

1. Uchida T., Furukawa M., Kikawada T., Yamazaki K., Gohara K. (2017) Intracellular trehalose via transporter TRET1 as a method to cryoprotect CHO-K1 cells, Cryobiology 77: 50-57.
2. Uchida T., Furukawa M., Kikawada T., Yamazaki K., Gohara K. (2019) Trehalose uptake and dehydration effects on the cryoprotection of CHO–K1 cells expressing TRET1, Cryobiology 90: 30-40.
3. Kikawada T., Saito A., Kanamori Y., Nakahara Y., Iwata K., Tanaka D., Watanabe M., Okuda T. (2007) Trehalose transporter 1, a facilitated and high-capacity trehalose transporter, allows exogeneous trehalose uptake into cells, Proc. Nat. Acad. Sci. 104: 11585-11590.

Assessment of biological functions and metabolic activity during embryogenesis by water analysis using near-infrared spectroscopy

Mika Ishigaki

Faculty of Life and Environmental Sciences, Shimane University, Japan
Raman Project Center for Medical and Biological Applications, Shimane University, Japan
ishigakil@life.shimane-u.ac.jp

The influence of embryonic bioactivity on the water structure was investigated using near-infrared (NIR) spectroscopy and imaging. The yolks of the activated eggs contained higher proportions of weakly hydrogen bonded water than those of non-activated eggs. A possible factor responsible for the significant changes in the water structure was revealed to be a protein secondary structural change from an α-helix to a β-sheet in the activated eggs. NIR images of the activated eggs successfully visualized the water structural variation in the yolk with a higher proportion of weak hydrogen bonds due to the activation of embryonic development.

Keywords: NIR spectroscopy, NIR imaging, Water structure, Embryogenesis

Introduction

NIR imaging has been a matter of keen interest because it provides the spatial distribution of chemical components nondestructively even for thick materials. In the present study, we investigated the relationship between bioactivity and water structure in Japanese medaka fish (Oryzias latipes) eggs using NIR imaging in situ. We aimed to better understand the differences between whether a new life will be born or not by investigating "water" as the main component of biology from the standpoint of molecular spectroscopy.

Materials and Methods

The variations in the components of the yolk, such as proteins, lipids, and water, were investigated and compared for four different kinds of egg samples: (a) eggs that were activated by fertilization and three kinds of non-activated eggs where embryogenesis was stopped or not started by (b) culturing under cold temperatures, (c) instant freezing or (d) the lack of fertilization. The NIR imaging data were obtained by a microscopic NIR system; Perkin-Elmer Spectrum One FT-NIR spectrometer equipped with a HgCdTe (MCT) detector (Spectrum Spotlight 300). To quantitatively evaluate the magnitude of a water peak shift ex vivo at approximately 5200 cm-1, four kinds of perturbations were given to ultrapure water: (i) temperature, (ii) ion concentration, (iii) protein concentration, and (iv) the secondary structural changes of proteins.

Results and Discussion

In NIR absorbance and second derivative spectra obtained from egg yolk, water, protein, lipid bands were observed. The broad features around 6950 and 5200 cm^{-1} are due to combination of the symmetric and antisymmetric O-H stretching modes and of antisymmetric O-H stretching and O-H bending modes of water, respectively [1]. The peaks at 4258 and 4340 cm^{-1} represent the combination of C-H stretching and bending modes, and the ones at 4864 cm^{-1} are assigned to amide modes relating of proteins [1].
In order to investigate the yolk component differences between activated and non-activated eggs, principal component analysis (PCA) was performed to the dataset of NIR second derivatives. The dataset was classified into two groups by principal component (PC) 1 and PC2 show in Figure 1, and the discriminant component between activated and non-activated was indicated to be related with water structure. Generally, water has mainly two components of water at normal temperature for organisms; strongly and weakly hydrogen bonding water [2, 3], and two bands at approximately 5200 and 5000 cm^{-1} to weakly and strongly hydrogen-bonded

water, respectively [4]. That is, the present results exhibited the activated eggs had higher ratio of weakly hydrogen bonding water than those of non-activated.The bioactivity was likely to have an impact on the hydrogen bonds of water. Figure 2 exhibits NIR imaging constructed by plotting second derivative intensities due to protein (4864 cm^{-1}) and strongly hydrogen donging water (5190 cm^{-1}). The differences of material variations and water distributions can be visualized between activated and non-activated eggs [5].

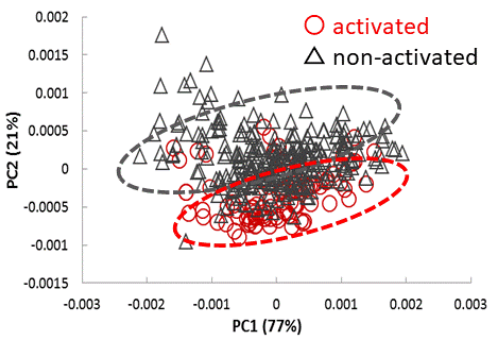

Figure 1: Score plots of PC1 vs PC2.

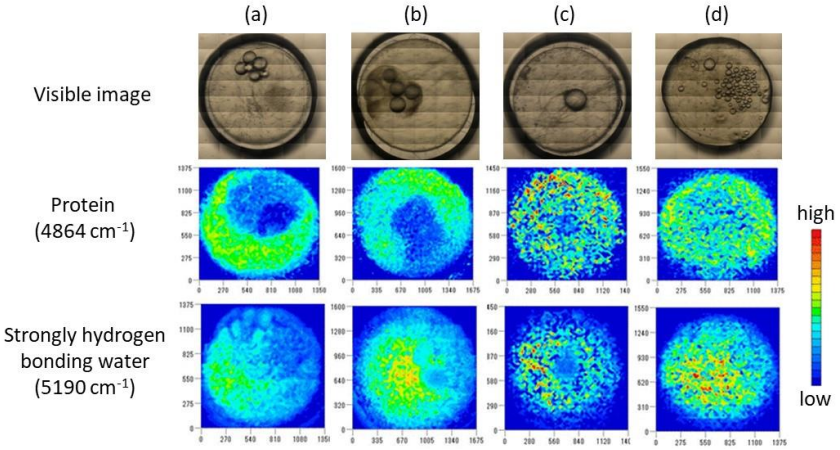

Figure 2: NIR images constructed by plotting second derivative intensities due to proteins and water.

Conclusions

The bioactivity of embryogenesis was assessed through changes in the water structure using NIR spectroscopy and imaging. In the activated eggs after fertilization, the water band at approximately 5250 cm^{-1} shifted to a higher wavenumber by 2-4 cm^{-1}, and the proportion of WHB water was higher than that in non-activated eggs. The water structure was likely to vary due to the higher proportion of WHB water associated with protein structural changes. NIR imaging successfully visualized the dynamic water structural changes depending on the embryogenetic activity. Whether a new life will be born or not was revealed through changes in the water structure.

References

1. Workman Jr, J., Weyer, L (2012). Practical guide and spectral atlas for interpretive near-infrared spectroscopy. CRC Press.
2. Šašic S, Segtnan V H, Ozaki Y (2002) Self-modeling curve resolution study of temperature-dependent near-infrared spectra of water and the investigation of water structure. *J. Phys. Chem. A*, 106:760–766.
3. Maeda H, Ozaki Y, Tanaka M, Hayashi N, Kojima T (1995) Near infrared spectroscopy and chemometrics studies of temperature-dependent spectral variations of water: relationship between spectral changes and hydrogen bonds. *J. Near Infrared Spectrosc.* 3:191-201.
4. Czarnik-Matusewicz B, Pilorz S, Hawranek J P (2005) Temperature-dependent water structural transitions examined by near-IR and mid-IR spectra analyzed by multivariate curve resolution and two-dimensional correlation spectroscopy. *Anal. Chim. Acta* 544:15-25.
5. Ishigaki M, Yasui Y, Kajita M, Ozaki Y (2020) Assessment of Embryonic Bioactivity through Changes in the Water Structure Using Near-Infrared Spectroscopy and Imaging. *Anal. Chem.* 92:8133-8141.

HYDRATION & INTERFACIAL WATER

Interfacial Water in Determining the Interactions of Proteins and Cells with Materials

Masaru Tanaka [1,*], Shingo Kobayashi [1], Daiki Murakami [1], Takahisa Anada [1], Tomohiro Hayashi [2] and Shigeaki Morita [3]

[1] Affiliation 1; Institute for Materials Chemistry and Engineering, Kyushu University, CE41 744 Motooka, Nishi-ku, Fukuoka 819-0395, Japan
[2] Affiliation 2; Department of Materials Science and Engineering, Tokyo Institute of Technology, 4259 Nagatsuta-cho, Midori-ku, Yokohama, Kanagawa 226-8502, Japan
[2] Department of Engineering Science, Osaka Electro-Communication University, 18-8 Hatsucho, Neyagawa 572-8530, Japan
***** Presenting author and Correspondence: masaru_tanaka@ms.ifoc.kyushu-u.ac.jp

To understand the role of water in the interaction of proteins and cells at biological interfaces, it is important to compare particular states of hydration water with various physicochemical properties of hydrated materials. Here, we discuss the fundamental concepts for determining the interactions of proteins and cells with hydrated materials along with selected examples, including poly(2-methoxyethyl acrylate) and other biomaterials. The states of water were analyzed by differential scanning calorimetry, in situ attenuated total reflection infrared spectroscopy, and surface force measurements. We found that intermediate water which is loosely bound to a biomaterial, is a useful indicator of the bioinertness of material surfaces.

Keywords: Water states, Polymeric Biomaterials, Aquatic Functional Materials

Introduction

Water molecules play a crucial role in biointerfacial interactions, including protein adsorption and desorption. Many studies have been conducted to understand the relationship between the protein adsorption and physicochemical properties of biomaterials. For instance, hydrophilicity/hydrophobicity, molecular mobility, charge, viscoelasticity, surface morphology of material surfaces can have an impact on the bioinertness of biomaterials. However, our molecular understanding of the mechanisms responsible for the protein behavior on biomaterials is incomplete. When biomaterials come in contact with blood, the water molecules present in blood immediately get adsorbed on the surface of the materials. This is followed by protein adsorption, protein. To understand the behavior of interfacial water around the biomaterials, interfacial water structure and dynamics on materials can be considered. Herein, we describe the role of the states of biointerfacial water in the bioinertness of the materials using thermal, spectroscopic, and surface force measurements to provide structure-based design guidelines for novel and effective biomedical surfaces.

Materials and Methods

The preparation of hydrated materials and analyses of the amount of hydration water and its states were performed using previously reported methods [1]. The amount and states of hydrated water and the presence of intermediate water in the materials such as water-insoluble poly(2-methoxyethyl acrylate) (PMEA)/PMEA derivatives, water- soluble poly(ethylene glycol), poly(vinyl pyrrolidone), and zwitterionic (betaine) polymers were evaluated by differential scanning calorimetry (DSC), solid-state NMR, time-resolved *in situ* attenuated total reflection infrared (ATR-IR) spectroscopy, and surface force measurement using atomic force microscopy (AFM) [2]. As reference materials, not only biomolecules/biopolymers but also inorganic materials or other chemicals, such as calcium phosphate minerals, and cholinium phosphate-type ionic liquids were used.

Results

The states of water at the biointerface differ from those of bulk water (non-bound water). Two types of bound water states exist in hydrated materials-tightly bound water (non-freezing water) and scarcely bound water (freezing water or free water). In addition, the intermediate state bound water (i.e., loosely bound water or

freezing bound water or intermediate water) is observed in hydrated PMEA/PMEA derivatives, which show low protein adsorption properties. The presence of intermediate water, rather than non-freezing water and free water, is a useful indicator of the bioinertness of the biomaterials. The characteristics and traditional names of the three types of water are listed in Table 1. The intermediate water is also observed in hydrated biomolecules and biopolymers (DNA, RNA, proteins, and polysaccharides). The intermediate water contents are dependent on the type of materials. The factors that affect the intermediate water content are molecular flexibility, mobility, and hydration forces.

Table 1. Classification of three types of hydrated water states

Mode of binding	Traditional name	Freezability	Time-resolved ATR-IR peak top of OH stretching region (cm^{-1})	Solid state NMR correlation time τ_c (s)	Surface force[#]
Scarcely bound water	Freezing water or Free water	Melting at 0 °C	3400–3200	10^{-12}–10^{-11}	No interaction
Loosely bound water	Freezing bound water or Intermediate water	Freezing and melting below 0 °C	3400	10^{-10}–10^{-9}	Repulsion at a long range (2–4 nm)
Tightly bound water	Non-freezing bound water	Non-freezing below 0 °C	3600	10^{-8}–10^{-6}	Repulsion at a short range (< 1 nm)

[#]This classification is based on the results of hydrophilic inorganic materials and self-assembled monolayers.

We found that the structured interfacial water (intermediate water) plays an important role in determining protein adsorption. A physical barrier of intermediate water of thickness of 2 to 3 nm is necessary for bioinertness. Our multiscale interfacial analysis integrates advanced analytical methods in biological hydrated conditions to clarify the role of intermediate water in biological functions. Our results will provide an in-depth understanding of biological mechanisms and guiding principles to design biomaterials.

Conclusions

Protein adsorption and cell adhesion were controlled by intermediate water contents. The intermediate water is the common state of water in hydrated biomolecules/polymers and bio-inert synthetic materials. The intermediate water is a useful index for determining the bioinertness/antifouling property. Surface force measurements revealed a protective barrier of interfacial water that prevents protein adsorption and cell adhesion. This finding on intermediate water provides novel insights and helps develop novel experimental models for Aquaphotomics.

References

1. Sonoda T, et al (2020) Macromolecules 53:8570. 2. Tanaka M, et al (2021) Colloids Surf B 198: 111449.

Investigation on the reaction mechanism of $Mg(OH)_2$ dehydration and MgO hydration by NIR spectroscopy

Masato Takeuchi [1,*] Atsushi Kondo [1,2], Ryo Kurosawa[3], Junichi Ryu[3]

[1] Department of Applied Chemistry, Graduate School of Engineering, Osaka Prefecture University
[2] Marketing & Planning Department, Magnesia Division, Ube Material Industries, Ltd.
[3] Graduate School of Engineering, Chiba University
* Presenting author and Correspondence: masato-t@chem.osakafu-u.ac.jp

The mechanism for the dehydration of Mg(OH)2 and hydration of MgO was investigated by NIR spectroscopy. Mg(OH)2 showed three absorption bands at 7339, 7306, and 7157 cm−1 (7339 cm−1, OH(e) and OH(c) located on the edge corner of the Mg(OH)2 sheet, 7306 cm−1, OH(t) located on the terrace of Mg(OH)2 sheet; 7157 cm−1, OH(i) located on the interlayer of Mg(OH)2 sheets). During the hydration of Mg(OH)2 into MgO, the OH(i) disappeared and the OH(t) on the Mg(OH)2 was converted to the hydrogen-bonded OH groups on the MgO (7309 cm−1). Furthermore, the mechanism for hydration of MgO was also clarified by NIR spectroscopy.

Keywords: Near infrared spectroscopy; Mg(OH)2 dehydration; MgO hydration

Introduction

To tackle global warming issue due to the escalating emission of CO2, researches have focused on the effective use of unharnessed thermal energy sources using chemical heat storage (CHS) materials [1−3]. For example, dehydration of Mg(OH)2 and hydration of MgO, regarding a reaction: Mg(OH)2 ⇄ MgO + H2O, correspond to storage and output processes of thermal energy, respectively. In this system, water molecule plays an important role as a heat carrier. In this study, we have applied the NIR spectroscopy to clarify the mechanism for the dehydration of Mg(OH)2 and hydration of MgO involving water molecules.

Materials and Methods

MgO was prepared by calcination of $Mg(OH)_2$ at 600 °C for 1 h in an electric furnace. Crystal structures of $Mg(OH)_2$ and MgO were characterized using an XRD, TG-DTA-MS measurements. Furthermore, the NIR spectra for dehydration of $Mg(OH)_2$ and hydration of MgO were monitored in a diffuse reflectance mode using FT-NIR spectrophotometer (FT/IR-4700, JASCO, Japan). The baseline was calibrated using an Al plate.

Results

Fig. 1(A) shows the NIR spectra for the dehydration process of Mg(OH)2 under heating conditions [4]. Before the heat treatment, the Mg(OH)2 showed three different absorption bands at 7339, 7306, and 7157 cm−1, which can be assigned to the first overtone (2νOH) of the hydroxyl groups of Mg(OH)2. The corresponding absorption bands were actually observed at 3702, 3687, and 3648 cm−1 (mid-IR region) in the FT-IR spectra (not shown here). Interestingly, the IR spectrum of Mg(OH)2 was first reported in 1905 by W. W. Coblentz [5]. Although the hydroxyl groups of Mg(OH)2 were not observed, the fundamental vibration modes (νOH and δ) of H2O were clearly detected at 3 and 6 μm. Moreover, the combination and first overtone bands were observed at 2 and 1.4 μm, respectively. Among the three absorption bands at 7339, 7306, and 7157 cm−1 (Fig. 1(A)), the former two bands can be assigned to less hydrogen-bonded hydroxyl groups located on the near-surface and the latter one to hydrogen-bonded hydroxyl groups positioned in the interlayers of Mg(OH)2. As the temperature increased to 400 °C, the intensity of the band at 7157 cm−1 gradually decreased, and the two bands at 7339 and 7306 cm−1 were combined into one at 7309 cm−1. At temperature higher than 450 °C, only one band was observed at 7309 cm−1, which can be assigned to the hydrogen-bonded hydroxyl groups of MgO surface. For further discussion on the dehydration process of the Mg(OH)2, second-derivative spectra are shown in Fig. 1(B). As the treatment

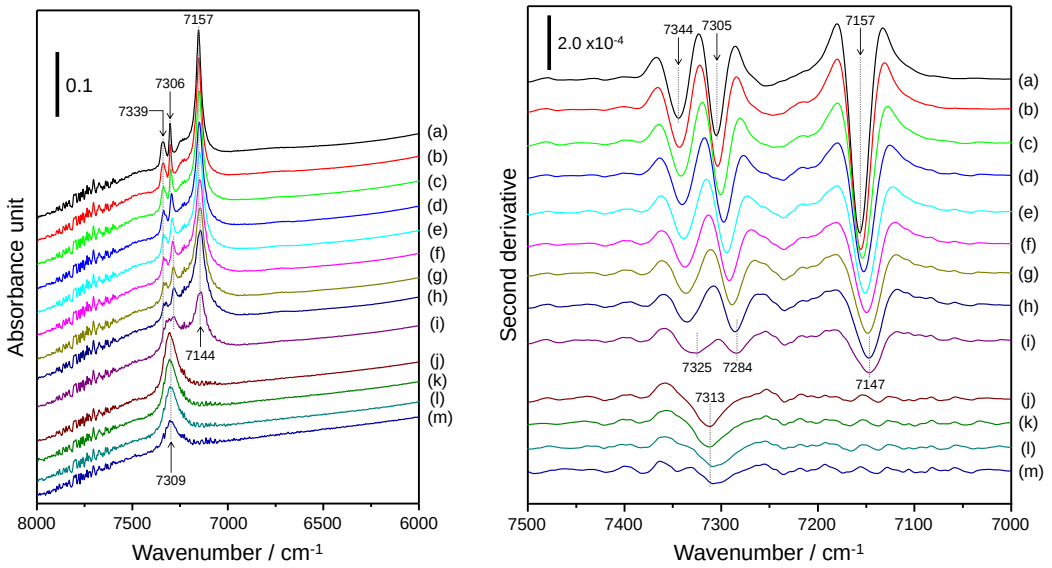

Figure 1. NIR spectra (left) and second-derivative spectra (right) for the dehydration process of $Mg(OH)_2$. (a) r. t., (b) 50 °C, (c) 100 °C, (d) 150 °C, (e) 200 °C, (f) 250 °C, (g) 300 °C, (h) 350 °C, (i) 400 °C, (j) 450 °C, (k) 500 °C, (l) 550 °C, (m) 600 °C.

Temperature increased, the absorption bands due to the OH groups of $Mg(OH)_2$ decreased but gradually shifted toward higher wavenumber regions. This behavior indicates that the hydrogen bond networks between the OH groups of Mg(OH)2 change into a dense state during the hydration process. A possible explanation could be that the MgO moieties, which are formed on the Mg(OH)2 surface, compress the bulk structure, especially in its interlayer direction. After these bands disappeared at 400−450 °C, a new band was observed at 7309 cm−1 due to the hydrogen-bonded hydroxyl groups of MgO surface. These observations were in good agreement with the results of the TG-DTS-MS and XRD measurements. In addition, hydration process of MgO was also discussed by NIR spectroscopy.

Conclusions

The dehydration of Mg(OH)2 and hydration of MgO were investigated by means of NIR spectroscopy. Three absorption bands could be detected for Mg(OH)2 at 7339, 7306, and 7157 cm−1, which were attributed to different OH groups of Mg(OH)2. As the Mg(OH)2 phase converted into MgO at approximately 400 °C, the OH groups of Mg(OH)2 surface were unified to hydrogen-bonded hydroxyl groups of MgO surface (7309 cm−1), and the interlayer OH of Mg(OH)2 disappeared via a condensation reaction. In the hydration process of MgO, the isolated OH groups of MgO surface were readily converted into hydrogen-bonded ones. When a monolayer Mg(OH)2 sheet was formed on the MgO surface, OH groups were observed at 7345 and 7309 cm−1. As several Mg(OH)2 sheets were stacked, the interlayer OH of Mg(OH)2 appeared.

References

1. Ishitobi H, Uruma K, Takeuchi M, Ryu J, Kato Y (2013) Dehydration and hydration behavior of metal-salt-modified materials for chemical heat pumps. Appl. Therm. Eng. 50, 1639–1644.
2. Kurosawa R, Takeuchi M, Ryu J (2019) Comparison of the effect of co-addition of Li compounds and addition of a single Li compound on reactivity and structure of magnesium hydroxide. ACS Omega 4, 17752−17761.
3. Kurosawa R, Takeuchi M, Ryu J (2021) Fourier-Transform Infrared Analysis of the Dehydration Mechanism of Mg(OH)2 and Chemically Modified Mg(OH)2. J. Phys. Chem. C (in print).
4. Kondo A, Kurosawa R, Ryu J, Matsuoka M, Takeuchi M (2021) Investigation on the mechanisms of Mg(OH)2 dehydration and MgO hydration by near-infrared spectroscopy. J. Phys. Chem. C (submitted to)
5. Coblentz W W (1905) Water of constitution of crystallization. Phys. Rev. 26, 252–258.

Water at biointerfaces: what makes surfaces bioinert?

Tomohiro Hayashi[1, 2,*]

[1] Department of Materials Science and Engineering, School of Materials and Chemical Technology, Tokyo Institute of Technology
[2] JST-PRESTO (Materials Informatics)
* Presenting author and Correspondence: tomo@mac.titech.ac.jp

Mechanism underlying anti-biofouling has been a matter of intense debate, although this is an essential issue in biomedicine, biosensing, etc. In this presentation, we overview the previous research works attempting to elucidate the underlying mechanism and introduce proposed mechanisms. Then, we present our recent progress on the analysis of interfacial behavior of water in the vicinity of various biomaterials, in particular, force induced by water.

Keywords: 3 - 5 keywords
Antibiofouling, surface force, interfacial water, interface analysis

Introduction

Antibiofouling property is highly demanded in various applications, including medical devices (stents, artificial blood vessels, heart valves, etc.) and marine coatings (coating of ships and marine sensors). Although many small or polymeric molecules have been developed to tailor solid surfaces bioinert, the mechanism of the anti-biofouling property has not been fully understood. [1, 2] To understand the mechanism, we have analyzed interfacial interaction induced by anti-biofouling surfaces. Among them, the speaker would like to introduce the interactions induced by protein- and cell-resistant self-assembled monolayers (SAMs) and discuss the interactions responsible for their anti-biofouling property

Materials and Methods

We performed surface force measurements using atomic force microscopy equipped with a colloidal probe (Fig. 1). This method enables us to measure the interaction between two surfaces with high accuracy and sensitivity. We fabricated SAMs listed in Table 1 on a substrate (Si) and probe (silica) and measured force-distance curves in phosphate-buffered saline solution.

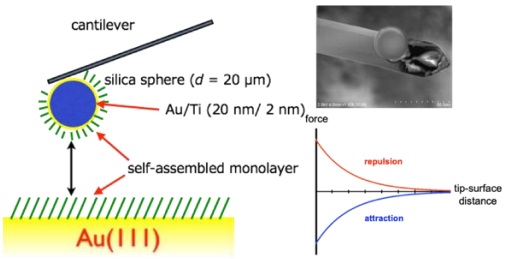

Figure 1. (left) Schematic illustration of surface force measurements using AFM equipped with a colloid-type probe (right) Scanning electron microscope image of a colloidal probe used for surface force and force-distance curves.

Table 1. Chemical structures of thiols used to fabricate SAMs in this work

abbreviation	Chemical structure
C8	$HS\text{-}(CH_2)_7\text{-}\mathbf{CH_3}$
EG3-OH	$HS\text{-}(CH_2)_{11}\text{-}\mathbf{(O\text{-}CH_2\text{-}CH_2)_3\text{-}OH}$
SA	$HS\text{-}(CH_2)_{11}\text{-}\mathbf{SO_3^-}$
TMA	$HS\text{-}(CH_2)_{11}\text{-}\mathbf{N^+(CH_3)_3}$
MC	SA + TMA
SB	$HS\text{-}(CH_2)_{11}\text{-}\mathbf{N^+(CH_3)_3\text{-}(CH_2)_3\text{-}SO_3^-}$

Results

The most important finding here is that we always observed water-induced repulsion between anti-biofouling SAMs (EG3-OH, MC, and SB). In sharp contrast, biofouling SAMs (C8, SA, and TMA) interacted attractively. [3-6] We also investigated surface forces for biomolecule (DNA and peptide)-based SAMs and found a clear correlation between water-induced repulsion and bioinertness (protein- and cell-resistance). [7, 8] These results strongly indicate that the interfacial water plays an essential role in anti-biofouling.

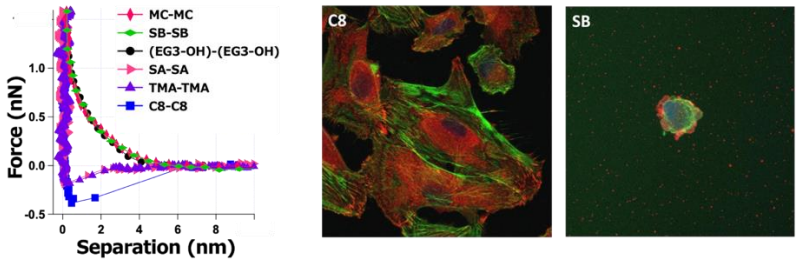

Figure 2. (left) Force-distance curves between SAMs measured on approaching in PBS (center & right) fluorescence microscope images of Human Umbilical Vein Endothelial Cells (HUVEC) on C8 and SB SAMs.

Conclusions

We found that the interfacial water in the vicinity of anti-biofouling SAMs of synthetic molecules and biomolecules plays a role of physical barrier to prevent biomolecules and cells' approach to the SAMs. Such findings may contribute to designs of biomaterials and a thorough understanding of smart molecular processes in biological systems.[9]

References

1. Tanaka, M.; Morita, S.; Hayashi, T. (2021) Role of interfacial water in determining the interactions of proteins and cells with hydrated materials. Colloids Surf B Biointerfaces 198:111449
2. Tanaka, M.; Hayashi, T.; Morita, S. (2013) The roles of water molecules at the biointerface of medical polymers. Polymer Journal 45:701-710
3. Hayashi, T.; Tanaka, Y.; Koide, Y.; Tanaka, M.; Hara, M. (2012) Mechanism underlying bioinertness of self-assembled monolayers of oligo(ethylene glycol)-terminated alkanethiols on gold: protein adsorption, platelet adhesion, and surface forces. Phys Chem Chem Phys 14:10196-206
4. Araki, Y.; Sekine, T.; Chang, R.; Hayashi, T.; Onishi, H. (2018) molecular-scale structures of the surface and hydration shell of bioinert mixed-charged self-assembled monolayers investigated by frequency modulation atomic force microscopy. Rsc Advances 8:24660-24664
5. Sekine, T.; Asatyas, S.; Sato, C.; Morita, S.; Tanaka, M.; Hayashi, T. (2017) Surface force and vibrational spectroscopic analyses of interfacial water molecules in the vicinity of methoxy-tri(ethylene glycol)-terminated monolayers: mechanisms underlying the effect of lateral packing density on bioinertness. J Biomater Sci Polym Ed 28:1231-1243
6. Sekine, T.; Tanaka, Y.; Sato, C.; Tanaka, M.; Hayashi, T. (2015) Evaluation of Factors To Determine Platelet Compatibility by Using Self-Assembled Monolayers with a Chemical Gradient. Langmuir 31:7100-5
7. Chang, R.; Asatyas, S.; Lkhamsuren, G.; Hirohara, M.; Mondarte, E. A. Q.; Suthiwanich, K.; Sekine, T.; Hayashi, T. (2018) Water near bioinert self-assembled monolayers. Polymer Journal 50:563-571
8. Kanayama, N.; Sekine, T.; Ozasa, K.; Kishi, S.; Nyu, T.; Hayashi, T.; Maeda, M. (2016) Terminal-Specific Interaction between Double-Stranded DNA Layers: Colloidal Dispersion Behavior and Surface Force. Langmuir 32:13296-13304
9. Kwaria, R. J.; Mondarte, E. A. Q.; Tahara, H.; Chang, R.; Hayashi, T. (2020) Data-Driven Prediction of Protein Adsorption on Self-Assembled Monolayers toward Material Screening and Design. ACS Biomater Sci Eng 6:4949-4956

Investigation of the electronic states of water in hydrate-melt

Nami Ueno[1], Masato Takegoshi [2] and Yusuke Morisawa[2]*

[1] Department of Analytical Chemistry and Radiochemistry, Innsbruck University,
[2] Faculty of Chemistry, School of Science and Engineering, Kindai University;
* Presenting author and Correspondence: morisawa@chem.kindai.ac.jp

There are series of studies investigated the FUV region of various molecules by ATR-FUV spectroscopy on the first electronic transition of liquid water in neat liquid, aqueous solutions of salts. The first electronic transition of water is observed in neat liquid at 157 nm by ATR-FUV. These studies show the electronic states of water were changed by ions in the solution and the changes in electronic states were reflected in the electronic transition of the solvents. In this presentation we will show the changes in electronic states of water in super concentrated aqueous electrolyte, called hydrate met using ATR-FUV.

Keywords: hydrogen bonding, hydrate melt, water in salt,

Introduction

Ultraviolet (UV) spectroscopy in the 145-200 nm region has recently been a matter of intense interest because many kinds of materials in the condensed phase. Rapid progress of the studies has been introduced by the development of attenuated total reflection spectroscopy in the FUV region (ATR-FUV), which has enabled us to measure the spectra in the complete Far-UV region for liquid and solid samples without facing problems such as peak saturation.1 Moreover, significant progresses of quantum chemical calculations for electronic excitation states of molecules improve our interpretations of the FUV spectra.2 There are series of studies investigated the FUV region of various molecules by ATR-FUV spectroscopy. 1-4 In the aqueous solution of alkali halides, charge-transfer-to-solvent bands of halide anions, I-, Br- and Cl- were observed in the region of 185-250, 175- 220, and 170-190 nm, respectively. Moreover, the effect of alkali cation (Li+, Na+, K+, Rb+ Cs+) on the first electronic transition of liquid water which is seen around 150 nm were studied by ATR-FUV spectroscopy. 3 We also have studied the changes in electronic states of polyethylene glycol by coordination with Li+ in the highly concentrated solution. 4 These studies show the electronic states of solvents were changed by ions in the solution and the changes in electronic states were reflected in the electronic transition of the solvents. In this presentation we will show results of ATR-FUV spectra of super-concentrated aqueous electrolytes (SAE) (>21 mol/kg), called hydrate melt (HM). These very concentrated aqueous solution have strong attention because Li-ion batteries used SAE as electrolyte have the high performance over 3.5V, although water is used as solvent. As a reason for a large potential window, Miyazaki et al. proposes that water's potential becomes higher than the counter anion when water coordinates to Li+ directly, using theoretical calculation. 4 We will have presented results of ATR-FUV spectra of SAE. We concluded that the band gap of water in SAE is very much enlarged by coordination with Li ion.

Results

This study aims to understand the electronic state of water molecules in HM by observing and analyzing the comparison with the ultra-pure water and the dependence on the concentration of Li salt and counter anion. Ultra-pure water shows a very broadband from 145 to 180nm, peak-top in around 157nm, and SAE also has a very broadband at 145 – 180nm, but table-top in 145 - 153nm is highest in this band and has a long tail to 180nm. Peak analysis using the second derivative found new bands in 151(water) and 149nm (HM). Dependence on the concentration of LiTFS, not included the electronic transition in the observation range, is investigated to clear the assignment of new bands. As a result, most affective bands into the spectra changes are varied with the concentration range of Li salt, $0 < \chi < 0.07$(range I), $0.07 < \chi < 0.15$(range II), $0.15 < \chi$ (range III). This correlation between the li salt concentration and spectra changes can be understood by the models that represented the number of water molecules surrounding the Li-ion. Additional experiments, comparison with

deuterated water and dependence on cations, are carried out to validate these models. Therefore, range-I, -II, −III is related to water's hydrogen-bonding condition, range-I reflects the changing of the number of the hydrogen-bonding between H_2O-H_2O, range-II is variation between the second-shell H_2O-H_2O, and range-III is the changes between the first-shell H_2O- first-shell H_2O. Finally, this study found the transition energy of water molecules of SAE is hugely higher than bulk water (A-X transition) because of the coordination with Li+ directly. However, it needs to compare the quantum chemical calculation to understand whether the blue shift's main reason is by the ground or excited state.

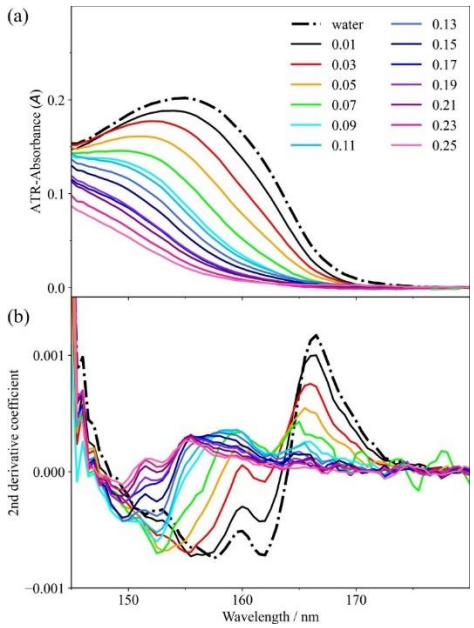

Figure 1. Use figure caption style. If there are multiple panels in the same figure, the figure legend contain description of each one for example: (a) Scores plot of PCA analysis; (b) Loading plots of PCA analysis.

Conclusions

We observed ATR-FUV spectra of HM and its dependences on concentration of Li salts. Absorption band of the first electronic transition of water in HM shows blue shift with increase of Li salts. These results shows that the band gap of water in SAE is very much enlarged by coordination with Li ion.

References

1. Y. Ozaki, S. Kawata, Far- and Deep-Ultraviolet Spectroscopy; Springer: Tokyo, 2015.
2. Y. Ozaki, Y. Morisawa, I. Tanabe, K. B. Beć, Spectrachim. Act. A. in press.
3. T. Goto, A. Ikehata, Y. Morisawa, N. Higashi, Y. Ozaki. "The Effect of Metal Cations on the Nature of the First Electronic Transition of Liquid Water as Studied by Attenuated Total Reflection Far-Ultraviolet Spectroscopy". Phys. Chem. Chem. Phys. 2012. 14(22): 8097–8104. doi:10.1039/c2cp40633k.
4. (a)N. Ueno, T. Wakabayashi, H. Sato, Y. Morisawa. "Changes in the Electronic Transitions of Polyethylene Glycol upon the Formation of a Coordinate Bond with Li+, Studied by ATR Far-Ultraviolet Spectroscopy". J. Phys. Chem. A. 2019. 123(50): 10746–10756. (b)N. Ueno, T. Wakabayashi, Y. Morisawa, "Determining the Coordination Number of Li+ and Glyme or Poly(ethylene glycol) in Solution Using Attenuated Total Reflectance–Far Ultraviolet Spectroscopy" Anal. Sci. 2020. 36: 723.
5. K. Miyazaki, N. Takenaka, E. Watanabe, S. Iizuka, Y. Yamada, Y. Tateyama, and A. Yamada, "First-Principles Study on the Peculiar Water Environment in a Hydrate-Melt Electrolyte", J. Phys. Chem. Lett. 2019, 10, 20, 6301–6305.

AQUAPHOTOMICS FOR FOOD QUALITY CONTROL

Food quality and process investigated through water absorption variations in NIR range

Tiziana M.P. Cattaneo[1,2] *

[1]Research Centre for Engineering and Agro-Food Processing, Council for Agricultural Research and Economics – Via G. Venezian, 26 – 20133 Milano, ITALY.
[2]PhD student, DAFNE, Tuscia University, Viterbo, ITALY.
* Presenting author and Correspondence: tiziana.cattaneo@crea.gov.it

The past two decades have seen much progress in water science with the establishment of a new common platform that can provide integration of knowledge. Aquaphotomics as a science was laid on a foundation provided by near infrared spectroscopy. The application of this holistic approach to food sector has been investigated by several groups of researchers. The usefulness of this discipline in understanding the role of water in food matrices has been already showed during the previous International and European Conferences. The aim of this presentation is to share recent results about the Aquaphotomics application to investigate the presence of food micro-components and to follow food dehydration processes, enlarging its application power in food sector.

Keywords: food, water absorption pattern, NIR

Introduction

The Aquaphotomics discipline has grown exponentially since 2005 [1]. NIR spectroscopy has been recognized for several decades as a useful technique in the study of the composition and quality of fresh and processed food, in particular fruit and vegetables [2], also if the combination of NIR and Aquaphotomics applied to food sector started about twelve years ago. In more recent years, several groups of researchers have used the information related to the modifications of the NIR response in aqueous systems [3] reflected through the variations in the water absorption profile [4]. This work aims to report recent Aquaphotomics applications in food sector with the scope to enlarge its use and suggest new application items.

Materials and Methods

Three different experiments are reported:

a. the investigation of the use of different salts during sturgeon caviar storage [6];
b. the evaluation of the efficiency of solar dehydration processes [7];
c. the continuous monitoring of sustainable food transformation processes [8].

The NIR spectra, in each trial, were collected in transflectance mode (spectral range: 900-1600 nm; 50 scans; 125 reading points) using a portable MicroNIR 1700 (VIAVI Solutions, Italy). The spectra pre-treatments were applied according to Tsenkova et al. [5]. Aquagrams, PCA, LDA and/or MBM (Moving Block Model) were then built up, depending on the goal.

Results

The main results are briefly reported for each experiment.

a. The goal was QC detecting the presence of preservatives in particular in organic products (borax in sturgeon caviar). The LDA applied to the validation set achieved high classification rates for both borax and no borax samples, based on the absorbance differences in the 1400-1430 wavelengths range. Differences in chemical structure between the two types of salt used allowed the detection of borax, due to its different hydration power, even if added in a small percentage.

b. The goal was the identification of the differences between two sustainable drying processes monitoring variations in water absorption pattern. LDA was performed on wavelegths selected by PCA: 1342, 1364, 1412, 1452, 1488 nm and allowed high discrimination between the two drying plants, with a respective correct prediction of 98% for plant 1, and 83% for plant 2.

c. In verifying the suitability of the use of Aquaphotomics for the continuous monitoring of a solar dehydration process, some critical points were identified: a) the positioning of the NIR probe; b) the working temperature and the NIR probe isolation; c) the sample size; d) the identification of the process end.

	Borax	**No Borax**
Borax	10	0
No Borax	0	12
Total	10	12
Correctly classified	10	12

Table 1. Classification matrix of the validation set (22 sturgeon caviar samples; 43 samples in classification matrix)

Conclusions

1. Aquaphotomics can be a fast useful tool for the identification of preservatives (such as sodium tetraborate) in food products (caviar batches).
2. These preliminary results suggested the use of Aquaphotomics, associated to NIR calibration for some chemical markers, in identifying the drasticity of different thermal processes in function of the final food quality.
3. The obtained results suggested the applicability of Aquaphotomics for the continuous monitoring of food drying processes using an adequate NIR probe.

References

1. Tsenkova, R. (2005) Visible-Near Infrared perturbation spectroscopy: Water in action seen as a source of information. In Proceedings of the 12th International Conference on Near-infrared Spectroscopy, Auckland, New Zealand, pp. 514–519.
2. Cattaneo, T.M.P., Stellari, A. (2019) Review: NIR Spectroscopy as a Suitable Tool for the Investigation of the Horticultural Field, Agronomy, 9, 9:503.
3. Muncan, J., Tsenkova, R. (2019) Review : Aquaphotomics - From Innovative Knowledge to Integrative Platform in Science and Technology. Molecules, 24, 2742.
4. Tsenkova, R. (2009) Aquaphotomics: Dynamic spectroscopy of aqueous and biological systems describes peculiarities of water. J. Near Infrared Spectrosc. 17:303–313.
5. Tsenkova, R., Muncan, J., Pollner, B., and Kovacs, Z. (2018) Essentials of aquaphotomics and its chemometrics approaches. Front. Chem. 6:363.
6. Brambilla, M., Buccheri, M., Grassi, M., Stellari, A., Pazzaglia, M., Romano, E., Cattaneo, T.M.P. (2020) The Influence of the Presence of Borax and NaCl on Water Absorption Pattern during Sturgeon Caviar (*Acipenser transmontanus*) Storage. Sensors, 20, 7174.
7. Cattaneo, T.M.P., Cutini, M., Stellari, A., Marinoni, L., Bisaglia, C., Brambilla, M. (2021) NIRS and Aquaphotomics for the Evaluation of the Efficiency of Solar Dehydration Processes, oral communication, Italian Symposium NIRItalia online "Waiting for Slovenia 2022", February 24-25, 2021.
8. Cattaneo, T.M.P. (2020) Non-destructive spectroscopic technologies applied to sustainable food transformation processes for monitoring the horticultural supply chain, 35th PhD cycle, EEE Dept., UNITUS, first year report, November 26, 2020.

Dairy products analysis – near-infrared spectroscopy and aquaphotomics approach

Stefka Atanassova[1,*], Dimitar Yorgov[1], Petya Veleva[1] and Todor Stoyanchev[2]

[1] Trakia University, Faculty of Agriculture, Stara Zagora, Bulgaria;
[2] Trakia University, Faculty of Veterinary Medicine, Stara Zagora, Bulgaria;
***** Presenting author and Correspondence: atanassova@uni-sz.bg

The results of several experiments, related to the application of near-infrared spectroscopy and aquaphotomics to study the degree of ripeness of white brined cheese and yellow cheese and discrimination of natural and imitation cheese and yogurt, will be presented.

Keywords: Cheese, yogurt, ripening, imitation dairy products, NIR, aquagram

Introduction

Dairy products are worldwide spread and have great commercial importance within the food industry. A rapid and reliable analysis of these products, including the determination of its chemical properties, ripening stage, adulteration and geographical origin, would be highly desirable both for the manufacturers and consumers. Near infrared (NIR) spectroscopy has been used as a method to predict the quality of different foods and real-time nondestructively monitoring of production processes due to the speed of analysis, minimal sample preparation and low cost [1,2]. Aquaphotomics added addition tools for spectroscopy analysis of food products [3].
The aim of this work was to assess the feasibility of NIR spectroscopy and Aquaphotomics to study the degree of ripeness of cheese and discrimination of natural and imitation cheese and yogurt.

Materials and Methods

Several experiment with white brine cheese, yellow cheese and yogurt were performed:

- Investigation of ripening process of Bulgarian white brine cheese and Bulgarian yellow cheese from cow milk, coagulated with cheese rennet and went through a process of ripening. Samples for spectral analysis were taken from first up to 74 days.
- Yogurt from cow milk (natural or mixed with 5, 10, 15 and 20% dry skim milk), prepared in laboratory conditions. The milk was pasteurized (95°C/30 min), cooled to 45°C, and inoculated with 1.5% yogurt culture consisting of *Lactobacillus delbrueckii ssp. bulgaricus* and *Streptococcus thermophiles*.
- Bulgarian white brine cheese - natural from cow milk, produced from mixture of cow milk and dry skim milk, imitation products with vegetable oil or produced with addition of hydrocolloids.

Spectra of all tested samples were obtained with a scanning NIRQuest 512 (Ocean Optics, Inc.) instrument in the range 900-1700 nm using reflection fiber-optics probe. A Pirouette 4.5 (Infometrix, Inc.) was used for performing spectral data processing. PLS models were developed for quantitative determination and SIMCA for classification. Aquagrams were calculated using transformed by MSC spectral data [3].

Results

Differences in near-infrared spectral data during ripening in the range of first overtone water region were found for both white brine cheese and yellow cheese samples. The biggest variation in spectral data were observed around 1368, 1417 and 1468 nm. The importance of this spectral region was confirmed by the analysis of the information from the models for classification of samples according to ripening stage and estimation of days of ripening. Aquagram pattern of cheese samples changed significantly in the process of ripening, showing changes in the water matrix.
Comparison of spectra of natural cheese or yogurt and imitation products, produced with adding a dry skim milk, vegetable oils or hydrocolloids also showed significant differences in the range of first overtone water

region. The models for discrimination of natural cheese or yogurt and imitation dairy products, based on spectral information in the region 1300-1550 nm, shower high accuracy.

Aquagrams of natural and imitation cheese or yogurt with additive of dry skim milk also showed significant differences. For example, aquagrams of white brine cheese samples from cow milk (natural and produced with adding hydrocolloids) with different water content were presented at figure 1. The aquagrams divided the samples into three groups according to augmented water content and differences in specific water molecular structures, caused by added hydrocolloid gums and their water retention properties.

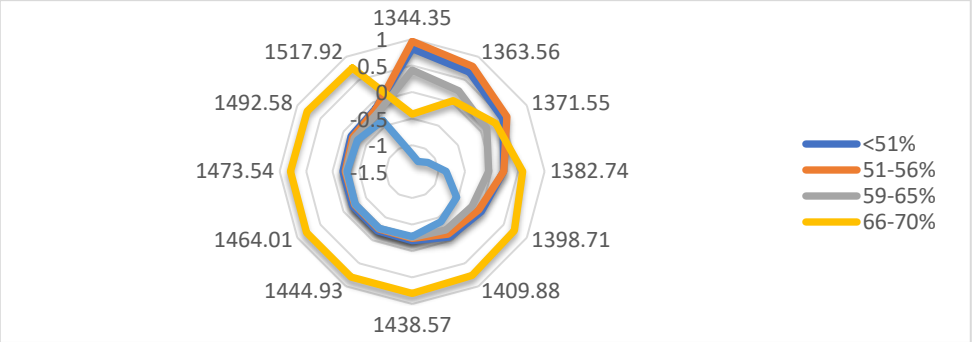

Figure 1. Aquagrams of white brine cheese samples from cow milk with different water content – natural and produced with adding hydrocolloids.

Conclusions

Differences in absorption spectra of natural and imitation dairy products and cheese at different ripening stages in the first overtone water region existed, which could be explained with different functionally structures of water in the investigated products. Near-infrared spectroscopy and aquaphotomics approach has a potential as a rapid screening tool for assessing cheese ripening and detecting the adulteration of dairy products.

Acknowledgement

This work was partially supported by the Bulgarian Ministry of Education and Science under the National Research Programme "Healthy Foods for a Strong Bio-Economy and Quality of Life" approved by DCM # 577 / 17.08.2018.

References

1. Yakubu H. G, Kovacs Z, Toth T and Bazar Ge (2020) The recent advances of near-infrared spectroscopy in dairy production—a review, Critical Reviews in Food Science and Nutrition, DOI: 10.1080/10408398.2020.1829540
2. De Marchi M, Penasa M, Zidi A, and Manuelian C. L. (2018) Invited review: Use of infrared technologies for the assessment of dairy products—Applications and perspectives. J. Dairy Sci. 101:10589–10604.
3. Tsenkova R (2009) Aquaphotomics: Dynamic spectroscopy of aqueous and biological systems describes peculiarities of water. J Near Infrared Spectrosc 17:303–313.

Recent Applications of Aquaphotomics in the Field of Food Science

Zoltan Kovacs[1,*], John-Lewis Z. Zaukuu[1], Zsanett Bodor[1], Balkis Aouadi[1], Flora Vitalis[1], Zoltan Gillay[1]

[1] Szent István University, Faculty of Food Science, Department of Physics and Control, Somlói street 14-16., 1118 Budapest, Hungary

***** Presenting author and Correspondence: Kovacs.Zoltan.food@etk.szie.hu

Keywords: near infrared spectroscopy, handheld spectrometer, authentication of food, food adulteration

Aquaphotomics, is a pioneer scientific discipline for exploring water molecular systems in nature. In food science, aquaphotomics has been acknowledged for food characterization in combination with near infrared spectroscopy (NIRS). As a molecular mirror, water aids to indirectly measure molecules by their spectral fingerprint in aqueous food systems. This presentation aims to highlight some recent progress of this technique in food science from both instrumental and application point of view.

From instrumental point of view, a handheld spectrometer (NIR-S-G1), produced by InnoSpectra Co. Taiwan proved to be a viable, affordable and reliable option that made it possible to measure liquids in a cuvette of 1 mm pathlength when it was modified by building an external light source and using a fiber optic cable to lead the light to the sample holder without heating it.

When the modified device was tested from application point of view with the aquaphotomics approach, classification of different origin Arabica and Robusta coffee drinks was possible with high accuracy using linear discriminant analysis (LDA) and quantification of the adulteration of Arabica coffee drinks with Robusta coffee drinks was also possible with good accuracy using the partial least squares regression (PLSR).

Structural changes of water as a result of adulteration made it possible to authenticate honey when samples from different botanical sources were mixed with rice syrup, self-produced sugar syrup and high fructose content sugar syrup. The level of adulteration could be predicted with high accuracy using PLSR.
NIRS and aquaphotomics were also successfully used to monitor germination time of mung bean and to predict the ascorbic acid content of the bean extract with high accuracy using PLSR.

Using benchtop spectrometers with the aquaphotomics approach, artificially manipulated low grade Tokaj wines with grape concentrate were clearly distinguished from the non-adulterated wines and high quality Tokaj wines with LDA. The concentration of the added grape concentrates in the low grade Tokaj wines could be predicted with high accuracy with PLSR.

Differently diluted aqueous solutions of paprika powder containing corn flour at different concentrations, showed that authentic paprika powder samples could be discriminated from its adulterated counterparts with high accuracy with LDA and the level of adulteration could be predicted with lower than five percent error with PLSR.

Multiple adulterants in tomato paste concentrate were correctly classified and quantified with lower than one percent error regardless of the type and number of applied adulterants.
Nine different concentrations of pork and beef meat mixtures could be classified with high classification rate with NIRS and aquaphotomics using LDA. The prediction of pork meat in beef meat was also possible with high accuracy using PLSR and the model presented prediction error as low as 1%w/w.
The recent studies of NIRS and aquaphotomics with the diverse variety of food matrixes prove the wide spectrum of applicability of the aquaphotomics approach in the field of food science.

Can Aquaphotomics Improve Quality Prediction of Intact Fruit?

Harpreet Kaur[1,*], Rainer Künnemeyer[2], and Andrew McGlone[1]

[1] The New Zealand Institute for Plant and Food Research Limited, Ruakura Research Centre, Hamilton, New Zealand;
[2] Dodd Walls Centre for Photonics and Quantum Technologies, University of Otago, Dunedin, New Zealand;
***** Presenting author and Correspondence: harpreet.kaur@plantandfood.co.nz

In our studies, we have explored aquaphotomics on simple aqueous systems, such as sucrose solution of various concentrations, kiwifruit juice, and finally on whole intact kiwifruit. Our analysis focuses on the first (1300 – 1600 nm) and the second (800 – 1100 nm) overtone regions of the OH stretch of water. For a simple aqueous system, water bands were identified in the first and second overtone regions that can explain water structure according to sugar concentration. The key question is: Can aquaphotomics help in developing better prediction models for intact fruit analysis? The partial least square regression (PLSR) model built in the second overtone region with 10 mm path length gave a standard error of prediction (SEP) of 0.11% which was comparable to the first overtone prediction using a 1 mm cell. This confirms that longer path-lengths are important for the short wavelength second overtone region and hence for solid samples such as kiwifruit, where light travels longer path lengths. The PLSR model built in the 800 – 1000 nm region (second overtone) gave a better result with a SEP of 0.41 % compared to 0.64% in the 600 – 1100 nm range implying that the important information exists in the tight window of the second overtone region.

Keywords: Fruit quality, Brix, Aquaphotomics, Aquagram

Introduction

Fruits like apples and kiwifruit whose quality parameters such as dry matter and Brix can be assessed non-destructively with near infrared (NIR) spectroscopy are more than 80% water. The NIR spectrum of fruit is dominated by water absorption peaks that shift and vary in shape with changes in quantities such as sugar content, temperature, etc. Aquaphotomics is a spectral analysis methodology that utilizes NIR spectroscopy and focuses on absorbance patterns related to water bands and the effect of perturbations due to variation in temperature, the concentration of solutes, environment, etc.[1] As the water peaks at 1450 nm (first overtone) and 970 nm (second overtone) in the samples vary due to soluble solids concentration (SSC), we investigated the aquaphotomics approach to learn more about changes in the water structure that are apparent in the 1300 – 1600 nm and 800 – 1100 nm wavelength regions. In the present study, we identified water bands for SSC variation in the first and second overtone regions. Models are built on aqueous samples using measurements from two transmission cuvettes of different path lengths, set to optimize the signal to noise for the first and second overtone region. We built calibration models for SSC prediction of kiwifruit juice at one temperature using measurements from an FT-NIR spectrophotometer. For intact whole fruit measurements, data were collected using a portable NIR spectrophotometer. Data modeling used PLSR and standard normal variate (SNV) pre-processing techniques.

Materials and Methods

A total of 100 Gold Kiwifruit "Actinidia chinensis" were purchased from New Zealand retail stores. Non-destructive NIR measurements were made on intact fruit, then the juice was extracted from squeezed endcaps. The juice was collected in Eppendorf tubes. FT-NIR analysis and reference measurements were performed at room temperature of 22 °C. For reference data, the SSC (°Brix) of the kiwifruit juice samples was measured by a digital refractometer (Atago Co. Ltd, Tokyo, Japan). Non-destructive NIR interactance measurements were acquired in the 300-1100 nm range using a handheld NIR instrument (F-750 Produce Quality Meter; Felix Instruments, Portland, USA) taking two separate measurements on opposite sides in the equatorial plane of each fruit. Transmittance spectra of the juice samples were measured at 22 °C (±1 °C) with an FT-NIR spectrometer (Tango, Bruker Corporation, Germany) equipped with a temperature-controlled holder. Two measurements were acquired for each juice sample using quartz cuvettes of 1 mm and 10 mm optical path length, respectively.

For each measurement, one spectrum, which was the average of 32 successive scans, was recorded for the range 870-2500 nm with a resolution of 16 cm^{-1}. Measurements with 1 mm and 10 mm path length cuvettes were also taken on Milli-Q water and sucrose solutions with SSC varying from 5 to 17.5 % with a step increase of 2.5 %. Predictive models were developed using MATLAB version R2018b (Math Works Inc., Natick, USA) and the PLS toolbox version 8.6.2 (Eigenvector Research Inc., Wenatchee, USA) with four-fold venetian blind cross-validation applied. The spectral data were pre-processed using SNV.

Results and Conclusions

Using a longer pathlength cell of 10 mm for second overtone region measurements (Fig 1(b)), the ambiguity of the water spectral pattern (WASP) compared to the 1 mm pathlength cell (Fig. 1(a)) is reduced. The aquagram in Fig. 1(b) illustrates that, as the sugar concentration rises, the number of strongly hydrogen-bonded water molecules (S2, S3, S4: water molecules with two, three, and four hydrogen-bonds, and (v1, v2): symmetrical stretching fundamental vibration) increases, resulting in highly organized water structures.

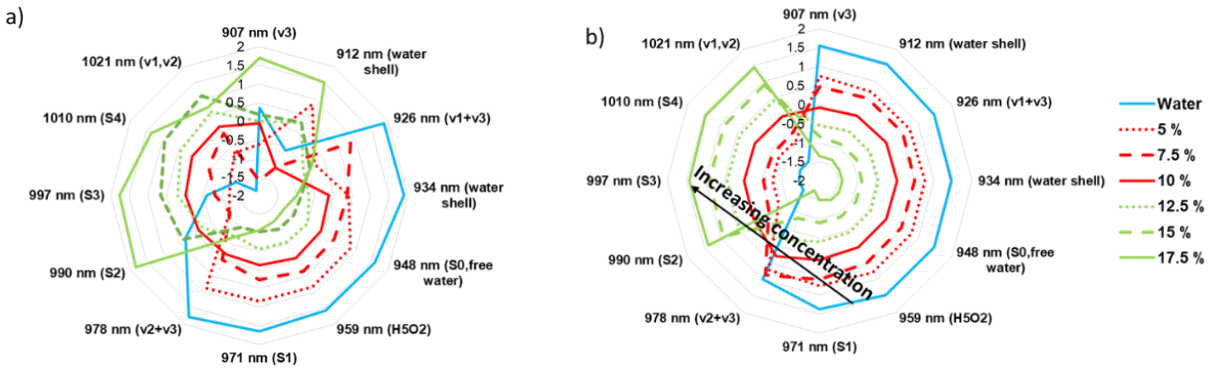

Figure 1. Aquagram of sucrose solutions in the second overtone region of OH stretch of water using a) 1 mm path length cuvette and b) 10 mm path length cuvette

There is an improvement in model performance for SSC prediction of kiwifruit juice with a 68% reduction in the standard error of prediction (SEP) when using the 10 mm path length cell measurements in the 870 – 1100 nm region (Table 1). Therefore, the path length of the sample cell is an important factor for improving aquaphotomics interpretation in short wave-NIRS because light has a longer penetration depth in this region. For the whole intact fruit, the PLRS model gives better results in the reduced 800 – 1000 nm region with a SEP of 0.41% in comparison to 0.64% in the 600 – 1100 nm region.

Table 1. Comparison of SSC prediction model performance for kiwifruit juice and for intact whole kiwifruit

PLS		**(N_{cal}=63 and N_{val}=33)**					
Pathlength/ Sample	**Wavelength range, nm**	**R^2_{cv}**	**RMSECV**	**R^2_p**	**RMSEP**	**Bias**	**SEP**
1 mm (Juice, FT-NIR)	1300-1600	0.99	0.13(± 0.01)	0.99	0.13(± 0.03)	0.02	0.13
	870-1100	0.94	0.31(± 0.04)	0.93	0.37(± 0.09)	0.09	0.35
10 mm (Juice, FT-NIR)	870-1100	0.99	0.13(± 0.02)	0.99	0.11(± 0.02)	0.01	0.11
Intact whole fruit (F-750)	600-1100	0.75	0.70(± 0.02)	0.79	0.65(± 0.09)	0.08	0.64
	800-1000	0.88	0.47(± 0.03)	0.91	0.43(± 0.06)	0.12	0.41

References

1. Tsenkova R, Munćan J, Pollner B, Kovacs Z. Essentials of Aquaphotomics and Its Chemometrics Approaches. Frontiers in Chemistry. 2018;6:363. doi: 10.3389/fchem.2018.00363.

WATER STRUCTURE - NEW INSIGHTS & IMPLICATIONS

Extending the spectrum: NIR spectroscopy of crystalline H_2O- ices

Christina M. Tonauer [1,*], Eva-Maria Köck [1], Christian W. Huck [2] and Thomas Loerting [1]

[1] Institute of Physical Chemistry, University of Innsbruck
[2] Institute of Analytical Chemistry and Radiochemistry, University of Innsbruck
***** Presenting author and Correspondence: christina.tonauer@uibk.ac.at

Keywords: high-pressure ice, polymorphism, cryo-conditions, NIR spectroscopy

Introduction

In the last four decades, the exploration of the solid part of water's state diagram has flourished. Within this timeline the structures of crystalline ices X - XIX have been resolved using diffraction methods. While these methods offer information on space group, size of unit cell and exact atom locations, infrared (IR) spectroscopy reveals the vibrational structure – with insights on chemical reactivity, e.g., after photoexcitation. After the pioneering works of Whalley and co-workers on mid-infrared (MIR) spectroscopy (4000-200 cm^{-1}) of ices I, II, IV, V, IX [1, 2], as well as the MIR studies of ices VII, VIII, X [3–5], no more work has been devoted to MIR characterisation of ice polymorphs. Moreover, the excitations in the near-infrared (NIR) range (10000-4000 cm^{-1}), that is, overtones and combination bands, of all ices, except for ice I_h [6], VI and VII [7], are unknown. The technique of NIR spectroscopy, however, is of high importance for the exploration of celestial bodies, since NIR waves pierce through interstellar dust, revealing objects lying behind. High-pressure ices make up the mantles of Saturn's and Jupiter's icy moons and are found on Earth in the form of diamond inclusions, and so NIR-spectroscopic data are highly desired.

Materials and Methods

High-pressure ices II, IV, V, VI, IX and XII were synthesized using the piston-cylinder setup established in the Loerting Lab. Quench-recovered samples were characterized using X-ray powder diffraction (CuKα1 radiation; diffractomer: Siemens D5000/Bruker D8 Advance). Near-infrared spectra were recorded at ambient pressure and liquid nitrogen temperature (~ 77 K), using a Büchi NIR Flex N-500 benchtop spectrometer in diffuse reflectance mode. Reflectance spectra were converted to Kubelka-Munk (K-M) function spectra. After baseline correction single spectra summed up and normalized to the corresponding maximum of K-M function. Peak centers and shoulders were identified by evaluation of first and second derivative spectra.

Results[8]

Here we present unprecedented spectroscopic data of crystalline H_2O-ices II, IV, V, VI, IX and XII in the near-infrared range. Fig. 1 depicts the NIR spectra of crystalline H_2O ices between 7800 and 4400 cm^{-1}. We want to highlight the blue-shift of the low-frequency wing (at ~ 6000 cm^{-1}) of the first overtone of the OH-stretching vibration (2 ν_{OH}; at ~ 6600 cm^{-1}), observed for high-pressure ices relative to low-pressure ice I_h.

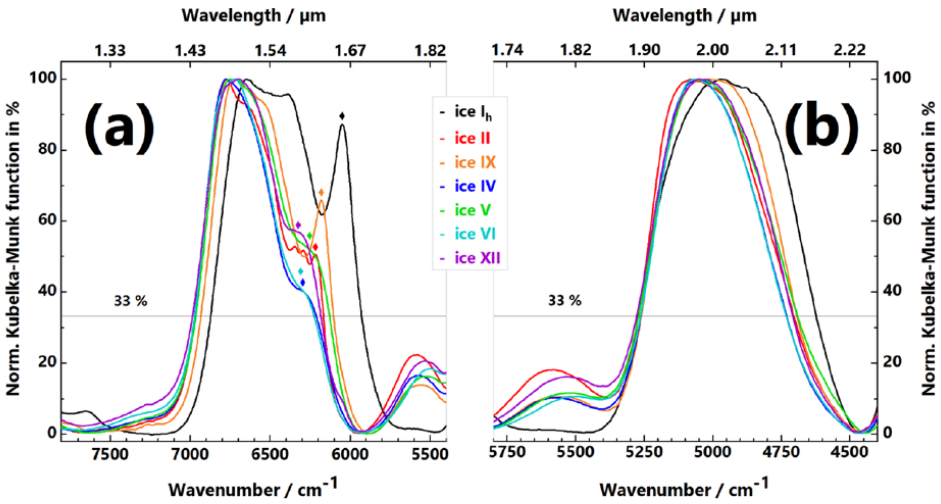

Figure 1. NIR spectra of ices I_h, II, IX, IV, V, VI and XII between (**a**) 7800-5400 and (**b**) 5800-4400 cm^{-1}.

Conclusions

The NIR-range (10000-4000 cm^{-1}) of high-pressure ices II, IV, V, VI, IX, XII was explored for the first time. Seven different overtone and combination bands for each ice polymorph could be assigned. The band at ~ 6000 cm^{-1} shows a correlation with (topological) density – the higher the wavenumber the higher the topological density of the high-pressure ice. Furthermore, the full width at one third of the maximum (FWTM) of the first overtone of the OH-stretching vibration (2 ν_{OH}) decreases with increasing density. Therefore, the 2 ν_{OH} band acts as an excellent marker for discrimination between different ices with different oxygen sublattices as well as discrimination between crystalline and different amorphous ices, which is subject to future work.

References

1. Bertie JE, Whalley E. Infrared Spectra of Ices Ih and Ic in the Range 4000 to 350 cm $^{-1}$. *J Chem Phys* 1964; 40: 1637–1645.
2. Bertie JE, Calvert LD, Whalley E. Transformations of Ice II, Ice III, and Ice V at Atmospheric Pressure. *J Chem Phys* 1963; 38: 840–846.
3. Hirsch K., Holzapfel W. Symmetric hydrogen bonds in ice X. *Phys Lett A* 1984; 101: 142–144.
4. Song M, Yamawaki H, Fujihisa H, et al. Infrared investigation on ice VIII and the phase diagram of dense ices. *Phys Rev B* 2003; 68: 014106.
5. Aoki K, Yamawaki H, Sakashita M, et al. Infrared absorption study of the hydrogen-bond symmetrization in ice to 110 GPa. *Phys Rev B* 1996; 54: 15673–15677.
6. Grundy WM, Schmitt B. The temperature-dependent near-infrared absorption spectrum of hexagonal H $_2$ O ice. *J Geophys Res Planets* 1998; 103: 25809–25822.
7. Kagi H, Lu H, Davidson P, et al. Evidence for ice VI as an inclusion in cuboid diamonds from high p-T near infrared spectroscopy. *Mineral Mag* 2000; 64: 1057–1065.
8. Tonauer CM, Köck E-M, Gasser TM, et al. Near-Infrared Spectra of High-Density Crystalline H $_2$ O Ices II, IV, V, VI, IX, and XII. *J Phys Chem A* 2021; 125: 1062–1068.

Water structure and water mirror effect in NIR region. A perspective from the quantum chemical simulations.

Justyna Grabska [1*], Krzysztof B. Bec [1] and Christian W. Huck [1]

[1] University of Innsbruck, Institute of Analytical Chemistry and Radiochemistry, Innrain 80-82, 6020 Innsbruck, Austria

***** Presenting author and Correspondence: Justyna.Grabska@uibk.ac.at

Keywords: Near-infrared spectroscopy, Carbohydrate, Vibration coupling, Hydration shell, Band assignment

Vibrational coupling between carbohydrates and the hydration shell was unveiled as the underlying mechanism that improves wavenumber-selectively the carbohydrate discrimination performance by near-infrared (NIR) spectroscopy. This effect has been previously identified as the "water mirror effect" and evidenced by empirical studies and observations [1]. It has been concluded in the literature as the driving factor behind the improved ability to detect the presence of an analyte in aqueous solution, because of its interaction with the surrounding water molecules [1]. Its existence, however, was only indirectly observed through its impact on analytical performance of NIR spectroscopy. In the present work, we took on the aim to obtain independent evidence and detailed insights into this fundamentally important phenomenon from quantum mechanical NIR spectra simulations [2]. A detailed information on the background of NIR spectra simulations is available in a recent review article [3].

The results of multivariate classification and quantification are interpreted by the theoretical ab initio simulation of the NIR spectra of the investigated carbohydrates and their first hydration shells. The simulation unveils that the water mirror phenomenon is vibration-selective and thus wavenumber-selective, and leads to an enhancement of the qualitative information contained in the specific spectral regions. The location of these regions and the related performance correspond fully to the appearance and magnitude of the cooperative vibration effect unveiled by multi-variate analysis (MVA).

The investigation into the effect of water mirror on the classification performance in low concentration of an analyte was based on NIR spectral measurement of six carbohydrates (fructose, glucose, mannose, ribose, xylose and sorbitol) in aqueous solution in different concentration levels. The limit of applicability of qualitative MVA analysis (discrimination between the six carbohydrates) was performed for two spectral regions (A: 6320-5564 cm-1; B: 4924-4096 cm-1; Fig. 1a) and two concentration levels (5 mg/mL, ~30 mmol/dm−3; and 20 mg/mL, ~100 mmol/dm−3). The applied methods included principal component analysis (PCA) and Linear Discriminant Analysis (LDA).

Subsequently, we investigated the manifestation of the water mirror effect in the limit of quantification and performance of various linear (PLSR, PCR) and non-linear regression methods (SVMR, GPR) and Artificial Neural Networks (ANNs). This was based on glucose in aqueous solution examined in a wide range of concentrations (1-200 mmol/dm−3).

Our investigation evidenced that the water mirror effect, understood as the vibrational coupling between the analyte (in this case, carbohydrate molecule) capable of forming hydrogen bonding with the solvent molecule (i.e., in this case, water) is vibration-selective and thus wavelength (wavenumber) selective. This picture obtained from the data independent from the experiment, spectra simulation, is fully consistent with the observations of the real-life systems. The improvement in selectivity of NIR spectra towards the solvated analyte (Fig. 1b; presented for qualitative analysis) appears only in those wavelengths, where this effect is observed (Fig. 1c). Therefore, we confirm the existence of the water mirror effect, and its role in enhancing the capability of NIR spectroscopy to sense lower concentrations of the hydrated analyte that it otherwise would be impossible without the vibrational cooperative effect between the analyte and the surrounding water molecules.

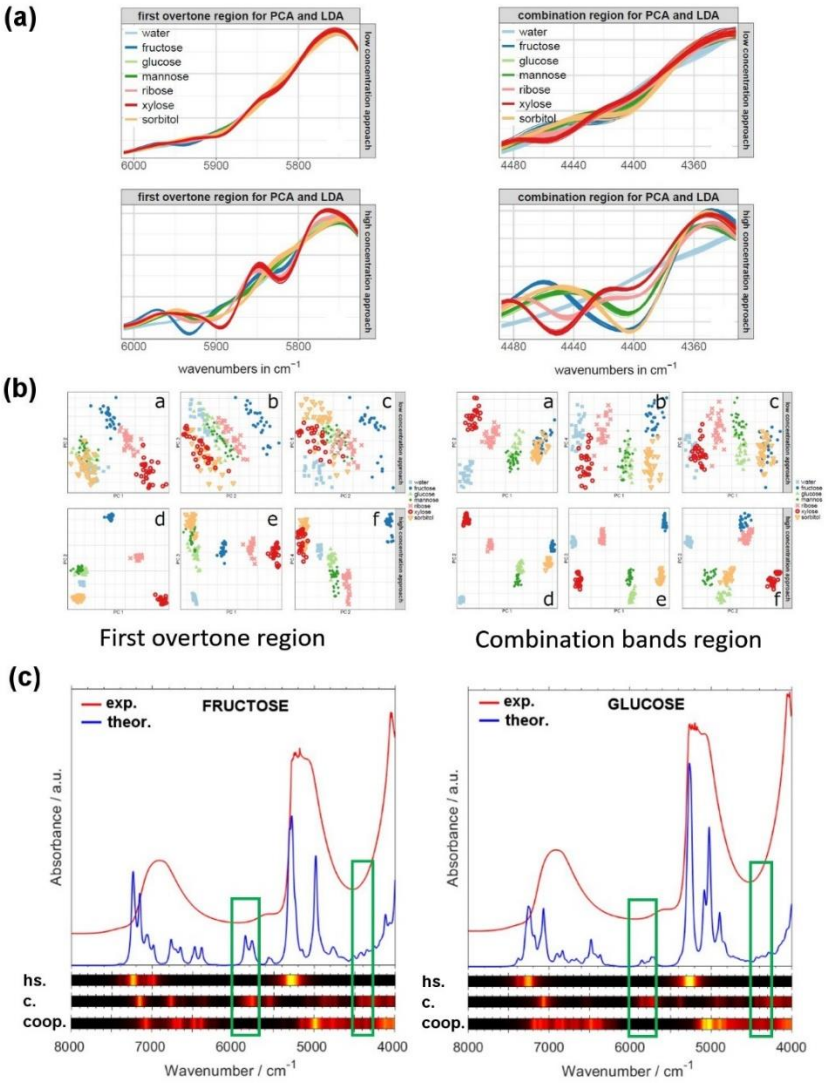

Figure 1. Cooperative effect in carbohydrate-water system (a) NIR spectra of carbohydrates in aqueous solution (top-5 mg/mL; bottom-20 mg/mL). (b) PCA plots (PC1 vs. PC2) presenting the corresponding discrimination performance. (c) Simulated spectra of the carbohydrate-hydration shell systems; pure vibrations of hydration shell (h.s.); pure vibrations of carbohydrate (c.); cooperative vibrations of carbohydrate and hydration shell (coop.).

References

1. Bázár, G, Kovacs Z, Tanaka M, Furukawa A, Nagai A, Osawa M, Itakura Y, Sugiyama H, Tsenkova R (2015) Water revealed as molecular mirror when measuring low concentrations of sugar with near infrared light, Anal. Chim. Acta, 896:52-62.
2. Beganović A, Beć KB, Grabska J, Stanzl MT, Brunner ME, Huck CW (2020) Vibrational coupling to hydration shell – mechanism to performance enhancement of qualitative analysis in NIR spectroscopy of carbohydrates in aqueous environment, Spectrochimica Acta A 237:118359.
3. Beć, KB, Huck, CW (2019) Breakthrough potential in near-infrared spectroscopy: spectra simulation. A review of recent developments. Front. Chem. 7: 48.

This work was supported by Austrian Science Fund (FWF): P32004-N28.

Detection of dissolved salts using the water spectrum

G.W.Steen[1], E.C. Fuchs[2] and H.L. Offerhaus[2,*]

[1] Wetsus, European Centre of Excellence for Sustainable Water Technology, Oostergoweg 9, 8911 MA Leeuwarden, The Netherlands;
[2] Optical Sciences Group, University of Twente, Postbus 217, 7500 AE Enschede, The Netherlands;
***** Presenting author and Correspondence: H.L.Offerhaus@UTwente.nl

Keywords: Optical absorption, spectroscopy, electrolytes, salts

Introduction

Dissolved ions interact with the water molecules surrounding them and thereby influence the (vibrational) motion of the water molecules. This can be detected as changes in the absorption spectrum of the water. These changes can also be seen in the overtones of the vibrational spectrum between 900nm and 1400nm. The changes are characteristic for different ions and can therefore be used to identify ionic content. The 900-1400nm window is a practical window that allows for the use of integrated optofluidic chips. However, the signals are quite weak at the overtones so that detection requires extensive control and very careful calibration.
In 2018 we characterized the influence of different salts on the vibrational overtones of the water spectrum [1] (see figure 1). We demonstrated that different salts have a different influence on the water spectrum so that the change in the water spectrum can be used to identify the salt. We used this knowledge to design optofluidic chips for the detection of the salts [2] and to further explore the identification of mixtures [3].

To quantify the effect of the salts on the water spectrum, the spectrum itself can be modeled using 4 Gaussian curves (each with a position, width and amplitude) and quantifying the changes to these curves that the salts induce to these 12 parameters. Each salt then represents a position in a 12-dimensional space. Additional information can be found when the temperature dependence of the effects is included. Disentangling mixtures of salts can be done by attempting to fit a measured spectrum by a combination of vectors and the temperature effect can be included for additional discrimination. We found that the influence of different salts on the water spectrum shows that the different salts influence each other but that this influence decreases with increasing temperature.

Materials and Methods

Transmission spectra were measured using Hellma cuvettes and a Shimadzu transmission-based spectrograph with a spectral resolution of 1 nm. The temperature of the light source was stabilized for one hour after which baseline spectra were recorded with the sample and reference cuvettes filled with 3 mL of demineralized water, both placed inside temperature-controlled holders set to 298.1 K. Five concentrations of aqueous electrolytes were prepared by serial dilution. The first one was made by replacing half of the demineralized water with 1.5 mL of 1 M stock solution, using a calibrated pipette. Subsequent concentrations were obtained by replacing half of the solution by demineralized water. The samples were allowed to thermally equilibrate and then measured. Stock solutions were prepared using commercial salts (Sigma-Aldrich), validated by chromatography and stored at 4°C in amber glass bottles. The effect of temperature on pure water was measured separately by raising the temperature in the sample arm, keeping the temperature in the reference arm constant.

Results

Figure 1 shows the absorption spectrum of water between 900nm and 1400nm and the (small) effect of 0.5M NaNO2. The differential absorption is converted to a differential absorbance and a deviation. Figure 1 also shows the differential absorbance for a full set of salts demonstrating their differences.

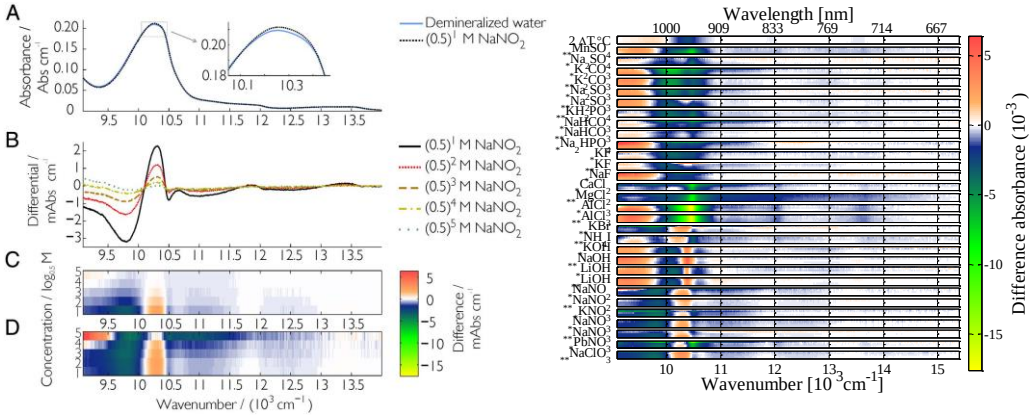

Figure 1. Left) A, Absorbance spectrum of demineralized water (blue circle) and _0.5_1 M NaNO2 dissolved in demineralized water (black square). B, Difference absorbance spectra of demineralized water and aqueous NaNO2, showing the effect of the dissolved salt at different concentration. C, A different representation of the effect of _0.5_1 M, _0.5_2 M, _0.5_3 M, _0.5_4 M, and _0.5_5 M dissolved salt: five 2D plots are stacked on top of each other with color coded absorbance difference. D, Multiplication of the difference absorbance spectra shown in C with the dilution factor of the electrolyte shows a deviation from the expected Beer–Lambert law, concentrations given in powers of (0.5). Right) 150 stacked 2D plots of the differential absorbance spectra for 30 salts tested at five different concentrations and a constant temperature of 298.15 _ 0.3 K. Deviations from Beer–Lambert law were observed even if the data is corrected using the dilution factor

The full absorption profile for demineralized water was characterized using four Gaussians (each with a center wavelength, a width and a relative amplitude). The twelve parameters create a 12-dimensional vector. After the salts are added the changes to the four parameters define a change in the 12D space that characterizes the differential absorption, that is particular to that salt. Once the characteristic differential absorption has been established, the effect of temperature on this differential absorption can be measured by changing the temperature. When we measured mixtures of salts it became clear that the (effect of the) salts (on the water vibration) interact, especially at higher concentrations, making it harder to disentangle a mixture. When we also measure the temperature dependence of the mixture this can be used to aid in the identification of the constituents.

Conclusions

We have characterized the changes in the water absorption in the 900-1400nm region (overtones of the water vibration) due to the presence of ions. We have looked at individual salts, their concentration and temperature dependence and at mixtures and their temperature dependence.

References

1. GW Steen, EC Fuchs, AD Wexler, HL Offerhaus, “Identification and quantification of 16 inorganic ions in water by Gaussian curve fitting of near-infrared difference absorbance spectra” Applied optics 54 (19), 5937-5942, http://dx.doi.org/10.1364/AO.54.005937
2. GW Steen, EC Fuchs, AD Wexler, HL Offerhaus “Design Considerations to Realize Differential Absorption-Based Optofluidic Sensors for Determination of Ionic Content in Water” IEEE Sensors Journal 18 (15), 6051-6058
3. GW Steen, AD Wexler, EC Fuchs, HA Bakker, PD Nguyen, HL Offerhaus “Role of temperature in de-mixing absorbance spectra composed of compound electrolyte solutions” Applied Optics 57 (27), 7871-7877

Abstract Title: Near Infrared and Aquaphotomic analysis of water absorption in lactate containing media

Nystha Baishya[1]

[1] Research Center for Biomedical Engineering, City, University of London, London, UK, EC1V 0HB;

***** Presenting author and Correspondence: Nystha.baishya@city.ac.uk

Keywords: Aquaphotomics, Lactate, Near Infrared Spectroscopy, Sepsis

Introduction

Sepsis is unobtrusive and one of the prominent causes of death around the world. The most recent spike in the cases is seen during the global pandemic happening right now because of COVID-19, where more than 2M deaths have been reported as in January 2021 [1]. Hence, there is a need for technology with the capability to continuously monitoring patients in intensive care and identify the onset of sepsis, which will enable clinicians to plan an optimum treatment strategy. According to the guidelines set by Surviving Sepsis Campaign in 2018, lactate levels in blood can serve as an early indication for the inception of sepsis and can be considered as a primary biomarker for the diagnosis of sepsis [2]. Therefore, there is an urgent need for a disruptive technology which can offer rapid, continuous, and non-invasive measurements of lactate in critical care environments. Hence, the motivation of this study was to establish Near Infrared (NIR) Spectroscopy as a possible alternative to existing methods and be used for non- invasive continuous monitoring of lactate. However, the dominant absorption of -OH overtone bands in the NIR poses a major challenge and complicates the accurate detection of lactate in this region for some aqueous systems. For this reason, comprehensive analysis of the -OH overtone bands with systematic lactate concentration changes in two different media has been investigated in this study.

Materials and Methods

The studies were conducted using state-of-the-art bench top spectrometers, for varying concentrations of lactate in different media (phosphate buffer saline (PBS) and whole blood) for in-vitro measurements. The spectra were collected using a Lambda 1050 (Perkin Elmer Corp, Massachusetts, USA) from 1200-1600 nm using an InGaAs detector for PBS samples and a 100 mm integrating sphere detector for whole blood samples. Preprocessing was performed in Matlab 2019b software (Mathworks, Massachusetts, United States). for both sets by spectral subtraction, Savitzky-Golay algorithm (Polynomial Order: 2, Derivative: 2 and Window Length: 71 for PBS and for whole blood samples) and Mean Scatter Correction.

Results

The work, thus far, reports on the analysis of NIR spectra of two aqueous systems of varying concentrations of lactate in saline and whole blood using the principles of Aquaphotomics. The results, as shown in Figure 1, show distinctive conformational and structural differences in lactate-water binding for both the aqueous systems [3]. The differences of the bonds could be manifested while predicting the concentrations of lactate, by multivariate analysis method, Partial Least Square, in both the aqueous systems, separately, as shown in Figure 2.

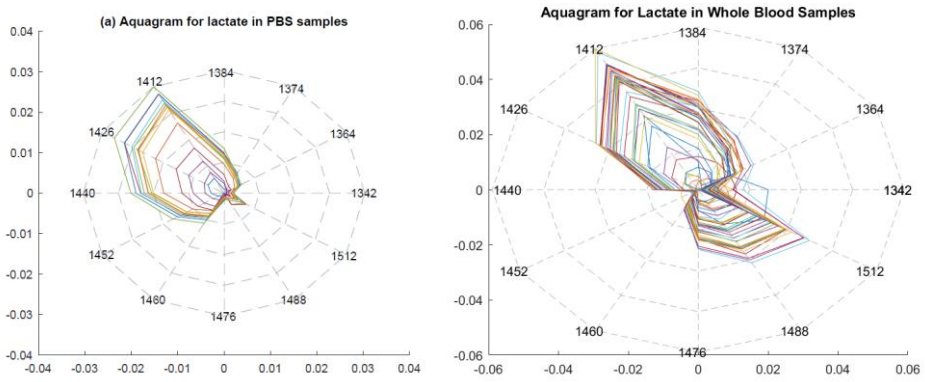

Figure 1. Aquagrams for aqueous systems of systemic variations in lactate: (**a**) in PBS; (**b**) in whole blood.

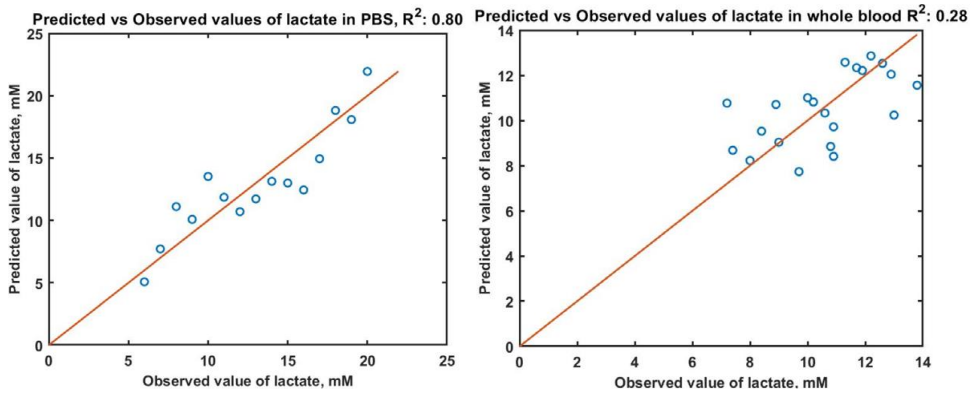

Figure 2. Concentration predictions of lactate: (**a**) in PBS (R2 =0.80); (**b**) in whole blood (R2 =0.28)

Conclusions

The research so far has comprehensively investigated the prominent Near Infrared (NIR) first OH overtone for systemic lactate concentrations in two aqueous media, namely saline and whole blood. This was performed to estimate the concentrations of lactate in-directly. It was found that there exist fewer lactate-OH molecular interactions in the PBS aqueous system, which activated lower wavelengths 1398-1418 nm in the Aquagram, (Figure 1 (a)). This was hence, affected by the concentration of the solute and could be determined with higher accuracy, with R2 of 0.80 (Figure 2 (a)). However, as shown in Figure 1 (b) and 2 (b), for the whole blood aqueous system, this was in fact the very opposite, with 1506-1516 nm wavelength activation and R2 of 0.28. Results from this study will assist in estimating lactate concentrations indirectly and to separate the presence of lactate in different media, which would be very crucial for in-vivo studies.

References

1. https://sepsistrust.org/
2. M. M. Levy, L. E. Evans, and A. Rhodes, (2018) “The Surviving Sepsis Campaign Bundle: 2018 update” Critical Care Medicine and Intensive Care Medicine, Special Edition, 44:925–928.
3. N. Baishya, M. Mamouei, K. Budidha, M. Qassem, P. Vadgama, and P. Kyriacou, (2020) “Near Infrared and Aquaphotomic analysis of water absorption in lactate containing media” 42nd Annual International Conference of the IEEE Engineering in Medicine and Biology Society (EMBC) in conjunction with the 43rd Annual Conference of the Canadian Medical and Biological Engineering Society.

WATER & OTHER BIOMOLECULES

The role of water activity in the thermodynamic response of lipid interphases

Cejas, J.[1] , O.A. Pinto[2], M.A. Frias[1] E. A. Disalvo[1]

1 Laboratorio de Biointerfases y Sistemas Biomiméticos, Centro de Investigaciones en Biofisica Aplicada y Alimentos (CIBAAL)(UNSE-CONICET). RN 9 Km 1125 Villa el Zanjón, Santiago del Estero, G4206XCP, Argentina.
2 Instituto de Bionanotecnología del NOA(INBIONATEC), Universidad Nacional de Santiago de Estero (UNSE), CONICET, RN 9 Km 1125, G4206XCP Santiago del Estero, Argentina.
*Correspondence to: disalvoanibal@yahoo.com.ar

Abstract

The consideration of water as a structural component gives biological membranes specific thermodynamic properties that explain its responsive behavior when chased by physical and chemical perturbations. These properties are derived from the peculiar surface tension of pure water and its variation due to the presence of hydrogen bonds arrangements between water and membrane components that determine a complex surface free energy profile.

In this regard, the intensive properties that act as driving forces are, at constant temperature, the surface pressure (surface tension) and the osmotic gradient (water chemical potential), which produce changes in its conjugated extensive properties such as membrane area and water content, respectively.

The formalism based on thermodynamics of irreversible processes (TIP) also allows to considered water –lipid and lipid-water friction to account for the exchange of water between the interphase and the bulk. Following this approach, the behavior of surface pressure vs. area per lipid isotherms are satisfactorily reproduced.

In addition, this formalism can also be applied to lipid vesicles subjected to an osmotic unbalance between the inner and the outer compartments. The water volume flux produces concomitant membrane expansion or compression and the same reasoning is applied.

This new approach for lipid membranes on thermodynamic grounds allows to overcome classical paradigms in the description of membrane structure and to compare the equivalence between lipid monolayers and bilayers as model systems.

Near infrared spectroscopy and multivariate analysis for the study of water in lipidic membranes

Jorge J. Wenz [1,2,*]

[1] Instituto de Investigaciones Bioquímicas de Bahía Blanca, UNS-CONICET, Bahía Blanca, Argentina;
[2] Departamento de Biología, Bioquímica y Farmacia, UNS, Bahía Blanca, Argentina.
* jwenz@criba.edu.ar

Keywords: Membranes; Water; Near Infrared Spectroscopy; Principal Component Analysis.

Introduction

The ability of near infrared spectroscopy to inform about the vibrations of the covalent O-H, by means of the first overtone of water around 1450/55 nm, was exploited to examine the water in membranes and the influence of the constitutive phospholipids on hydrogen bonding. The less the number and/or the strength of H-bonds, the more the strength of the O-H bonds and so they vibrate and absorbs radiation at higher frequencies. This shift is employed to evaluate the water status in membranes composed of two phospholipids having the same acyl chain but different polar head, the part of the molecule typically associated in the interaction with water.

Materials and Methods

Membrane production: solvent from phospholipids solution was removed with nitrogen flux while rotating the container, in order to obtain a thin film. MiliQ water was next added, vortexing and sonicating to form the vesicles, working at temperatures higher than the highest transition temperature of the lipids. NIR spectra and analysis: absorbance of the suspensions was registered in the 1100-2300 nm interval, between 13-58 °C every 5°C. Principal Components Analysis was employed to disclose the spectral changes [1].

Results

Figure 1 shows the sixty spectra, quite overlapped and unfeasible to discriminate according to phospholipid (DMPA or DMPC) or concentration (250 or 500 µM). Only the effect of temperature can be barely advised in some regions (shown by arrows). The localization of the first overtone of water (1450/55 nm) matches with previous reports [2-4]. The isosbestic region at 1425-1430 nm, is not far from the 1440-1442 nm reported by [5] and 1446 nm reported by [4] for pure water.

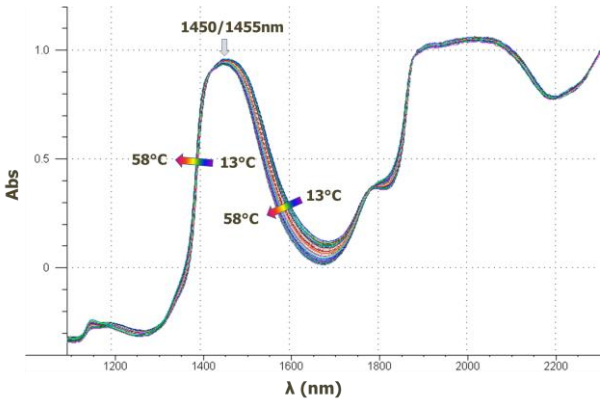

Figure 1. The sixty NIR spectra includes: two water control samples (Milli-Q), a sample of DMPA (1,2-dimyristoyl-sn-glycero-3-phosphate) and a sample of DMPC (1,2-dimyristoyl-sn-glycero-3-phosphocholine) at two concentrations (250 and 500 µM). All samples measured at ten temperatures (every 5°C in the 13-58 °C interval).

The simultaneous analysis of scores (Figure 2, left) and loadings (Figure 2, right) discloses useful information. Scores along PC1 capture the effect of temperature on the hydrogen bonding, whereas scores on PC2 capture the effect of phospholipids. By far, temperature in the assayed range is the dominating affecting factor (PC1 ≈ 97 %). As temperature increases, the differences in the effect of phospholipids become smaller, as series become closer at the highest temperatures.

Loadings reveal that increasing temperatures and the presence of phospholipids (particularly DMPC) weaken water H-bonds, as the O-H vibration band (first overtone) shift to higher frequencies, i.e. higher energy. As temperature increase, the absorbance increases at shorter (1391 nm) and it decreases at longer (1546 nm) wavelengths of the water band. To a lesser extent, phospholipids cause similar changes around 1385 and 1494 nm, respectively.

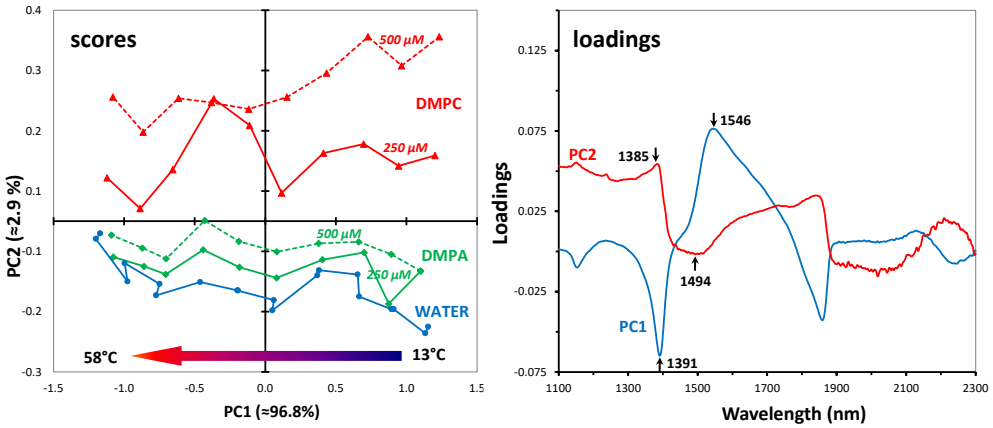

Figure 2. Output of the PCA, considering the first two PCs. Left panel: scores, where the connecting lines denote the evolution of samples with temperature, increasing from right to left every 5°C, as indicated by the arrow. Right panel: loadings plotted against the original variables.

Conclusions

As occurs with increasing temperature, DMPA and DMPC disrupt H-bonding in membranes, and the effect increases with the concentration.

Having identical acyl chain (myristoyl), the absence of OH in the polar head of DMPC may explain why it has a stronger disrupting effect on H-bonds than DMPA (OH acts as a H-bond donor).

References

1. Beeve KR, Pell RJ, Seasholtz MB (1998) Chemometrics: A Practical Guide1998, John Wiley & Sons, New York.
2. Maeda H, Ozaki Y, Tanaka M, Hayashi N, Kojima, T (1995) Near infrared spectroscopy and chemometrics studies of temperature-dependent spectral variations of water: relationship between spectral changes and hydrogen bonds. Journal of Near Infrared Spectroscopy 3:191-201.
3. McCabe WC, Subramanian S, Fisher HF (1970) Near-infrared spectroscopic investigation of the effect of temperature on the structure of water. The Journal of Physical Chemistry 74(25):4360-4369.
4. Segtnan VH, Sasic S, Isaksson T, Ozaki Y (2001) Studies on the structure of water using two-dimensional near-infrared correlation spectroscopy and principal component analysis. Anal Chem 73(13): 3153-3161.
5. Gowen A.A., Amigo jM, and Tsenkova R 2013) Characterisation of hydrogen bond perturbations in aqueous systems using aquaphotomics and multivariate curve resolution-alternating least squares. Anal Chim Acta 759: 8-20.

Understanding Hyaluronic Acid Induced Variation of Water Structure by Near-Infrared Spectroscopy

Qin Dong[1], Xueping Guo[2], Lian Li[1], Chen Yu[1], Lei Nie[1], Weilu Tian[1], Hui Zhang[1], Siling Huang[2] & Hengchang Zang[1,3,4,*]

[1] School of Pharmaceutical Sciences, Shandong University, Wenhuaxi Road 44, Jinan, 250012, China;
[2] Bloomage Biotechnology Corporation Limited, Tianchen Street 678, Jinan, 250012, China;
[3] Key Laboratory of Chemical Biology (Ministry of Education), Shandong University, Wenhuaxi Road 44, Jinan, 250012, China;
[4] National Glycoengineering Research Center, Shandong University, Binhai Road 72, Qingdao, 266200, China.
***** Presenting author and Correspondence: zanghcw@126.com

Keywords: Hyaluronic Acid, Near-Infrared Spectroscopy, Aquaphotomics, Water Structure

Introduction

Hyaluronic acid (HA) is a natural polysaccharide and one of the main components of the extracellular matrix. It is widely distributed in various tissues and organs of animals as well as the capsules of some bacteria, and plays a significant role in life process. Due to its high water retaining capacity, biocompatibility and non-immunogenicity, HA is an attractive material for various cosmetic, food and medical applications. Analysis of the hydration water in aqueous solution is challenging, and the structural changes in water induced by HA are yet to be fully understood. Near-infrared (NIR) spectroscopy, as a powerful analytical method, has unique advantages in studies of molecular structure and interaction. The proposal of Aquaphotomics provides a Venus-like foundation for studying the structure of water. The purpose of this study is to continue and extend the research on the hydration behaviors of HA, but particular attention is paid on investigating the water structure changes induced by HA. NIR spectra of water and aqueous HA solutions with a range of concentration were measured at different temperatures. Principal component analysis (PCA) was conducted on the spectra data to extract the information of different water species. Aquaphotomics was employed to analyze the effect of HA on water structure.

Materials and Methods

HA was provided by Bloomage Biotechnology (Jinan, China) with Mw of 7775 Da. Continuous concentration of HA solutions (1 mg/mL, 5 mg/mL and 10–100 mg/mL with a step of 10 mg/mL) were prepared.
All NIR spectra were recorded using Antaris II FT-NIR spectrometer (ThermoFisher scientific Inc., American) equipped with a 1 mm cuvette, tungsten-halogen light source, and InGaAs detector. The spectral range is from 10000 to 4000 cm−1 and the spectra are digitalized with 4 cm−1 intervals in Fourier transform. The temperature-dependent spectra of water and HA solutions were collected between 25 °C and 55 °C with 5 °C interval.
Spectra were imported into Matlab R2015a (The Math Works Inc., Natick, MA, USA), which was used for data transformation and processing. PCA was performed on spectral data of HA aqueous solution to extract information related to water changes and the reconstructed spectra were calculated accordingly. Then, a radar chart named aquagram was established to visualize water spectral pattern at different concentrations.

Results

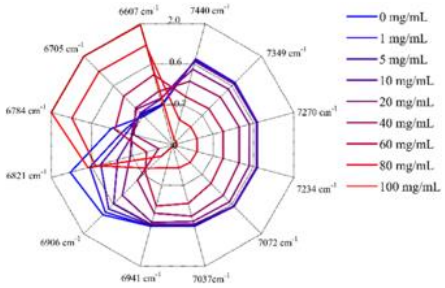

Figure 1. Concentration dependency of water spectral changes depicted by aquagram patterns at 25 °C.

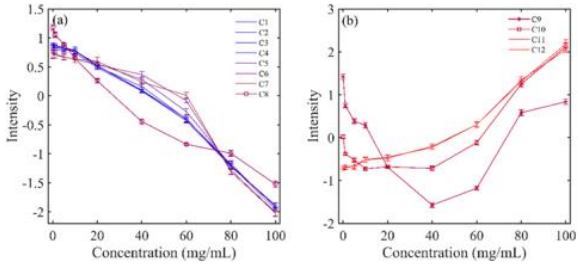

Figure 2. Intensity variation of different water species with different HA concentrations at 25 °C (a) for C1-C8 and (b) for C9-C12.

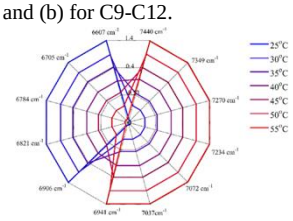

Figure 3. Temperature dependency of water spectral changes depicted by aquagram patterns in 100 mg/mL HA aqueous solution.

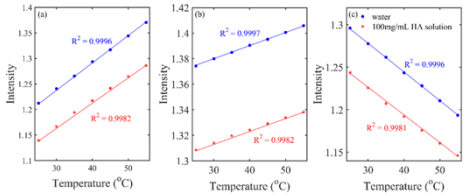

Figure 4. Variation of the peak intensity of S_0 (a), S_1 (b) and S_2 (c) in the reconstructed spectra of water and HA solution (100 mg/mL) with temperature. The solid lines were obtained by linear fitting.

Conclusions

The study found that HA acted as a structure maker to make water structure ordered in aqueous solutions and different water network was promoted at different HA concentrations. Meanwhile, HA had the function of improving the thermal stability of water structures. The results provide new information of HA hydration and possibly shed more light on the function of water in bio-systems.

References

1. Ozaki Y (2012) Near-infrared spectroscopy — its versatility in analytical chemistry. Anal. Sci. 28:545–563.
2. Cui X., Liu X., Yu X., Cai W. & Shao X. (2017) Water can be a probe for sensing glucose in aqueous solutions by temperature dependent near infrared spectra. Anal. Chim. Acta 957:47–54.
3. Dong Q (2019) Near-infrared spectroscopic study of molecular interaction in ethanol-water mixtures. Spectrochim. Acta Part A 222,117183.
4. Dong Q (2019) Analysis of hydration water around human serum albumin using near-infrared spectroscopy. Int. J. Biol. Macromol. 138,927–932.
5. Cui X., Cai W. & Shao X. (2016) Glucose induced variation of water structure from temperature dependent near infrared spectra. RSC Adv. 6:105729–105736.
6. Tsenkova R (2009) Aquaphotomics: dynamic spectroscopy of aqueous and biological systems describes peculiarities of water. J. Near Infrared Spectrosc. 17:303–313.

Details of glucose solution near-infrared band assignment revealed using deuterium oxide and glucose isotopes

Sae Tanaka1,2*, Roumiana Tsenkova2,3, Masato Yasui1,2,4

[1] Department of Pharmacology, Keio University School of Medicine, 160-8582 Japan
[2] Keio Advanced Research Center for Water Biology and Medicine, Keio University, 108-8345 Japan
[3] Department of Agricultural Engineering and Socio-Economics, Kobe University, 657-8501 Japan
[4] Keio Global Research Institute, 108-8345 Japan
***** Presenting author and Correspondence: sae-tanaka@keio.jp

Keywords: glucose, structural isomers, deuterium oxide, isotopes, specific rotation

Introduction

Carbohydrate is one of the most important materials in living organisms, and especially glucose is widely used in energy storing, cell structure and molecular recognition. Hexose like glucose has streochemical isomer, termed anomers, in aqueous solution and equilibrated glucose solution contains β-D-Glucose (~62%) and α-D-Glucose (~38%) (Figure 1). The stability of each anomer in solution is determined depending on hydrogen bonding with water molecules and is different from that in gas or crystal. In this study, to elucidate the difference of the water structure around each glucose anomer, we analyzed the near-infrared spectra of both glucose anomers using deuterium oxide and four glucose isotopes.

Materials and Methods

Sample α-D-glucose (purity > 96%, powder), D-glucose-1-d1 (purity > 99%, D enrichment >98%, powder), D-glucose-6,6-d2 (purity > 99%, D enrichment > 98%, powder), D-glucose-1-13C (purity > 99%, 13C enrichment > 99% powder), and D-glucose-1,2,3,4,5,6,6-d7 (purity > 99%, D enrichment > 97%, powder) were purchased from Sigma-Aldrich (St. Louis, MO, USA), and β-D-glucose (purity > 98%, powder) was purchased from Cayman Chemical (Ann Arbor, MI, USA). 200 mM sugar solution was prepared just before measurement.
Spectral acquisition A NIR spectrophotometer MPA (Bruker Optics, Ettlingen, Germany) was used for spectral acquisition. The NIR spectra were measured with cuvettes in the wavelength region of 12,000 cm^{-1} (833 nm) to 4,000 cm^{-1} (2500 nm) with 8 cm^{-1} intervals. A polarimeter RePo-5 (Atago, Tokyo, Japan) was used to acquire the optical rotation.
Data analysis Data analysis was performed with Pirouette software (Infometrix, Bothell, WA, USA). Spectral pretreatments of smoothing and first derivative were applied. Principal component analysis (PCA) and partial least squares (PLS) regression was performed.

Results

NIR spectra of α-D-Glucose and β-D-Glucose solution showed obvious difference and the difference in C-H region has a concentration dependency. On the PLS regression analysis with optical rotation, a linear regression model with a high accuracy was developed using near-infrared spectral data, and absorbance at 1,742 nm showed highest peak in regression vector (Figure 2). Moreover, absorbance at 1,742 nm had a strong correlation with the optical rotation after normalization for spectra, suggesting this absorbance reflects the structure of anomers and is useful for quantification of glucose anomers. To analyze the spectra more detail, we used deuterium oxide as solvent and four glucose isotopes as solute (Figure 3). Consequently, we found that difference spectra of glucose anomers in the region of 1,682–1,823 nm contains two glucose bands and a solvent water band. The two glucose bands are considered to originate from an exocyclic hydroxymethyl CH2 group and a CH group on the C1 carbon.

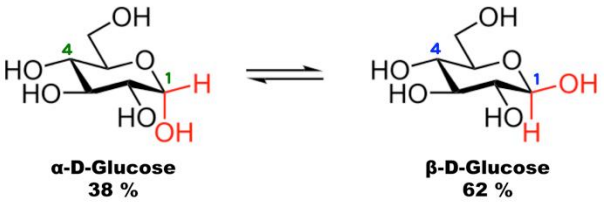

Figure 1. Glucose anomers

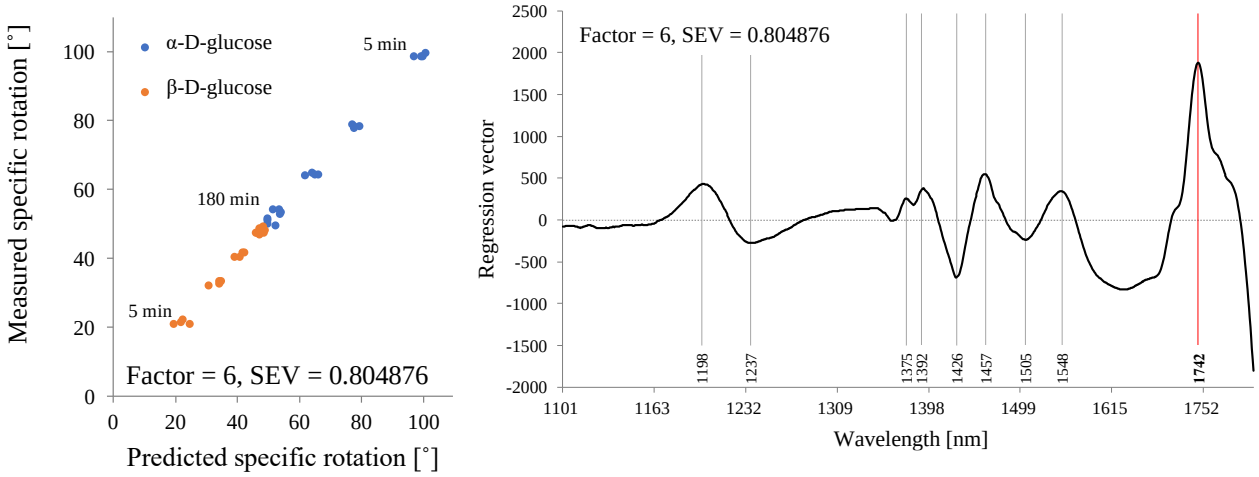

Figure 2. Regression analysis of optical rotation and near-infrared spectra

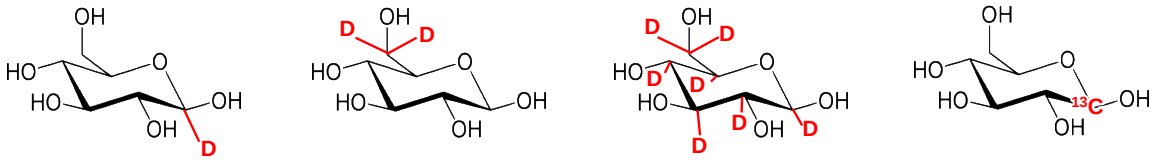

Figure 3. Glucose isotopes

Conclusions

In this study, detail of the spectra of glucose aqueous solution by using specific rotation, deuterium oxide and glucose isomers.

References

1. Tanaka S., Kojić D., Tsenkova R. and Yasui M., Quantification of anomeric structural changes of glucose solutions using near-infrared spectra. *Carbohydr. Res.*, 463:40-46. 2018,
2. Tanaka S, Tsenkova R, Yasui M., Details of glucose solution near-infrared band assignment revealed the anomer difference in the structure and the interaction with water molecules. *Journal of Molecular Liquids*, in press, 2020

WATER STRUCTURE & HYDRATION

Recent and Future X-ray Measurements of Pure Water

Craig Schwartz [1,*] and Richard Saykally [1,2]

[1] Lawrence Berkeley National Laboratory;
[2] University of California, Berkeley;
***** Presenting author and Correspondence: craigpschwartz@gmail.com

Despite the recent coronavirus pandemic, several interesting papers on liquid water at ambient and deeply supercooled temperatures as studied by X-ray techniques have been published. A recent spectroscopic study has provided evidence, based on a combination of X-ray Absorption, X-ray Emission and resonant inelastic X-ray scattering that water is fully consistent with a continuous model of water. Seemingly contradictorily, scattering data of deeply supercooled water showed maximum values in thermodynamic response and correlation functions, implying a phase transition in liquid water. This was then complemented by ultrafast melting of amorphous ice, which showed two distinct timescales and crystallization, suggesting a liquid-liquid phase transition. We will attempt to explain these seemingly contradictory results and propose new experiments which could sort out these results.

Keywords: X-ray Diffraction, Resonant Inelastic X-ray Scattering

Introduction

Recently, there have been tremendous improvements in X-ray spectrometers and X-ray sources. The improvement in spectroscopic methods has been employed by the group of Alexander Föhlisch using a variety of techniques to try to understand the structure of liquid water and supporting it as a continuous model.(Niskanen et al. 2019) The group of Anders Nilsson recently used XFELs to show anomalous properties of supercooled water which appear to support a liquid-liquid phase transition in the deeply supercooled regime in two different ways. First his group examined the thermodynamics of deeply supercooled liquid water droplets (Kim et al. 2017) and subsequently they used an ultrafast laser pulse to heat amorphous ice (Kim et al. 2020). These papers, their implications and possible follow up studies will be discussed.

Materials and Methods

The measurements detailed here were taken using standard X-ray techniques at a synchrotron (spectroscopy measurements) and X-ray free electron lasers (scattering measurements). Temperature was controlled in the X-ray free electron laser measurements by either evaporatively cooling droplets or by heating the amorphous solid with an ultrafast laser pulse.

Results

Based on a series of X-ray spectroscopy results, (X-ray absorption, X-ray emission, resonant inelastic X-ray scattering(RIXS)), Alexander Föhlisch and coworkers found water at ambient conditions to be entirely consistent with a single distribution of water molecules.(Niskanen et al. 2019) For instance, as shown in Figure 1 the RIXS data can be fit with a single distribution. In contrast, recent results by Nilsson (Kim et al. 2017, 2020)and coworkers have shown properties that are better explained by a two-state model of water, including maxima in thermodynamic properties. This is shown in Figure 2. This is further complemented by a recent study from the same group where they laser heated amorphous ice, and the ice went through a short-lived metastable intermediate before crystallizing, strongly supporting a liquid-liquid phase transition. The differences in these two studies will be discussed.

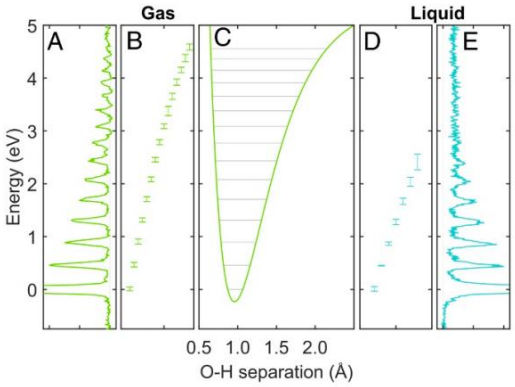

Figure 1. Resonant inelastic X-ray scattering data from gas phase and ambient liquid water. Both can be fit with a single morse potential, providing evidence for a single continuous distribution of water. From (Niskanen et al. 2019)

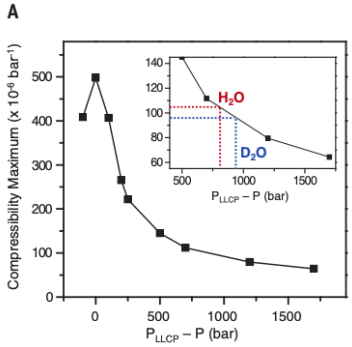

Figure 2. Compressibility of liquid water as a function of pressure difference from the believed liquid-liquid critical point. Significantly, it shows a maximum value, providing evidence for a two-state model of water being necessary. From (Kim et al. 2017)

Conclusions

These recent X-ray studies provide seemingly contradictory results about the nature of liquid water. While these studies did occur at significantly different temperatures and conditions, it does pose a challenge for our understanding of liquid water. If there are two states of water, particularly at supercooled temperatures, it should be possible, at least in principle to determine what this second state of water would be. Some possible method will be briefly discussed.

References

1. Kim KH, Amann-Winkel K, Giovambattista N, et al (2020) Experimental observation of the liquid-liquid transition in bulk supercooled water under pressure. Science (80-) 370:978–982. https://doi.org/10.1126/science.abb9385
2. Kim KH, Späh A, Pathak H, et al (2017) Maxima in the thermodynamic response and correlation functions of deeply supercooled water. Science (80-) 358:1589–1593. https://doi.org/10.1126/science.aap8269
3. Niskanen J, Fondell M, Sahle CJ, et al (2019) Compatibility of quantitative X-ray spectroscopy with continuous distribution models of water at ambient conditions. Proc Natl Acad Sci U S A 116:4058–4063. https://doi.org/10.1073/pnas.1815701116

Concentration-Dependent Near-Infrared Spectra of Water-Aprotic Organic Solvents Binary Systems

Shigeaki Morita [1,*]

[1] Department of Engineering Science, Osaka Electro-Communication University;
***** Presenting author and Correspondence: smorita@isc.osakac.ac.jp

Concentration-dependence of binary liquid mixtures using water and aprotic organic solvents such as acetonitrile (MeCN) was investigated by means of near-infrared (NIR) spectroscopy. A higher wavenumber contribution in the first overtone of the O-H stretching arising from water was observed by adding MeCN, while a lower wavenumber contribution by pyridine (Py). These results will be discussed in detail.

Keywords: multivariate curve resolution (MCR), partial molal volume, donor number

Introduction

Fundamental and overtones of the O-H stretching vibration of molecules which containing hydroxy group in the structure are known to be sensitive to hydrogen-bonds structures via the hydroxy groups. Hydrogen-bonds structures in water have also been discussed based on vibrational spectroscopy such as infrared spectroscopy, Raman scattering spectroscopy and near-infrared (NIR) spectroscopy.1,2 In the present study, hydrogen-bonds structures of binary liquid mixtures using water and aprotic organic solvents, e.g., acetonitrile (MeCN), were investigated by means of NIR spectroscopy.

Materials and Methods

Two independent solvents were mixed and pumped by a liquid chromatograph (LC) having a gradient mixer. The mixed sample was sent to a flow cell in a NIR spectrometer. A mixing ratio of the binary liquid mixture was controlled as a function of time by the LC-NIR system. Concentration-dependent NIR spectra were collected automatically at a constant time interval. A mole fraction of water in the mixture □ was checked and calculated by mass of the mixture. The density of the mixture was independently measured by a pycnometer after the spectroscopic observations.

Results

Figure 1 shows concentration-dependent NIR spectra of binary liquid mixtures of MeCN + water in the first overtone region of the O-H stretching. Red and blue lines in the figure represent NIR spectra of neat MeCN ($\phi = 0$) and neat water ($\phi = 1$), respectively. Gradual increase of the signal in the region as a function of water content ϕ shows change in the spectral waveform. This spectral waveform variation was analyzed based on multivariate curve resolution (MCR) and at least two independent components were identified by the analysis. A higher wavenumber contribution was observed by adding MeCN, while a lower wavenumber contribution by pyridine (Py).

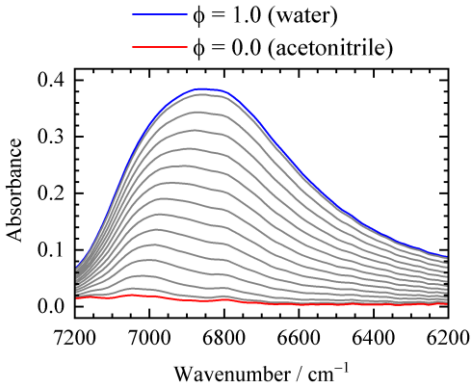

Figure 1. Concentration-dependent NIR spectra of binary liquid mixtures of acetonitrile and water. Red and blue lines represent neat acetonitrile (f = 0) and neat water (f = 1), respectively.

Conclusions

Spectral waveform variations in the first overtone of the O-H stretching region were observed by adding aprotic organic solvents to water.

References

1. Tanaka M, Morita S, Hayashi T (2021) Role of interfacial water in determining the interaction of proteins and cells with hydrated materials. Colloids and Surface B: Biointerfaces 198:111449-111457.
2. Morita S, Tanaka M (2014) Effect of sodium chloride on hydration structures of PMEA and P(MPC-*r*-BMA). Langmuir 30:10698–10703.

Highly precise characterization of the hydration state upon thermal denaturation of globular protein

Keiichiro Shiraga [1,2,*], Mako Urabe [2], Takeshi Matsui [2], Shojiro Kikuchi [3] and Yuichi Ogawa [1]

[1] Graduate School of Agriculture, Kyoto University;
[2] RIKEN Center of Integrated Medical Sciences (IMS);
[3] Department of Reverse Translational Research, Hyogo College of Medicine;
* Presenting author and Correspondence: shiraga.keiichiro.3a@kyoto-u.ac.jp

Keywords: Hydration number, complex dielectric constant, thermal denaturation of globular protein

Introduction

Biochemical processes are inherently built on molecular fluctuations, bathed in the flexible and dynamic hydrogen bond (HB) network of liquid water. It is well known that at least a single layer of water molecules surrounding the protein surface yields the biological functionality of proteins, and dehydrated enzymes lose their activity. In fact, the rigidity of the water HB networks correlates with the flexibility of the protein side-chains that are directly related to the protein activity. However, even when hydrated, protein turns to a glassy-like state and as such its biological functions are suppressed below −70°C. This fragile-to-strong dynamical transition arises from the interplay with hydration water in the vicinity of the protein surface, because reduced water mobility in turn inhibits protein side-chain motions. At high temperatures, the second dynamical transition commonly referred to as the thermal denaturation, is observed. Unlike the first transition at low temperatures, the second transition lets the protein to unfold its conformation irreversibly but how hydration water is engaged in this process is not yet fully understood. In this study, we aimed to quantitatively characterize the number of hydration water upon thermal denaturation of human serum albumin (HSA), based on a state-of-art CMOS dielectric sensor operating at 65 GHz.

Materials and Methods

The CMOS dielectric sensor embedding 65 GHz LC resonator structures, manufactured by Sharp Corporation, was used in this study. Because the electric field is localized within several dozens of micrometers from the chip surface, each resonator feels the effective capacitance C_{eff} that includes the contribution from the passivation layer and the sample placed on it. Assuming a dielectric sample with a complex dielectric constant at 65 GHz resting upon the resonator, the LC oscillation frequency f is consequently described as

$$f = \frac{1}{2\pi\sqrt{L_0 C_{\mathrm{eff}}}} = \left[2\pi\sqrt{L_0\left\{C_0 + C_1\frac{C_1C_2 + {C_2}^2 + {G_2}^2}{(C_1 + C_2)^2 + {G_2}^2}\right\}}\right]^{-1} \quad (1)$$

where, $C_2 = C\varepsilon'$and $G_2 = C\varepsilon''$ (C: constant) are the capacitance and conductance of the sample, respectively [1]. Eqn. (1) indicates that f undergoes a low-frequency shift in the presence of the sample, demonstrating the potential of this sensor as a quantitative index to estimate the complex dielectric constant of the sample at 65 GHz. The rear surface of the sensor was attached to a Peltier control unit so as to vary the sample temperature from 25°C to ~ 80°C, at nearly regular intervals, in a stepwise manner and then similarly reversed to 25°C, with the aim of examining the temperature dependence of f.

Results and Discussions

As presented in Fig. 1(a), $\Delta f(T) = f_{\mathrm{BKG}}(T) - f(T)$ (where, f_{BKG} is the oscillation frequency without a sample) of pure water undergoes a monotonous upshift with temperature, and the reversed route is perfectly followed when cooling. In contrast, the 10 wt% HSA solution heated up to ~ 80°C obviously exhibits hysteresis behavior, showing smaller $\Delta f(T)$ in the recovery process (open circles) compared with that in the forward (closed

circles). The measured frequency shifts $\Delta f(T)$ of pure water and the HSA solution at each temperature were then converted to the bulk water ratio based on our novel algorithm, and finally, the hydration number N_{hyd} was determined. As summarized in Fig. 1(b), N_{hyd} monotonously increases as raising temperature with a huge jump at around 55°C where the helical-rich secondary structure of HSA starts to fall apart. The rapid rise in N_{hyd} perfectly in phase with replacement of α-helices with water-exposed extended chains clearly declares that hydration to exposed backbone and side-chains is responsible for the increased N_{hyd} when a globular HSA moves to a thermally denatured form. In other words, the increased amount of hydration water should be the result of protein unfolding. Meanwhile, Mallamace and his co-workers experimentally revealed that subtle enhancement of hydration water mobility due to weakened HBs at high temperatures lets protein to unfold, due to conformational flexibility of backbone and side-chains [2]. These complementary evidences lead to the conclusion that the loosened hydration shell upon heating triggers thermal denaturation by increasing conformational entropy of protein, and the hydration number N_{hyd} is increased as a consequence. Nevertheless, the highly stable hydration shell consisting of a minimum quantity of water molecules around native protein is disappeared and becomes more unstable upon thermal denaturation, owing to less restricted exposed backbone and side-chains.

The slight increase in N_{hyd} below 55°C may have its roots in the overall expansion involving growth of solvent-accessible surface area (SASA) while keeping the native secondary structures. With regard to the recovery process from ~ 80°C to 25°C, the downward trend in N_{hyd} via a different path from the heating process is undoubtedly ascribed to irreversible thermal denaturation. This is not the case with reversible unfolding by heating up to 45°C, where the hydration number traces its forward path. In the recovery process, the constant hydration number around 3700 turned to decline with $T \approx 55$°C as a boundary, at the similar rate to that in the forward process. Since the secondary structure content is kept at constant values in this temperature range, the observed decrease of N_{hyd} may be attributed to reduction in SASA without restoring the native secondary structure.

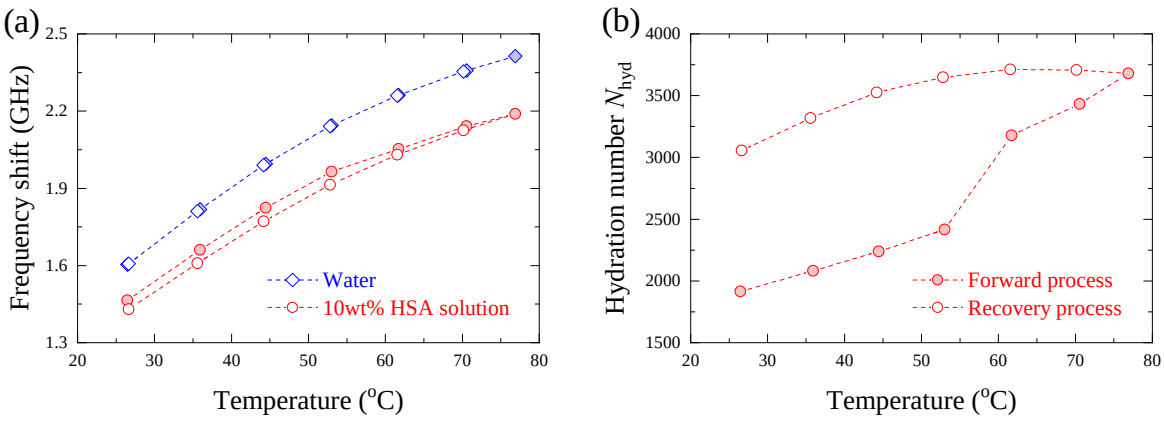

Figure 1. (a) Temperature dependence of the frequency shift $\Delta f(T)$ of pure water and the 10 wt% HSA aqueous solution when the sample temperature shifts step-by-step up to nearly 80°C. Closed and open symbols represent the heating and cooling processes, respectively. (b) Derived hydration number as a function of temperature, $N_{\mathrm{hyd}}(T)$, of the 10 wt% HSA aqueous solution.

References

1. Shiraga K, Urabe M, Matsui, T, Kikuchi S, Ogawa Y (2020) Highly precise characterization of the hydration state upon thermal denaturation of human serum albumin using a 65 GHz dielectric sensor. Phys Chem Chem Phys 22:19468–19479.
2. Mallamace F, Corsaro C; Mallamace D, Cicero N, Vasi S, Dugo G, Stanley H. E. (2015) Dynamical changes in hydration water accompanying lysozyme thermal denaturation. Front Phys 10: 1–7.

Study on the dynamic state of free, hydrogen-bonded water with wood by near-infrared hyperspectral imaging

Te Ma[1], Tetsuya Inagaki[1] and Satoru Tsuchikawa[1,*]

[1] Graduate School of Bioagricultural Sciences, Nagoya University
***** Presenting author and Correspondence: st3842@agr.nagoya-u.ac.jp

This work was aimed to provide a rapid and nondestructive imaging method for visualizing the dynamic state of free, hydrogen-bonded water with lignocellulosic material. Near-infrared (NIR) spectral images in the wavelength range 1002–1847 nm was firstly used to visualize the distributions of moisture content (MC) over the surface of Japanese cedar by partial least square regression. Then, principal component analysis and curve fitting methods were utilized to explore the changes in water-wood structure characteristics based on peak shifts to longer wavelength in spectral signals caused by increasing MC. The experimental results were clear showing that the earlywood regions have higher MCs in the initial stage of drying, but their free water evaporates more rapidly than that in other regions. Furthermore, the edge of the samples dried most rapidly into strongly bonded water. It is concluded that NIR hyperspectral imaging has the potential to be a complementary methodology for studying the transient changes of wood-water interactions.

Keywords: Lignocellulose, air drying, dynamics state of free and hydrogen-bonded water, near-infrared hyperspectral imaging, principal component analysis

Introduction

Wood is a natural hygroscopic material able to exchange water molecules with its surrounding environments. Water in wood is generally classified as free and bound water (where hydrogen bonds with the cell walls of wood). The latter has profound effects on the properties of wood, causing it to shrink, swell, and crack[1]. Monitoring the dynamic state of water molecular structure in wood is challenging, but important both for theoretical studies and industrial applications. Near-infrared (NIR; wavelength range: 800–2500 nm) spectroscopy is a proven method for evaluating simple water content by mass and effectively determining its molecular dynamics, since vibrational NIR spectra contain information about the light absorbance of oxygen and hydrogen (O–H) structures in the analyzed samples[2]. However, conventional NIR spectrometry based on point measurement is not suitable for spatially resolved relaxation analysis. NIR hyperspectral imaging (HSI) is an appropriate technique for capturing a large number of images at different wavelengths and provides a spectrum at each pixel, thus enabling comprehensive evaluation across the entire sample surface. This study aims to visualize the dynamics of free and hydrogen-bonded water in three typical wood samples which have fundamental differences among their anatomical structures.

Materials and Methods

Twelve samples [5 mm (longitudinal) × 12 mm (tangential) × 24 mm (radial)] were cut from wood blocks of Japanese cedar (Cryptomeria japonica), beech (Fagus sylvatica), and Manchurian ash (Fraxinus mandshurica). In order to prepare the wood in a water-saturated state, all samples were immersed in distilled water under vacuum state for 12 h. Then, the wood samples were dried at ambient temperature (25 °C), and their weights were determined before and after the collection of hyperspectral images. After 12 cycles, the samples were weighed after being dried for 24 h at 103 °C. In total, 144 data sets (12 samples in 12 cycles) were collected from each type of wood in order to build its MC calibration model. Following the weight measurement, NIR hyperspectral diffuse reflectance images were acquired from the radial surface of each sample using a push-broom line scanning system (Compovision, Sumitomo Electric Industries, Ltd., Osaka, Japan). The camera possesses a spectroscope and a two-dimensional photosensitive element capable of receiving NIR light from 1002 to 2350 nm at a spectral resolution of approximately 6.2 nm. In this study, wavelengths in the region 1002–1847 nm were selected for the purpose All collected spectral images of the wood samples were then converted to relative reflectance values for further PLS regression analysis. Standard normal variate (SNV) spectral pretreatments were firstly used to correct for the baseline offset and enhance absorption characteristics.

Then, the spectral data was mean centered for further partial least square (PLS) regression analysis. Principal component analysis (PCA) has been utilized in the visualization of free and bound water distributions because it is a useful tool for characterizing spectral data variance and dimension reduction. The O-H band at the almost totally dried areas subtracted from various MC levels is expected to achieve a good signal difference.

Results

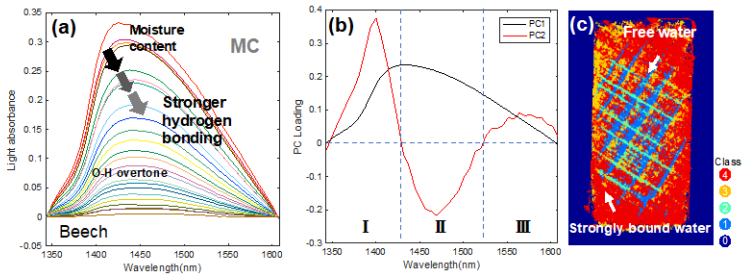

Figure 1. (a) Difference spectra of Beech wood sample; (c) Loading plots of PCA analysis; (d) Mapping of the relative variation of free and bound water distribution during air drying.

Figure1 (a) shows the difference spectra of Beech for wavelengths between 1340 and 1610 nm after baseline correlation. Figure 1 (b) shows the PC1 and PC2 loading plots, the contribution rate to the spectral variation of PC1 and PC2 of which were approximately 99% and 0.2%, respectively. PC1 loading and difference spectra have similar shapes. This means that PC1 loading mainly correlates with simple water content by mass in the wood samples, whereas PC2 loading suggests more detailed water–wood interactions. The combination of PC1 and PC2 scores explores the relative variation of free and bound water distribution during air drying (Figure1 (c)). The edge of the samples dried most rapidly into strongly bonded water[3].

Conclusions

This study proposes a nondestructive, rapid, high spatial resolution (62.5 um/pixel) method for monitoring of dynamic state of water structure within lignocellulosic material by the NIR-HSI technique. PCA was used to characterize the baseline corrected NIR difference spectral data variance between 1340 and 1610 nm for showing the distribution changing from free to bound water during air drying in three typical wood samples that have fundamental differences in the anatomical structure.

Acknowledgments

The authors are grateful for the financial support provided by JSPS (KAKENHI, no. 25292102).

References

1. Wagner L, Bos C, Bader TK, de Borst K (2015) Effect of water on the mechanical properties of wood cell walls - Results of a nanoindentation study. BioResources 10:4011–4025. https://doi.org/10.15376/biores.10.3.4011-4025
2. Tsuchikawa S (2007) A Review of Recent Near Infrared Research for Wood and Paper. Appl Spectrosc Rev 42:43–71. https://doi.org/10.1080/05704920601036707
3. Ma T, Inagaki T, Tsuchikawa S (2020) Rapidly visualizing the dynamic state of free, weakly, and strongly hydrogen-bonded water with lignocellulosic material during drying by near-infrared hyperspectral imaging. Cellulose 27:4857–4869. https://doi.org/10.1007/s10570-020-03117-6

Poster Specials

NIR Spectroscopy and Aquaphotomics in Carambola B10 Averrhoa

Siti Anis Dalila Muhammad Zahir[1] and Ahmad Fairuz Omar [2]

School of Physics, Universiti Sains Malaysia, 11800 Penang, Malaysia
***** Presenting author and Correspondence: sitianisdalila@gmail.com

Carambola fruit is well known for its attractive star-shape and pleasant taste. It is composed of up to 91% of water and is classified into index 1 to index 7 according to its maturity level. This study investigates the feasibility of near-infrared spectroscopy related to aquaphotomics in the quality measurement of B10 Averrhoa carambola. The spectra measurement is conducted using the interactance method towards fifty samples of carambola of different maturity levels. The value of firmness, pH, and SSC of respective samples were determined. The NIRS measurement performed were in the wavelength range of 800-1100nm using a Jaz Spectrometer (Ocean Optics Inc., Dunedin, FL, USA). The aquagram coefficient and correlation coefficient were calculated and constructed. The wavelengths in the range of 970 nm and 975 nm are found to provide information on the SSC, pH, and firmness of the carambola.

Keywords: Carambola, Vis-NIR spectroscopy, aquaphotomics

Introduction

The near-infrared (NIR) range provide an ideal circumstance for aquaphotomics under various perturbations. The characteristic of NIR light that has a high penetration rate and does not fully absorb by the water allows the remaining light that interacts with the matter and energy to be measured. Moreover, the NIR spectra provide physical information such as scattering, and this region consist of two broad peaks known as the first and second overtones [1]. The methodology in this paper discussed the absorbance bands of carambola fruits under various perturbations. A fresh carambola is mainly composed of up to 91% of water and is usually harvested at the color break (one-quarter yellow) stage [2]. The changes in the color of the peel in fruits had been used as an indicator of desirable characteristics in fruit quality grading. Moreover, the color of the peel could provide information on the firmness, pH, as well as soluble solid contents in the fruits [3-5]. Thus, this paper assesses the use of water absorbance in the near-infrared spectrum corresponding to different perturbations such as soluble solid contents (SSC), acidity (pH), and firmness.

Materials and Methods

The fruit sample used in this experiment is the premium quality B10 Arrvohea carambola L. (starfruit) contributed by the Malaysian Federal Agricultural Marketing Authority (FAMA). In this study, fifty carambola samples from different grading index are being chosen. Based on the color features, the maturity index is classified into 1-7 standard indexes [6]. The weight, pH, SSC, and firmness of the respective fruits are being measured. Next, the interactance technique had been performed by using a Jaz Spectrometer to measure the NIR spectra. Data analysis was executed using Matlab R2019b and Excel.

Results

The mean value of SSC, pH, and firmness calculated for each index shows that as carambola ripen, the fruit is less firm, and the value of pH and SSC increases. Figure 1 shows the absorbance spectra of the carambola after pre-processing and smoothing spline. The local quadratic regression using second-degree polynomial is performed. The absorbance spectra of the carambola show a water absorbance curve and a distinctive bottom peak lies in the wavelength range of 950 nm to 1000 nm.

(a) 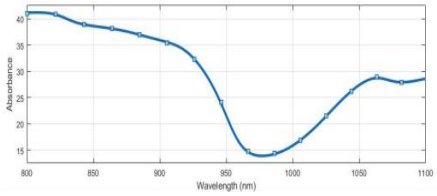 (b) 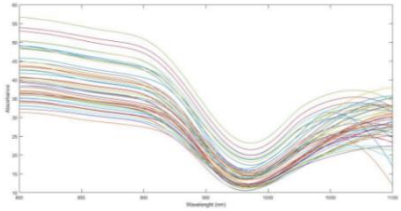

Figure 1. absorbance spectra of the carambola after pre-processing and smoothing spline (a) Mean absorbance; (b) Absorbance spectra after local quadratic regression smoothing

The aquagram constructed using spectral data information of carambola is illustrated in Figure 2. All 7 indexes showed a uniform pattern in the wavelength of 800.34 nm to 1050.02 nm. The smallest value of aquagram can be observed at approximately 825 nm in carambola of index 6 and the highest value of aquagram can be observed at approximately 850 nm in carambola index 2.

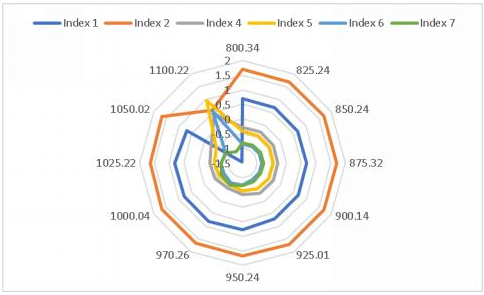

Figure 3. Aquagram values according to carambola index

Conclusions

The results interpret that firmness has a larger absolute value, which shows a stronger relationship with the aquagram values. The relationship between aquagram values and correlation coefficient explains that water can be used indirectly to measure other components such as SSC, pH, and firmness. Future research in the spectral analysis technique could be done in various types of fruit samples to observe the differences in the absorbance pattern.

References

1. Tsenkova R (2010) Aquaphotomics: Water in the biological and aqueous world scrutinized with invisible light. Spectroscopy Europe 22(6)
2. Warren O, Sargent SA (2011) Carambola (Averrhoa carambola L.). Postharvest Biology and Technology of Tropical and Subtropical Fruits, pp 397-414e. doi:10.1533/9780857092762.397
3. Emanuel MA, Benkeblia N (2013) Variation of reducing and total sugars, total phenolics and anthocyanins in otaheite (Syzygium malaccense L.) during three "on tree" ripening stages. Acta Horticulturae 1012:161–164. https://doi.org/10.17660/ActaHortic.2013.1012.15
4. Muhammad Zahir SA, Yahaya OK, Omar AF (2020) Correlating the natural color of tropical fruit juice with its pH. Color Research & Application. https://doi.org/10.1002/col.22575
5. Omar AF, Matjafri MZ (2013) Near infrared spectral linearisation in quantifying soluble solids content of intact carambola. Sensors (Switzerland) 13(4):4876–4883. https://doi.org/10.3390/s130404876
6. FAMA. (n.d.). Siri Panduan Kualiti Carambola. Retrieved January 7, 2020. http://www.fama.gov.my/en/spesifikasi-gred-dan-piawaian1

Water Changes Spectral Patterns When Perturbed by Sound Frequencies

Ryo Takagi[1], R. Tsenkova[2], S. Shigeoka[1] -

[1] Yunosato Aquaphotomics Lab
[2] Kobe University, Bio measurement Technology Laboratory

Introduction

Post-dispersive spectroscopy can be used for flowing, continuous water measurement. Running with fixed speed water in flow water cuvette cells was continuously measured by NIR spectrophotometer, which enabled us to conduct real-time, high precision monitoring of water spectral changes.
With this newly developed device, we conducted real time monitoring of water spectra when perturbed by several sound frequencies.

In the world, a fundamental tone of 432Hz was mainstream 100 years or more ago. However, it was authorized to 440Hz formally in 1953 by ISO. Various things are said for these two fundamental tones, but will the difference in this 8Hz have a different influence to water?

Also, just temperament which the frequency of the chord becomes the integral multiple was used for music in old days, but in later years, used the equal temperament that it is not divisible.

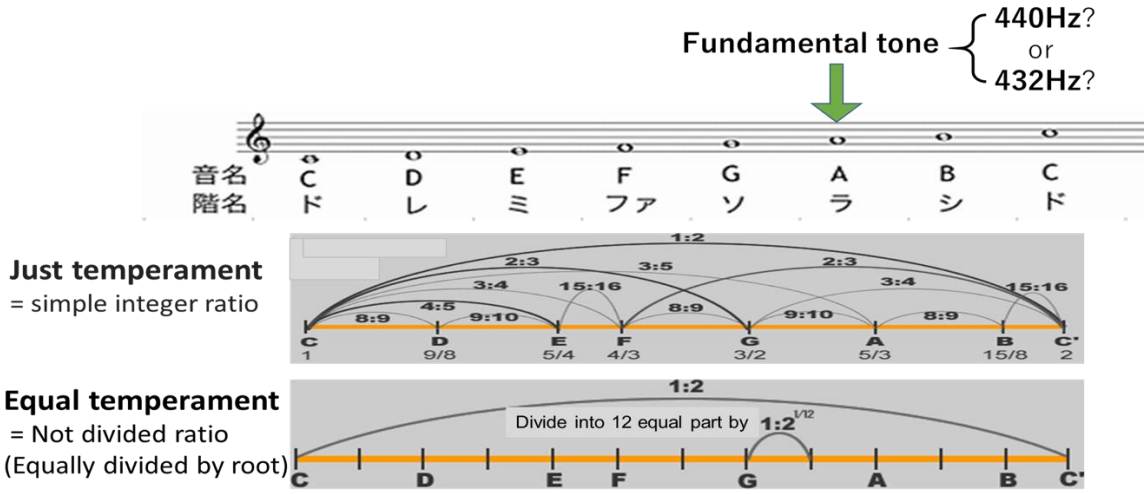

The analyzed flowing water spectra revealed with high precision characteristic water spectral patterns for each of the sound frequencies played to the analyzed water.

Materials and Methods

In this study, one type of water was used. (Gold Water mineral water from Yunosato Spa underground well) The flowing in a cuvette cell water which falls from a tank was exposed to one specific frequency in each experiment.

During the experiment, the two type of sound: 440Hz only, 440+ 329+ 659Hz(close to equal temperament) and 432 only, 432+324+ 648Hz(just temperament) was turned on and off, respectively, in separate experiments.
Water spectra were measured using Hamamatsu-photonics spectrometer, applying temperature control and sound insulation box.

Results

Water flow was exposed to the respective sound frequency for 1 minute, as well as it was flowing for 1 minute with no exposure. 15 spectra were consecutively acquired within each minute and the same procedure was repeated 5 times (for a total of 10 minutes). For each frequency, this experiment was repeated 3 times for consistency.

PLS-DA classification model was developed using the acquired spectral data. It was validate using 5-out-cross-validation. (sound on:1 off:0) 440Hz water spectral data was very well fitted to the PLS-DA model, but 432Hz water spectral data fitting ratio seemed to decrease. The difference of the fitting ratio was expanded when the same experiments were carried out for the 2 chords:
440, 329, 659Hz and 432, 324, 648Hz.

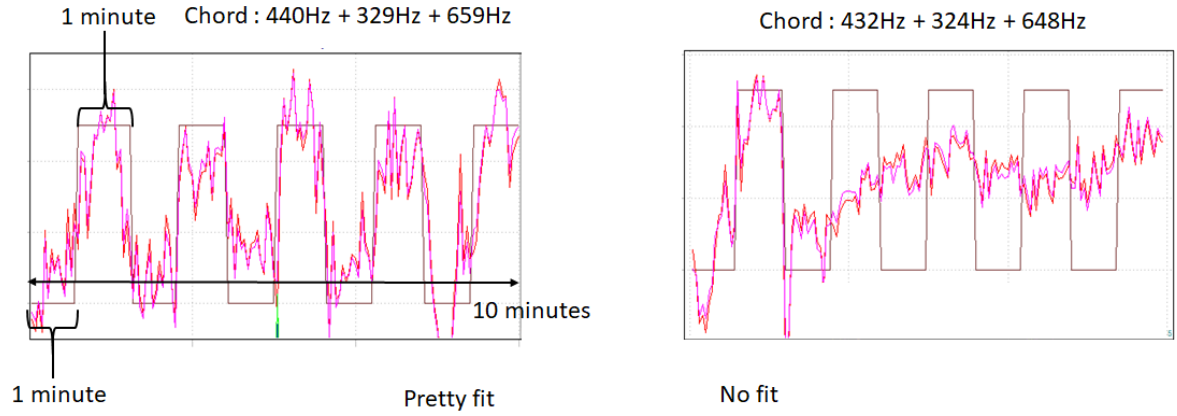

Figure 1. PLS-DA Y fit line of the 2 chords

To further investigate the differences in 2 chords, additional experiments had been conducted. Water was measured 40 times without any sound, and then, measured 80 times with sound. PLS models of the consecutive measurements with sound and without sound were developed. The Y fit plots and regression vectors showed the differences of the nature of the 2 chords. (Interclass distance between the 2 groups was 2.064 , by SIMCA classification)

Conclusions

By flowing water device, continuous flowing water spectral measurements can be performed and subtle changes of the water can be accurately measured in real-time, without touching the cuvette cell. New phenomena and factors influencing water can be easily observed by using the Water Mirror Approach and Near-infrared Aquaphotomics.

Bacteria growth evaluation and understanding

Aleksandar Stoilov [1] and Roumiana Tsenkova [2]

[1] Yunosato Aquaphotomics Lab;
[2] Kobe University;
***** Presenting author and Correspondence: alex.stoilov@abv.com

Keywords: microbiology, bacteria, broth, supernatant, metabolites, abnormality prediction

Introduction

Bacteria are everywhere around us, however, a non-invasive technique for understanding their behavior, or for predicting subsequent changes accurately and fast enough, has not yet been developed. Commonly used detection methods require time, experience, and knowledge. For a quick, accurate and non-invasive bacteria metabolism, growth abnormality detection and metabolites quantitative measurement, NIRS have been successfully applied.

Table 1. Microbial detection methods

Method	Time required	Required conditions / Notes
Agar medium	2~3 days	Selectivity of medium
Flow cytometry	50 minutes	Pretreatment and knowledge
ATP	Few minutes	Possibility of ATP from food
Impedance method	6~24 hours	Environmental stability
Aquaphotomics	**3 minutes**	**NIR spectrometer**

Materials and Methods

In this study a single species of industrial bacteria was used, displaying abnormalities in its growth. Samples were divided into batches and were provided in various hours of cultivation, in order to better observe the microbial metabolism. Their spectra were measured using FOSS XDS-RLA spectrometer, applying temperature control and recording environmental conditions. Also results from Mass Spectroscopy were provided on metabolites detected in each sample and later used as reference for the modeling of spectral data.

Results

Optical density of 600nm provided by CE-MS, displayed the differences between the normal and abnormal growth rates (Figure 1). Results were consistent with the data acquired by NIRS. When MVA were applied, groupings of samples were observed, where the type of growth process and its phases were detected using specific bands in the 1100-1300nm and 1300-1600nm regions.

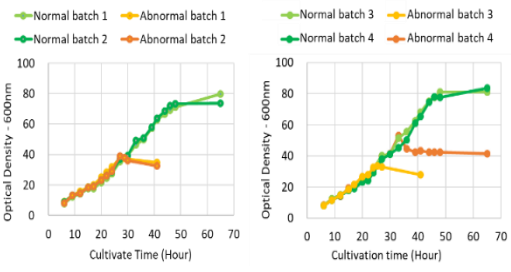

Figure 1. Bacteria growth curve of samples

By examining the changes in spectral patterns, it was possible to observe and evaluate metabolic abnormality with less hydrogen bonds in the early hours of cultivation and with increase in hydrogen bonds after the bacteria stop growing (Figure 2-3).

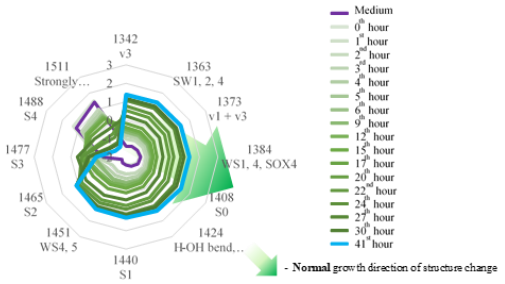

Figure 2. Aquagram of Normal broth growth process

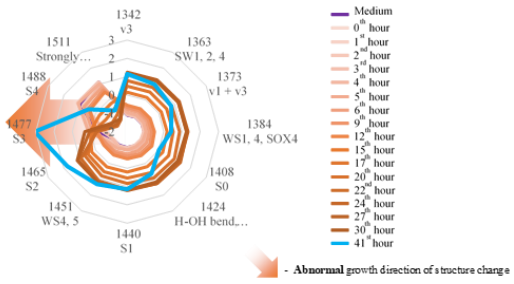

Figure 3. Aquagram of Abnormal broth growth process

When building models for each growth process, based on early cultivation hours PLS Time Regressions, predictions for each sample were made, where their standard error of prediction value (SEP) was used as a method for categorizing all spectra to their growth type. After expanding the initial models, better categorization of growth process was accomplished (Figure 4). Highest accuracy for predicting growth processes was seen for media, 0th and 6th hours samples, due to those periods of cultivation being present in all experiments. Being able to observe abnormality in media provided evidence of the phenomenon occurring due to difference in the preparation and mixing of bacterial nutrients.

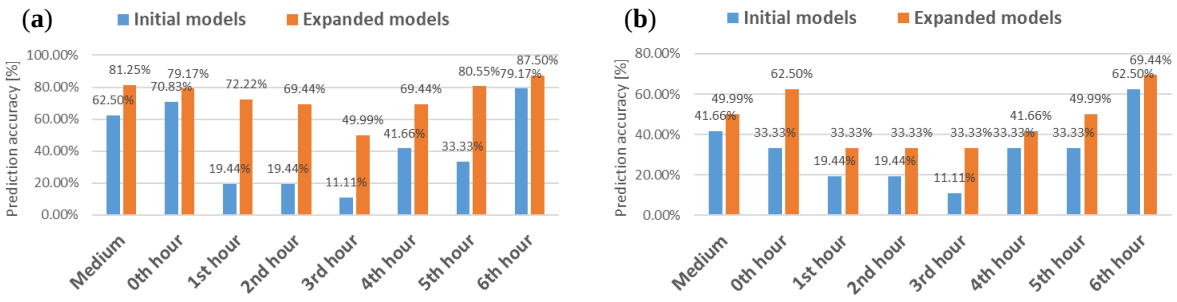

Figure 4. PLSR on cultivation hours prediction accuracy of growth processes at 1300-1600nm for: (**a**) broth (**b**) supernatant

Conclusions

Using the Water Mirror Approach of Near-infrared Aquaphotomics, fast and accurate methods for non-invasive bacteria growth stage, abnormality detection and metabolites measurement were developed.

References

1. Tsenkova, R. 2009. "Aquaphotomics: dynamic spectroscopy of aqueous and biological systems describes peculiarities of water." Journal of Near Infrared Spectroscopy 17 (6):303-313.
2. Slavchev, A., "Monitoring of Water Spectral Pattern Reveals Differences in Probiotics Growth When Used for Rapid Bacteria Selection," PloS One, vol. 10 (7), 2015

FORCES SHAPING THE WATER - BEYOND SENSING TO BIOMODULATION

Microwaves and nanosecond electric pulses for analysis and influencing of microtubule systems

Michal Cifra [1,*]

[1] Institute of Photonics and Electronics of the Czech Academy of Sciences;

***** Presenting author and Correspondence: cifra@ufe.cz

Keywords: microwaves, nanosecond pulsed electric field, microtubules, tubulin, proteins

Here I review our recent works on microwave dielectric sensing of tubulin-to-microtubule self-assembly state and on the effects of intense nanosecond electric pulses on microtubule systems.
Microtubules (MTs), biologically ubiquitous protein structures, are self-assembled from tubulin proteins. MTs are tube-like structures that are essential in cellular functions such as cell division and intracellular transport and also a major target in cancer therapies. Therefore, it is crucial to develop efficient methods for monitoring and influencing tubulin self-assembly at the molecular level.

We proposed a new approach based on a microwave lab-on-a-chip method to monitor tubulin self-assembly states. To that end, we designed a dedicated microwave platform with integrated microfluidics with nanoliter scale sensing. Using our chip, we demonstrated that the microwave microfluidics technology can be used for monitored using self-assembly state of tubulin into microtubules [1].

In order to influence the tubulin and microtubules, we explore the effects of ultrashort duration intense pulsed electric field (PEF), which represent a unique tool to modulate the function of biological systems with potential applications in bionanotechnology and biomedical therapies. At first, in molecular dynamics simulations, we showed that 20 - 100 MV/m nanosecond PEF affects tubulin conformation and dipole moment [2]. We used these insights in interpreting our findings on nanosecond PEF ability to modulate tubulin conformation to control the self-assembly of tubulin to microtubules in vitro [3]. Then we demonstrated that nanosecond PEF are capable of remodeling microtubule network in cells [4] and how combination of advanced microfabrication technology and super-resolution technology brought us tools to observe effects of nanosecond PEF on microtubule network in cells [5].

Our results introduce a novel label-free probing and controlling electromagnetic methods for bionanotechnology and biomedicine applications that can potentially be integrated into advanced microscopy systems.

Acknowledgements

We acknowledge Czech Science Foundation (GAČR), project no. GA20-06873X.

References

1. Krivosudský O, Havelka H, Chafai DE, et al. (2021) Microfluidic On-Chip Microwave Sensing of the Self-Assembly State of Tubulin. Sens and Act B Chem 328:129068
2. Marracino P, Havelka D, Průša P, et al. (2019) Tubulin Response to Intense Nanosecond-Scale Electric Field in Molecular Dynamics Simulation. Sci Rep 9:10477
3. Chafai DE, Sulimenko V, Havelka D, et al. (2019) Reversible and Irreversible Modulation of Tubulin Self-Assembly by Intense Nanosecond Pulsed Electric Fields. Adv Mat 31:1903636
4. Chafai DE, Vostárek F, Dráberová E, et al. (2020) Microtubule Cytoskeleton Remodeling by Nanosecond Pulsed Electric Fields. Adv Biosys 4:2000070
5. Havelka D, Chafai DE, Krivosudský O, et al. (2020) Nanosecond Pulsed Electric Field Lab-on-Chip Integrated in Super-Resolution Microscope for Cytoskeleton Imaging. Adv Mat Tech 5:1900669.

Heretics or pioneers: *Viktor SCHAUBERGER* and *Wilhelm REICH* - a fresh look

Pierre MADL[1*] and Herbert Lettner[1]

[1] Radiological Laboratory Salzburg, University of Salzburg;
***** Presenting author and Correspondence: pierre.madl@sbg.ac.at

In the past, personalities like Viktor Schauberger and Wilhelm Reich were viewed with great skepticism; some scholars even classified them both as charlatans. But in recollection of their achievements and the re-evaluation by renowned scientists showed that their ideas and concepts deserve a closer look.

Moreover, as new tools such as NIR spectroscopy become available along with the advancement of modern theories in the fields of biology and physics, together enable new insights and as such allow us to re-evaluate their discoveries.
The aim of this paper is therefore to provide an incentive to review their achievements by means of the novel methodological approaches as available by aquaphotomics; doing so would imply a detailed study of the postulated effects on the absorption bands of water in the NIR range, and in the light of the radically new framework that has been elaborated in physics and biology, to find evidence how to bridge theory with practice.

Keywords: Schauberger, Reich, EMF, QED, Aquaphotomics

Introduction

In this literature review, we present some of the highlights and achievements that both individuals have made in their professional life and relate them with recent publications that are accessible by numerous scientific investigations in support of their claims. In view of the diversity of their findings, we only can a) limit ourselves to selected aspects, and b) in order to keep our contribution straight forward, we do so by approaching the respective aspects in a rather "general" way, without diving too deep into the various topics as specialists in the respective fields usually would do. The common denominator that connects both Schauberger and Reich particularly regards the special properties of aqueous media. Thus, the entire contribution aims at pointing the finger at possible research applications which are possible via NIR spectroscopy.

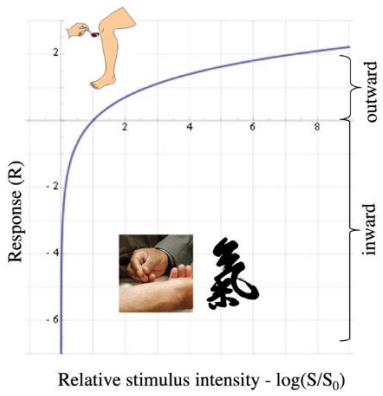

Figure 1. The graph shows that when the stimulus (S) is larger than the threshold value (S0), the lowest stimulus intensity resulting in no response) the response is positive. The response turns towards the outside: If our knee is hit by a hammer, we will react with a kick. The response grows much more slowly than the stimulus; that is very useful for protecting the organism from stimuli that are too big. In the case when the stimulus S is smaller than the threshold stimulus S0, the response grows as S decreases, but in the negative direction; it is a response turned towards the inside. In other words, the organism acts on itself, it re-structures and re-organizes itself, even more as the entity

becomes smaller. Here we have a rational basis for the formulation of the principle of minimal stimulus: the smaller the stimulus, the bigger the power of the organism to re-form and re-organize itself (adapted from: Tosi M, delGiudice E (2013) The Principle of Minimal Stimulus in the Dynamics of the Living Organism. ISIS Report Vol.60: 26-29).

Conclusions

Given the lack of understanding of mainstream science, specifically when it comes to comprehend the properties of water, the achievements of both Schauberger and Reich provide a reservoir of inspiration to unfold a broader understanding of water - specifically in the context of the living. It all starts with the basic principles of vortex formation, which encompass the micro- and extend well beyond the macroscopic domains, whereby fractality is the underlying cross-related entity. On the various levels of dimensions, this dynamic generates rhythms (pulsations), that in turn generate solitons, which are in essence coherent structures directly influencing the living. Since such an approach does not correspond to the conventional dose-effect-principle but much more to hormesis, it then becomes possible both in medicine as well as in biology or in the life sciences in general to radically re-evaluate hitherto one-sidedly interpreted relations (such as ecosystem destabilisation, electro-magnetism and life, chronic diseases, etc.) with regard to the fundamental role of water, whereby currently prevailing, mechanistically accentuated, dogmas can no longer be hold. Through the theoretical framework offered by modern physics, here in particular by QFT, a coherent picture emerges with which many of the peculiar observations associated to these two scientists appear in a completely new light. The basic assumption whereby water is just considered a solvent and in which the substances dissolved are given supremacy becomes reversed, whereby water becomes that what it is: LIFE.

References

1. Coats C (1995) Living Energies – Viktor Schauberger's Brilliant Work with Natural Energy Explained. Gateway Books, Bath, UK
2. Peitgen HO, Juergens H, Saupe D (1986) Chaos and Fractals. New Frontiers of Science. Springer, Berlin, FRG
3. Shen YR (1997) Solitons made simple. Science 276: 1520
4. Renati P (2021) QED coherence in Condensed and Living Matter - Theoretical frameworks, experimental results, and epistemological implications. PhD Thesis, University of Catania, Italy
5. Volodyaev I, Ivanovsky RN, Krasilnikova EN, Beloussov LV (2009) A Partial Verification of the A. Gurvich Mitogenetic Effect; Biological faculty of M.V. Lomonosov Moscow State University, Russia.
6. Strick J (2015) Wilhelm Reich, Biologist. Harvard University Press, Cambridge, USA
7. Smithers DW (1962) Cancer: an Attack on Cytologism. Lancet, 279(7228): 493–499
8. Chukova YP (2010) The Weber-Fechner Law. Gigiena, Moscow, RUS

SPECTRAL PATTERN OF BIOMATERIAL - WATER INTERACTION

Spectral imaging and spectroscopic methods for characterizing and monitoring biomaterial/water interactions

Aoife Gowen, Ronan Dorrepaal, Sindhuraj Mukherjee, Jose Martinez-Gonzalez, Junli Xu.

Spectral Imaging Research Group, UCD School of Biosystems and Food Engineering
Presenting author and Correspondence: aoife.gowen@ucd.ie

Keywords: spectral, imaging, FTIR, water, biomaterial

Spectral imaging and spectroscopic methodologies were developed to characterise interactions between biomaterials and water. These methods were evaluated for a range of biomaterials, including biopolymers, bone cements, hydrogels and coatings in contact with water [1,2,3]. Vibrational spectral features were related to conventional surface measurements, such as contact angle, and interactions between water and biomaterials were monitored using Near infrared, Mid infrared and Raman spectral imaging. Method 1 is based on Attenuated total reflectance – Fourier transform infrared (ATR-FTIR) imaging of wetted polymers [1]. IR light is passed through a germanium crystal in contact, under pressure, with a biomaterial surface confined under water. The biomaterial sample is submerged in a water well, through which ATR measurements are taken within the wavenumber range 750-4000 cm^{-1}. This enables spectral images of both the biomaterial surface and the water interface to be obtained simultaneously, within a sampling area of approximately 1 um from the biomaterial surface. This method, when combined with chemometrics, enabled spatially localised assessment of contact angle over a wide range of surface types. Method 2 consists of a set of parallel glass windows between which a biomaterial is deposited, followed by the introduction of water through the window and around the biomaterial via capillary motion [2]. This method, more suitable for bone cements and hydrogels, has two advantages over method 1: firstly, the method is non-contact, therefore the range of biomaterial surfaces that can be sampled is increased; secondly the lateral setup enables easier separation of the water and biomaterial signal (these are mixed in the spectra obtained using method 1). The main drawback if this technique is that spatial resolution is limited to that of the CI technique used (i.e. 1 um for Raman – 300 um macroscopic NIR). This method has been applied to monitor the interaction of water with bone cement biomaterials and biopolymers. When combined with chemometrics, this enabled monitoring of the degradation of these biomaterials over time. Method 3 is based on transmission spectroscopy of biomaterials in a controlled relative humidity environment. Relative humidity was controlled by flowing humid air through a sealed cell with calcium fluoride window which was accommodated in the sample compartment of FTIR system. This approach enabled monitoring of the structure of water vapor molecules on biomaterial surfaces [3]. Using Method 1, it was demonstrated that the degree to which protein and cell adhesion occurs on polymeric biomaterials could be predicted based on the Mid infrared spectra representing the interaction between water and the surface [4, 5]. Our results showed that predictive models built with spectra from wetted surfaces performed much better than models built using spectra acquired from dry surfaces, proving that the water-polymer interaction is critically important to the prediction of subsequent protein and cell adhesion behaviour. These results offer new insights into cell-biomaterial behaviour in the framework of the water/biomaterial interface.

References

1. Mukherjee S, Martínez-González JA, Dowling DP, Gowen AA (2018). Predictive modelling of the water contact angle of surfaces using attenuated total reflection-Fourier transform infrared (ATR-FTIR) chemical imaging and partial least squares regression (PLSR), Analyst 143(15): 3729-3740.
2. Dorrepaal RM, Gowen AA (2018). Identification of Magnesium Oxychloride Cement Biomaterial Heterogeneity using Raman Chemical Mapping and NIR Hyperspectral Chemical Imaging. Scientific Reports, 8: 13034
3. Xu, J, Gowen, A (2021). Time series Fourier transform infrared spectroscopy for characterization of water vapor sorption in hydrophilic and hydrophobic polymeric films. Spectrochimica Acta Part A: Molecular and Biomolecular Spectroscopy, 250, 119371.
4. Mukherjee S, Martinez-Gonzalez JA, Gowen AA (2019). Feasibility of attenuated total reflection-fourier transform infrared (ATR-FTIR) chemical imaging and partial least squares regression (PLSR) to predict protein adhesion on polymeric surfaces, Analyst 144(5): 1535-1545.
5. Xu JL, Lesniak A, Gowen AA (2020). Predictive Modeling of the in Vitro Responses of Preosteoblastic MC3T3-E1 Cells on Polymeric Surfaces Using Fourier Transform Infrared Spectroscopy. ACS Applied Materials and Interfaces, 12: 24466-24478.

Aquaphotomics for revealing the interaction between water molecular and surface: Potential applications to predict cell response and biofilm formation

Jun-Li Xu[1*], Mariateresa Ferone[2], Anna Lesniak[1], Aoife A. Gowen[1]

[1] School of Biosystems and Food Engineering, University College Dublin, Belfield, Ireland.
[2] School of Agriculture and Food Science, University College Dublin, Belfield, Ireland.
*****Presenting author and Correspondence: Junli.xu@ucd.ie

Keywords: Water-surface interaction, FTIR, Modelling, Cell behavior, Biofilm

Introduction

Fourier transform infrared (FTIR) spectroscopy is well recommended for the characterization of physico-chemical structure of materials due to its versatility in determining composition, conformation and crystallinity. Attenuated total reflectance Fourier transform infrared (ATR-FTIR) spectroscopy has been reported to investigate protein adsorption [1], surface segregation [2] and material degradation [3]. ATR-FTIR spectra of dry surfaces manifest molecular structure of materials, while the wet spectra obtained from wetted surface enable to represent both the chemical structure and the water-surface interaction information. In this sense, this work aims to investigate the potential of ATR-FTIR collected at wetted surfaces combined with multivariate modelling methodology for cellular responses and biofilm formation prediction.

Materials and Methods

The selected materials include poly-L-lactic Acid (PLLA), polysulfone (PSU), polystyrene (PS), polypropylene (PP), poly-vinyl chloride (PVC), polyethylene (PE), polyurethane (PU), silicone rubber (SR) film, polytetrafluoroethylene (PTFE), and glass coverslip. Mouse calvaria-derived, pre-osteoblastic cell line (passage 1- 22 after defrosting form liquid nitrogen, MC3T3-E1; ATCC CRL-2593) was used to produce diverse cellular responses on surfaces. The biofilm formation capacity of E. coli on different surface materials was monitored in 2 mL aerobic cultures in 12-well plates at 37 °C using minimal media (M9 glucose media). Quantification of biofilm formation was performed by crystal violet staining.

A Thermo ScientificTM NicoletTM iN10 Infrared Microscope was used to collect ATR-FTIR chemical images in the spectral range of 4000 – 1000 cm^{-1} with a 4 cm^{-1} resolution. Using the technique developed by Mukherjee, Martínez-González [4], wetted spectra were acquired after hydrating the sample at room temperature (21-25 °C and 40-60% relative humidity) with an equilibration time of ~ 30 minutes. Partial least squares (PLS) regression models were developed to predict cellular responses (the response variable, e.g., cell viability, morphological features) from the mean spectra (the predictor variable).

Results

The big difference between dry and wet spectra occurs in 4000-3000 cm^{-1} [ν(OH)] [5] and vibration near 1640 cm^{-1} [δ(HOH)] [6], since water is in contact with these surfaces. The dissimilar spectral change trends from dry to wet condition implicated different interactions happened between water and surfaces. PSU, PS, PP, PE, PTFE and SR share a similar band shape showing a peak shift to a higher frequency compared to glass, indicating that a weakened hydrogen bonding network at the surface due to its hydrophobic character. Strong biofilms formed on PLLA while weaker biofilm formed on PTFE. A relationship between wet spectra and biofilm growth has been witnessed.

Noticeably, PLS models using wet spectra outperformed dry spectra for prediction of cell behaviors. PLS models from wet spectra exhibited good performance to predict morphological features of the actin cytoskeleton and focal adhesions (FAs), as shown in Figure 1. For prediction of FAs, the developed model was further applied on PSU, PS and PE which were not included in the training set, yielding satisfying predictive ability with $R^2{}_P$ of 0.94 and RMSEP of 2.57 µm. Combining the analysis of regression vector, wet and difference spectral profiles, water contact angle and cellular response of FAs area, results suggested that carbonyl-to-water interactions occurred between polymer and water molecules tended to discourage cell adhesion.

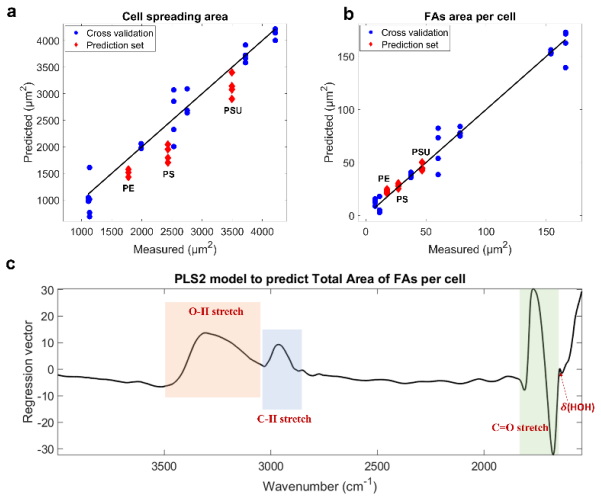

Figure 1. (a) Comparison of measured and predicted cell spreading area for cross-validation and prediction for PSU, PS and PE which were not used in model development. (b) Comparison of measured and predicted FAs area for cross-validation and prediction for PSU, PS and PE. (c) Regression vector obtained from PLS model for predicting FAs area. The major spectral features are highlighted with color shadows.

Conclusions

In this work, the approach of predicting cellular behavior on surfaces using ATR-FTIR chemical imaging combined with PLS modelling is proposed. Better performance was witnessed when spectra of wetted surfaces was used due to the incorporated information of water-surface interaction via hydrogen bonding. This work offers new insights into our understanding of cell-surface interactions based on the use of water-surface interaction.

References

1. Chittur, K.K., *FTIR/ATR for protein adsorption to biomaterial surfaces.* Biomaterials, 1998. **19**(4-5): p. 357-369.
2. Edith, D. and J.-L. Six, *Surface characteristics of PLA and PLGA films.* Applied Surface Science, 2006. **253**(5): p. 2758-2764.
3. Dorrepaal, R.M., et al., *Hyperspectral chemical imaging reveals spatially varied degradation of polycarbonate urethane (PCU) biomaterials.* Acta biomaterialia, 2018. **73**: p. 81-89.
4. Mukherjee, S., et al., *Predictive modelling of the water contact angle of surfaces using attenuated total reflection–Fourier transform infrared (ATR-FTIR) chemical imaging and partial least squares regression (PLSR).* Analyst, 2018. **143**(15): p. 3729-3740.
5. Tammer, M., *G. Sokrates: Infrared and Raman characteristic group frequencies: tables and charts*. 2004, Springer.
6. Bellamy, L., *Alkanes*, in *The Infrared Spectra of Complex Molecules*. 1980, Springer. p. 1-23.

SPECTRAL PREPROCESSING FOR AQUAPHOTOMICS

New trends in the preprocessing of Near Infrared spectra

Jean-Michel ROGER [1]*

[1] ITAP, INRAE, Institut Agro, University Montpellier, Montpellier, France;
* Presenting author and Correspondence: jean-michel.roger@inrae.fr

Keywords: NIRS, preprocessing, standardization, VSN, SPORT

Introduction

For decades, near-infrared spectrometry (NIRS) has made it possible to access the properties of matter, such as the chemical composition, physical structure and bonding state of its major components, as proposed by aquaphotomics. Thus, NIRS is extensively used to determine and predict product quality during the product development and manufacturing processes. This use is based on the calibration of chemometric models. Spectra preprocessing methods are a part of the strategy to build a robust calibration model representative of the property to be predicted. In addition, a proper use of spectral preprocessing can lead to a better understanding of the material being studied [1].

It is therefore very important to control the pre-processing phase of the spectra and to understand their effects, instead of just pressing buttons and observing the decrease in model error. The theoretical bases of spectral preprocessing will be presented, and the main methods will be illustrated with examples.

How to optimise spectrum standardisation?

Measurement conditions might induce various additive (baseline) or multiplicative effects on the collected signals which jeopardize the building of estimation models. A common answer to this concern is signal normalization and, when the baseline is constant, in particular the Standard Normal Variate (SNV) transform [2].

SNV has important drawbacks, in terms of physical interpretation and robustness of estimation models, because all the variables are equally considered, independently on what their actual relationship with the response(s) of interest is. Since SNV is very efficient, it is widely used in chemometrics. However, it produces spectral distortions that make interpretation very difficult and prohibit the discovery of fine spectral phenomena, such as those sought in aquaphotomics. As a consequence, alternative normalisation methods have been developed.

A state of the art of these methods will be briefly listed and a new method, named VSN (Variable Selection for Normalization) [3] will be presented. This algorithm automatically produces, for a given set of multivariate signals, a weighting function favoring signal variable that are only impacted by additive and multiplicative effects, and not by the response(s) of interest. When introduced in classical methods, as SNV, this weighting function significantly improves signal shape and model interpretation.

How to combine several pre-treatments?

Preprocessing NIRS spectra are intended to suppress the effects of unwanted variations, in order to improve the calibration model performance or to make clearer the sought features. Because there are many types of background noise, there are many pre-treatment methods. It is therefore tedious to select and/or combine the best pre-treatments. Only few methods have been proposed in this aim, mainly based on the exhaustive search. A set of new methods, based on the ensemble paradigm, will be presented. A focus will be put on the SPORT method [4], which uses sequential and orthogonalized partial least squares (SO-PLS), thus leading to a boosting method. The performances and properties of this new method will be compared to those of a previously published stacking method.

Perspectives

Based on the methods presented, but also on the current state of the art, perspectives for future research will be presented, including a special focus on aquaphotomics.

References

1. Roger, J. M., Boulet, J. C., Zeaiter, M., & Rutledge, D. N. (2020). Pre-processing Methods⋆. Reference Module in Chemistry, Molecular Sciences and Chemical Engineering.
2. Barnes, R. J., Dhanoa, M. S., & Lister, S. J. (1989). Standard normal variate transformation and de-trending of near-infrared diffuse reflectance spectra. Applied spectroscopy, 43(5), 772-777.
3. Rabatel, G., Marini, F., Walczak, B., & Roger, J. M. (2020). VSN: Variable sorting for normalization. Journal of Chemometrics, 34(2), e3164.
4. Roger, J. M., Biancolillo, A., & Marini, F. (2020). Sequential preprocessing through ORThogonalization (SPORT) and its application to near infrared spectroscopy. Chemometrics and Intelligent Laboratory Systems, 199, 103975.

Non-linear regression and artificial neural networks in NIR spectroscopy: insights into fundamental phenomena and impact on practical applications in water-related scenarios.

Krzysztof B. Bec[1*], Justyna Grabska[1], and Christian W. Huck[1]

[1] University of Innsbruck, Institute of Analytical Chemistry and Radiochemistry, Innrain 80-82, 6020 Innsbruck, Austria

***** Presenting author and Correspondence: Krzysztof.Bec@uibk.ac.at

Keywords: near-infrared spectroscopy, miniaturized (handheld) spectrometers, water content analysis, natural medicine, Gaussian Process Regression (GPR), Artificial Neural network (ANN)

In the past decade, the continuous progress in technology has led to dynamic development of portable, miniaturized near-infrared (NIR) spectrometers, enhanced the potential of this spectroscopic technique by enabling analysis directly on-site and enabled a new spectrum of applications of this technique in science and industry [1,2]. The miniaturization required implementing a number of distinct engineering solutions, and these sensors differ by the key elements used for their construction, e.g. wavelength selectors and detector configurations [2]. Different design philosophies make the performance and applicability of various miniaturized NIR spectrometers specific, governed by the operating spectral region, resolution and sensitivity. As the result, their analytical performance is often inferior in absolute terms to the benchtop laboratory instrumentation [1,2].

The advantages of miniaturized NIR spectroscopy are particularly exposed in several field of natural products, because of their chemical diversity that can vary depending on the medicinal plant cultivation conditions, geographical origin or harvest time [3]. One of the most critical quality parameters of natural medicines, essential in the production process and also the suitability of the final retail product, is the moisture content. Flexible, efficient and rapid analytical method for monitoring water content in natural medicinal material has critical importance. Miniaturized NIR spectroscopy offers great potential in this role. However, these kinds of samples feature a complex chemical matrix, typical for plant material.

Our investigation evidenced that the analytical performance of miniaturized spectrometers in a challenging scenario, i.e., that involves chemically complex plant matrices, can be significantly improved with advanced calibration methods [4]. In the explored analytical scenario, the quantification of the moisture content in 192 samples of dried plant extract composed of five different plants from different geographical origins harvested at various times within two years. The spectra measurements involved a rich suite of spectrometers; two benchtop (NIRFlex N-500 and MPA I) and three miniaturized (microPHAZIR, MicroNIR 2200 and MicroNIR 1700ES) instruments were used to acquire the spectral datasets for all 192 investigated samples. For the needs of the calibration, reference analysis of the moisture was performed with the use of Karl Fischer titration method, which is the industry standard for this purpose. Moisture content is one of the most important quality parameters of the intermediate and final products in the area of natural medicines. It determines the market suitability, stability and shelf life of the product and requires to be constantly monitored. The calibration step involved development and evaluation of PLSR, Gaussian process regression (GPR) and artificial neural networks (ANN) models that were constructed for the spectral sets from each instrument. The non-linear GPR and ANN methods are known to offer substantially improved performance in the case of less than ideal data-sets, e.g. resulting from difficult nature of the analyzed sample (i.e. chemically complex plant matrix), reduced quality of the spectra (i.e. narrow spectral region, lower resolution and poorer S/N typically accepted for the miniaturized spectrometers). The prediction performance of those calibration models was evaluated through the root-mean square error of prediction (RMSEP) determined for an independent test set (Table 1).

Thus, the penalty to the accuracy resulting from the hardware miniaturization can be compensated by using GPR or ANN calibration. In this case, the miniaturized spectrometers offered the prediction performance at the

level of the benchtop instruments (Table 1). Moreover, the samples in native state proved to be more difficult to analyze for all evaluated instruments when using PLSR calibration (Table 2).

Table 1. RMSEP values for an independent test set validation resulting from PLSR, GPR and ANN. Bolded values highlight are the models with highest performance of prediction for a given spectrometer and sample configuration.

		PLSR	GPR	ANN			
				1 HN	2 HN	3 HN	4 HN
drying agent	NIRFlex N-500	0.27	0.31	0.35	0.36	0.32	0.39
	MPA I	0.27	0.32	0.39	0.35	0.39	0.33
	microPHAZIR	0.37	0.30	0.27	0.30	0.31	0.48
	MicroNIR 2200	0.32	0.30	0.33	0.29	0.33	0.33
	MicroNIR 1700ES	0.28	0.28	0.25	0.33	0.30	0.34
native	NIRFlex N-500	0.45	0.36	0.73	0.55	0.41	0.43
	MPA I	0.47	0.44	0.54	0.68	0.56	0.59
	microPHAZIR	0.54	0.60	0.59	0.53	0.58	0.48
	MicroNIR 2200	0.43	0.38	0.32	0.35	0.44	0.44
	MicroNIR 1700ES	0.50	0.43	0.46	0.70	0.67	0.72

Table 2. The difference between the RMSEP values for independent TSV performed for the plant material in two states, native samples vs. the samples laced with the drying agent, summarized for two benchtop and three miniaturized NIR spectrometers.

	PLSR	GPR	ANN
NIRFlex N-500	0.18	0.05	0.05
MPA I	0.20	0.12	0.21
microPHAZIR	0.17	0.30	0.21
MicroNIR 2200	0.11	0.08	0.03
MicroNIR 1700ES	0.22	0.16	0.21
average	0.18	0.14	0.14

References

1. Beć, KB, Grabska, J, Siesler, HW, Huck, CW (2020) Handheld near-infrared spectrometers: Where are we heading? NIR News 31:28–35.
2. Beć, KB, Grabska, J, Huck, CW (2021) Principles and applications of miniaturized near-infrared (NIR) spectrometers, Chemistry - A European Journal 27:1514-1532.
3. Beć, KB, Grabska, J, Huck, CW (2020) NIR spectral analysis of natural medicines supported by novel instrumentation, methods of data analysis and interpretation, JPBA 193:113686.
4. Mayr, S, Beć, KB, Grabska, J, Wiedemair, V, Pürgy, V, Popp, MA, Bonn, GK, Huck, CW (2021) Determination of water content: Challenging handheld NIR spectrometers with sophisticated plant matrices. Spectrochimica Acta A 249:119342.

This work was supported by Austrian Science Fund (FWF): M2729-N28.

The effects of water on scattering: taking into account path-length modifications

Alexandre Mallet [1, 2, 3, 4, *], Roumiana Tsenkova [5], Jelena Muncan [5], Cyrille Charnier [3], Éric Latrille [1, 4], Ryad Bendoula [2], Jean-Philippe Steyer [1], and Jean-Michel Roger [2, 4]

[1] INRAE, Univ Montellier, LBE, 102 Av des Etangs, Narbonne F-11100, France
[2] INRAE, UMR ITAP, Montpellier University, Montpellier, France
[3] BIOENTECH Company, F-11100 Narbonne, France
[4] ChemHouse Research Group, Montpellier, France
[5] Kobe University, Graduate School of Agricultural Science, Biomeasurement Technology Laboratory, 1-1 Rokkodai, Nada-ku, Kobe 657-8501, Japan
***** Presenting author and Correspondence: alexandre.mallet@bioentech.eu

Keywords: near infrared spectroscopy; scattering; preprocessing; water content; EMSC

Introduction

The Beer-Lambert law (ie. the linear relationship between absorbance and an absorbing constituent concentration) is valid in very strict conditions: the medium should be a fully transmitting solvent. Thanks to sound chemometrics involving signal processing and multivariate statistics, the lack of linearity observed in scattering media (soil, biomass, water suspensions) has been compensated and successful quantitative calibration have been developed [1]. However, when interested in the specific spectroscopic assignments (both relative intensity and position of the absorptivity coefficients), a special care in the pre-processing steps should be given [2]. In this study, near infrared spectra were acquired during the drying of aluminum pellets mixed with water. This model system allowed to study specifically the scattering effects induced by moisture content variations. The path-length modifications are shown to be related to water content by a power law. Implications of such relationship are discussed, in particular, for the improvement of specific spectral assignments made on water structure.

Materials and Methods

Aluminum paper pellets mixed with water were put into an in-house built drying system with automatic dynamic acquisition of near infrared reflectance spectra and water content determination [3].
A new formulation of the relationship between absorbance and water content is proposed:

$$A_{\lambda,c} = \varepsilon_\lambda . l_0 . c^{a_\lambda + 1} + f_{\lambda,c}. \quad \text{(Eq. 1)}$$

With ε_λ the extinction coefficients, $l_0 . c^{a_\lambda}$ the path-length dependent of c due to scattering events, and $f_{\lambda,c}$ the additive baselines due to the photon loss. Applying the logarithm results in the following equation:

$$log\left(A_{\lambda,c} - f_{\lambda,c}\right) = log(\varepsilon_\lambda . l_0) + (a_\lambda + 1) . log(c). \quad \text{(Eq. 2)}$$

In order to obtain the absorbance corrected from additive effects ($A_{\lambda,c} - f_{\lambda,c}$), the EMSC framework was used [4]. For each wavelength, an ordinary least squares (OLS) log-log regression was fit: both intercept $log(\varepsilon_\lambda . l_0)$ and slope $(a_\lambda + 1)$ were evaluated.

Results

As seen in Figure 1A, the raw absorbance measurements at 1430 nm do not follow a linear relationship with water content. After correcting additive effects using EMSC (Figure 1B), the log-log regression shows a perfect fit with an R^2 of 0.995 (Figure 1C). This analysis was run for all wavelengths of the spectrum, and it was shown that this law fitted perfectly on the whole spectrum.

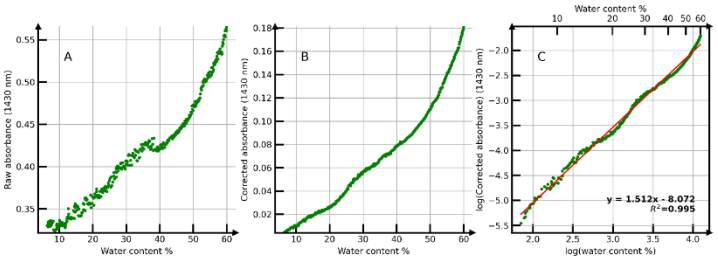

Figure 1. Evolutions with water content % of (A) raw absorbance, (B) corrected absorbance, and (C) log-transformed corrected absorbance. In the (C) subplot, the OLS regression line is plot in red, with the slope, intercept and coefficient of determination (R^2).

The intercepts obtained with the log-log regression (corresponding to $log(\varepsilon_\lambda . l_0)$ in Eq.2) are the logarithm of the pure extinction coefficients ε_λ. These are presented in Figure 2 (blue curve), and second derivative using Savitzky-Golay (red curve) shows the subpeaks of the first overtone OH region. The negative peaks at 1405 nm and 1469 nm correspond well to observed peak positions in transmission spectra of water [5].

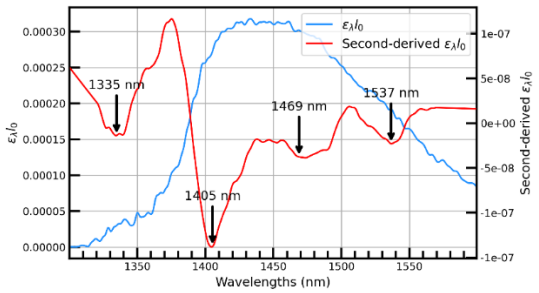

Figure 2. The exponential of the fitted intercept values ($\varepsilon_\lambda . l_0$) in Eq.2 (in blue) and the corresponding Savitzky-Golay second derivation (in red).

Conclusions

This work highlights the effect of water on the scattering properties of the measured material. It is shown that path-length modifications can be related to water content by a power law. It is suggested that by correctly preprocessing additive effects, and taking into account this new modeling of path-length, the relative intensity and position of the extinction coefficients can be correctly studied. Such framework may benefit to Aquaphotomics studies where specific absorbance bands of water are looked for.

References

1. C. Charnier, E. Latrille, L. Lardon, J. Miroux, J.P. Steyer, Water Res. 95 (2016) 268–279.
2. P. Oliveri, C. Malegori, R. Simonetti, M. Casale, Anal. Chim. Acta 1058 (2019) 9–17.
3. A. Mallet, C. Charnier, É. Latrille, R. Bendoula, J.-P. Steyer, J.-M. Roger, Waste Manag. 122 (2021) 36–48.
4. H. Martens, E. Stark, J. Pharm. Biomed. Anal. 9 (1991) 625–635.
5. V.H. Segtnan, Š. Šašić, T. Isaksson, Y. Ozaki, Anal. Chem. 73 (2001) 3153–3161.

Poster Session

POSTER SESSION I SUNDAY March 21, 2021

Poster No.	Name	Country	Title
I1	David Tjandra Nugraha	Hungary	Evaluation of Mung Bean (Vigna radiata) Sprout and Quantification of Ascorbic Acid Content Using Near-Infrared Spectroscopy and Aquaphotomics
I2	Vladyslav Bozhynov	Czechoslovakia	Comparison of different types of error in Visible Aquaphotomics
I3	Anastasia Surkova	Russia	Near infrared spectroscopy and aquaphotomics – a possible tool for cancer diagnostics?
I4	Petya Stoykova	Bulgaria	Detection and quantification of hydrophobic pollutants in aqueous solution
I5	Vladimir Beskoski	Serbia	Is aquaphotomics suitable for the determination and analysis of perfluorinated compounds?
I6	Zsanett Bodor	Hungary	Application of aquaphotomics to detect different sugar syrup adulteration of honeydew honey
I7	John-Lewis Zinia Zaukuu	Hungary	Application of NIRS and aquaphotomics for diluted meat extract characterization
I8	Flora Vitalis	Hungary	Monitoring of brown rot caused by Monilia fructigena on plums with the aquaphotomics approach

POSTER SESSION II MONDAY March 22, 2021

Poster No.	Name	Country	Title
II1	Xiaoyu Cui	China	Temperature-dependent variable selection in near-infrared spectra for aquaphotomics
II2	Vladimi Beskoski	Serbia	Can carbohydrates change the shape of water?
II3	Yasuhiro Miwa	Japan	Spectral study on low frequency Raman of hydrogen-bonded substances on the surface of icy moons
II4	Sukkrita Anantawittayanon	Japan	The investigation of water spectra and water activity using Aquaphotomics approach
II5	Lian Li	China	Characterization of moisture absorption process of rebaudioside using near infrared spectroscopy and aquaphotomics
II6	Makoto Sakai	Japan	Investigation of different types of water using aquaphotomics
II7	Chongwen Xiong	China	Understanding the interaction between water and polymer in thermo-sensitive hydrogel phase transition system by near-infrared spectroscopy
II8	Xihui Bian	China	Spectrophotometric simultaneous determination of trace Cu2+ and Co2+ in aqueous solution by membrane preconcentration coupled with chemometrics
II9	Siti Anis Dalila Muhammad Zahir	Malaysia	NIR Spectroscopy and Aquaphotomics in Carambola B10 Averrhoa
II10	Ryo Takagi	Japan	The changes in spectral pattern of water perturbed by different sound frequencies – Measurements using newly developed flowing water device
II11	Aleksandar Boykov Stoilov	Japan	Understanding of Yogurt Bio-Functional Water

Poster Session I

Evaluation of Mung Bean (*Vigna radiata*) Sprout and Quantification of Ascorbic Acid Content Using Near-Infrared Spectroscopy and Aquaphotomics

David Tjandra Nugraha [1,*], John-Lewis Zinia Zaukuu [1], Juan Pablo Aguinaga Bósquez [1], Zsanett Bodor[1], Flora Vitalis [1], and Zoltan Kovacs [1]

[1] Institute of Bioengineering and Process Control, Department of Measurements and Process Control, Faculty of Food Science, Szent István University, 1118 Budapest, Hungary;
***** Presenting author and Correspondence: dtdavidtjandra@gmail.com

Mung bean is a leguminous crop with distinct disadvantages in its consumption, namely its anti-nutrient components. Processing techniques especially sprouting process is one of the solution for better nutritional quality, while producing important components such as ascorbic acid. Production of mung bean sprout in large scale does not have definite standard for the sprouting process, thus there is a need for rapid and effective quality check for mung bean sprout. Near-infrared spectroscopy (NIRS) as a sensitive technique is proposed to describe the quality parameters (water content, pH, and ascorbic acid) of mung bean sprout relative to the conventional analytical methods. Mung bean was sprouted for 120 h in 6 h interval, analyzed using conventional methods and NIRS instrument, and evaluated using statistical methods, chemometrics approach (principal component analysis (PCA), discriminant analysis (DA), partial least squares regression (PLSR)), and aquaphotomics analysis by calculating an aquagram in the range of 1300-1600 nm interval. Scanning the bean sprout extract showed classification and 100% accuracy of prediction using DA. The PLSR model developed for quality parameters showed dependable R2CV of above 0.95 with RMSECV ranging from 0.02%-0.05%. The aquagram showed a trend of strong bound water forming during the sprouting, peaking in 1462, 1477, 1489, and 1513 nm.

Keywords: germination; chemometrics; water spectral pattern

Introduction

Mung bean (Vigna radiata) is one of the most significant crop in Asia, but it contains anti-nutrient components in the form of phytate, which reduce the bioavailability of mineral in its consumption [1]. Some processing techniques, especially sprouting have been proven to reduce anti-nutrient components, and increase the quality of mung bean. Sprouting process also reduce flatulence-related sugar, and produce phenolic components and vitamins; especially ascorbic acid [2]. Rapid evaluation of mung bean sprout quality and monitoring of sprouting process over time would prove an objective means of assessment of one of the most important sprouting parameter: time. As water changes and organic acid formation in bean sprout product happened in the function of time, developing rapid analysis and continuous monitoring technique for industrial scale is essential. The use of NIRS within 700-2500 nm interval has been reported to be able to classify bean sprout based on sprouting time for quality purpose [3]. However, the complex aqueous system of the mung bean sprout suggests that water matrix coordinates play a key role at the molecular level. It is therefore, necessary to understand the changes in the hydrogen bonding network of water molecules occurring in the mung bean during sprouting. [4]. The usage of Aquaphotomics is suitable, due to the appropriate sample preparation from the conventional analytical techniques. The objective of this study was to understand the possibility of rapid quality check and observation of mung bean sprouting process through NIRS and Aquaphotomics and test the potential of NIR and Aquaphotomics to make a correlative model for quality parameters evaluation and ascorbic acid.

Materials and Methods

The bean was sprouted for 120 h in 6 h interval. The bean was soaked with distilled water for 12 h, and rinsed every 12 h. The sprouting was done on cellulose paper in an incubator of a constant temperature (35oC). Grown bean sprout is crushed, mixed with water (1:2 ratio), and filtered with filtration paper. This sample liquid is called the bean sprout extract, used for NIRS scanning. Water content determination was based on AOAC

method, pH and conductivity determination utilized benchtop instrument, and ascorbic acid determination was based on direct redox titration using iodine solution. NIRS measurement was done using DLP NIRScanNano instrument (Texas Instrument, Dallas, Texas, United States) in transmission mode using a quartz cuvette of 1 mm path length. The NIRS scanning was done in triplicate and three consecutive scans. Result from conventional analytical techniques were analyzed using descriptive statistics and one-way ANOVA, followed by differentiation test. The spectral data was analyzed using chemometrics methods (PCA and LDA), correlative model was made using PLSR technique and n-fold cross-validation technique, and aquagram was made from spectral data in the first O-H overtone range (1300-1600 nm).

Results

The aquagram showed a trend of strong bound water formation during germination (Figure 1a.), and its comparison with the ascorbic acid standard (Figure 1b.). PLSR model was made from the spectral data of bean sprout extract, and predicted quality parameters (water content, germination time, and ascorbic acid content). The ascorbic acid content was analyzed for independent prediction of sample with unknown concentration of ascorbic acid. The prediction result was then compared with conventional technique (Figure 1d.)

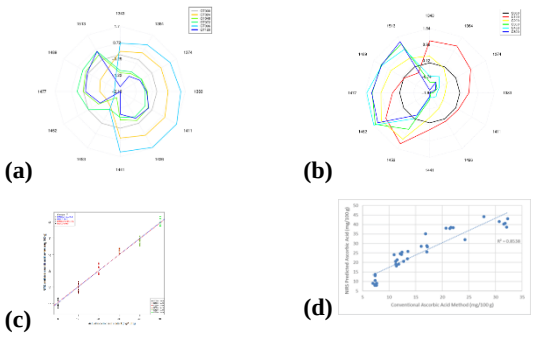

Figure 1. Aquagram (1300-1600 nm) and PLSR plot, after Savitzky-Golay smoothing (SG) and standard normal variate (SNV) pretreatment of the spectra: (a) Aquagram plot of sprouted mung bean sprout with 24-hour interval; (b) Aquagram plot of ascorbic acid (0-500 mg/100 g); (c) Regression of ascorbic acid prediction; (d) Ascorbic acid content plot of NIR predicted values against conventional technique result.

Conclusions

The result from the experiment showed NIR reliability for mung bean sprout quality evaluation, where it prominently predicted water content of mung bean sprout and its sprouting time parameter. Further prediction of ascorbic acid showed satisfactory prediction capability, as well as similarity to the prediction by conventional techniques. PLSR regression models showed high accuracies even after cross-validation (R2CV) and low errors (RMSECV) for predicting water content, germination time and ascorbic acid. Aquagrams from aquaphotomics evaluations showed similarity in trend. Both mung bean sprout and ascorbic acid initially showed the abundance of weaker bonded water molecules (first and fourth quadrant), and stronger bonded water (1513 nm) was observed under higher concentration of ascorbic acid, and longer germination time. This indicated the potential of ascorbic acid detection for complex food matrixes on a sub-percent level.

References

1. Lorensen E, Prevosto R, Wilson KA (1981) The Appearance of New Active Forms of Trypsin Inhibitor in Germinating Mung Bean (Vigna radiata) Seeds . Plant Physiol 68:88–92. https://doi.org/10.1104/pp.68.1.88
2. Medhe S, Jain S, Anal AK (2019) Effects of sprouting and cooking processes on physicochemical and functional properties of moth bean (Vigna aconitifolia) seed and flour. J Food Sci Technol 56:2115–2125. https://doi.org/10.1007/s13197-019-03692-y
3. Geneve RL, Al-Amery M, Sanches MF, et al (2018) Near-infrared spectroscopy used to predict soybean seed germination and vigour. https://doi.org/10.1017/S0960258518000119
4. Muncan J, Tsenkova R (2019) Aquaphotomics-From Innovative Knowledge to Integrative Platform in Science and Technology. Molecules 24:. https://doi.org/10.3390/molecules24152742

Comparison of different types of error in Visible Aquaphotomics

Vladyslav Bozhynov [1,*], Jan Urban [1]

[1] Laboratory of Signal and Image Processing, Faculty of Fisheries and Protection of Waters, South Bohemia Research Center of Aquaculture and Biodiversity of Hydrocenoses, Institute of Complex Systems, University of South Bohemia in České Budějovice, Zámek 136, 373 33 Nové Hrady, Czech Republic;
***** Presenting author and Correspondence: vbozhynov@frov.jcu.cz

Keywords: Aquaphotomics; Visible Spectrum; Biophysics; Sampling Error; Cuvettes.

Introduction

Aquaphotomics, the modern application of near infrared spectroscopy, introduced by Prof. Tsenkova in 2005, has been successfully used to study and systematize the knowledge about water-light interaction [1,2]. The study of water spectral analysis in the visible range of spectrum (visible Aquaphotomics) is a potential extension of the knowledge of NIR Aquaphotomics. The use of absorption analysis requires experimental precision and, therefore, minimization of measurement errors. The aim of the following study is to determine the main errors that occur during experiments in visible Aquaphotomics, and their significance (influence) on the results.

Materials and Methods

For data collection, the SHIMADZU UV-2401PC UV-VIS spectrophotometer was used, range limited from 380 to 800 nm, with step 1 nm and absorption measurement mode. Acquisition was performed in transmittance mode using optical rectangular glass cuvettes providing 2 mm and 5 mm of technical pathlengths, chosen as optimal for visible spectral during previous research [3,4]. Distilled water was used for the experiments as an aqueous sample. Glass cuvettes Starna Scientific were completely new and never used before. After unpacking, the cuvettes were washed by Ethanol 96 % and before measurements, each cuvette washed by distilled water three times. For the experiments three cuvettes of each pathlength were used. The volume of the sample was kept constant: 8 mL and 20 mL for 2 mm and 5 mm, respectively. To test the device error, three consecutive scans were performed for each measurement. Three sampling (refilling) for each cuvette were carried on and to test error of the place each cuvette was taken off and placed back with the same sample three times. There were three cuvettes of each pathlength to evaluate given error by different cuvettes. To estimate the device error, standard deviations between all consecutive scans of the same sample were calculated for each wavelength using the error propagation rules. For the position error, the standard deviation between all cuvette positions for each cuvette were evaluated. Sampling error was given by calculation of standard deviation between all the samples (refilling) for one cuvette. Finally, the cuvette error is represented by the standard deviation between the different cuvettes sets of measurements.

Results and Conclusions

Calculated standard deviations between the measured spectra with 5 mm cuvette are presented on the Fig. 1. There are 4 curves representing the deviations between consecutive scans of the same sample (StDevCS), samplings (refilling) of the same cuvette (StDevS), physically different cuvettes but same type (StDevC), and different positions (StDevP). As expected, the smallest values has the deviation between the consecutive scans, which represents the error of the device. The error given by the cuvette replacement is small and comparable with the device error. Error given by the sampling is expected in each experiment, usually due to the inaccuracy of the used pipettes and human factor. This error is often the highest in the experiment. However our results show that there is error, the impact of which is even greater than that of the sampling error. The cuvettes from the same box of the same producer are not exactly equal and give the highest deviation during the measurement.

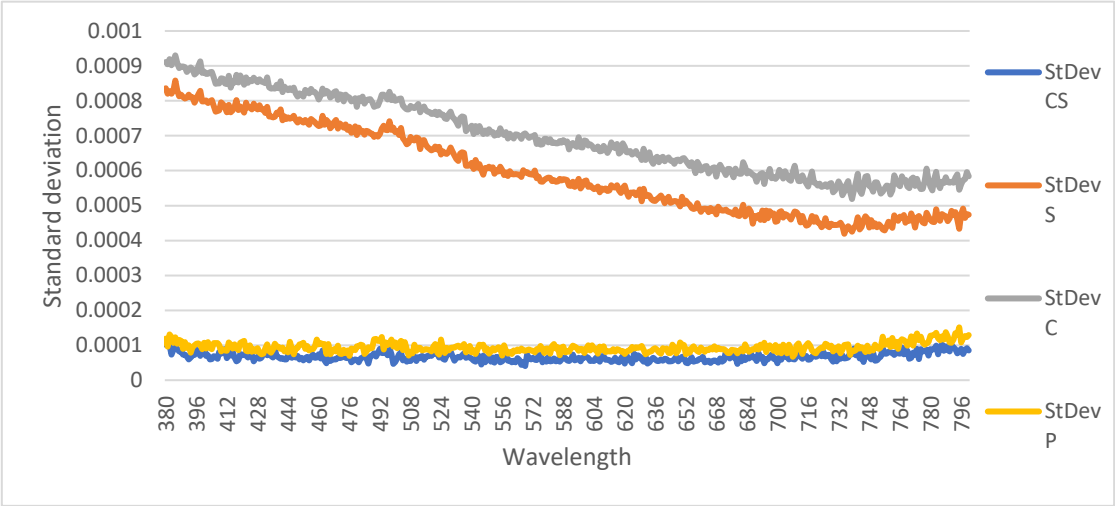

Figure 1. Standard deviations between the measured spectra with 5 mm pathlength cuvette.

Table 1 presents the errors of the device (Ed), sampling (Es), cuvettes (Ec) and positions (Ep) from the measured spectra, together with the average values of the absorption (Av_abs), for the 2 mm and 5 mm pathlengths. As can be seen, errors differ for the 2 mm and 5 mm cuvettes. The errors of the device and position are small, while the sampling and cuvettes errors are much higher. The highest error with 2 mm is the cuvette error, when with 5 mm cuvettes it is error of the sampling. We assume that this is directly related to the amount of sample being measured.

Table 1. The calculated errors of the device, sampling, cuvette and position.

	2 mm	**5 mm**
Av_abs	4.424E-2	3.994E-2
E_d	4.057E-6	3.316E-6
Es	2.302E-5	2.94E-5
E_c	4.292E-5	1.749E-5
E_p		3.205E-6

Our results show the presence and influence of errors presented in spectral experiments. Most of these errors are well known and are taken into account by experimenters. The sampling error is often considered as the largest. However, the error presented by the difference between cuvettes from the same manufacturer (from the same box) can have a significant impact on the expected result. In this regard, it is necessary to consider this error and, possibly, apply correction methods that can reduce its affect.

Acknowledgments

Supported by the MEYS Czech Republic – CENAKVA LM2018099, No.CZ.1.05/2.1.00/19.0380, Biodiversity CZ.02.1.01./0.0/0.0/16/025/0007370, GAJU 013/2019/Z, and TAČR-GAMA2-PoC 01-08.

References

1. R. Tsenkova. “Visible-Near Infrared perturbation spectroscopy: Water in action seen as a source of information”. Proceedings of the 12th International Conference on Near-infrared Spectroscopy. 2005. pp. 607–612
2. R. Tsenkova, J. Muncan, B. Pollner, Z. Kovacs. “Essentials of Aquaphotomics and Its Chemometrics Approaches”. Frontiers in chemistry. 2018. 6. https://doi.org/10.3389/fchem.2018.00363
3. V. Bozhynov, O. Mashchenko, P. Urbanova, Z. Kovacs. “Steps to Visible Aquaphotomics”. In: I. Rojas, O. Valenzuela, F. Rojas, L. Herrera, F. Ortuño, editors. Bioinformatics and Biomedical Engineering. Cham, Switzerland: Springer International Publishing, 2020. Vol. 12108, pp. 287-297
4. V. Bozhynov, P. Soucek, A. Barta, P. Urbanova, D. Bekkozhayeva. “Dependency Model for Visible Aquaphotomics”. In: I. Rojas, O. Valenzuela, F. Rojas, F. Ortuño, editors. Bioinformatics and Biomedical Engineering. Cham, Switzerland: Springer International Publishing, 2019. Vol. 11465, pp. 105-115

Near infrared spectroscopy and aquaphotomics – a possible tool for cancer diagnostics?

Anastasiia Surkova [1, 2] *, Andrey Bogomolov [2], Olga Bibikova [3], Urszula Zabarylo [3], Viacheslav Artyushenko [3], Thaddäus Hocotz [4], Andrey Legin [1], Dmitry Kirsanov [1] Jelena Muncan [5], and Roumiana Tsenkova [5]

[1] Institute of Chemistry, St. Petersburg State University, St. Petersburg, Russia;
[2] Samara State Technical University, Samara, Russia;
[3] artphotonics GmbH, Berlin, Germany;
[4] Charité – Universitätsmedizin Berlin, Germany;
[5] Kobe University, Japan;
* Presenting author and Correspondence: melentosik89@mail.ru

Keywords: cancer screening and diagnostics, biological fluids, NIR spectroscopy, aquaphotomics

Introduction

Late cancer diagnosis is one of the causes of high mortality rate. Biopsy and histopathology, being a gold standard in cancer diagnosis, are complex, invasive and expensive. The development of new low-cost and rapid methods for mass screening of patients and early cancer diagnosis is an urgent need in modern medicine. The detection of compositional changes in a patient's biological fluids (blood and urine) caused by cancer distribution is a perspective direction of the research in this field [1].
Optical spectroscopy has great potential in cancer diagnostics. Using fiber optic probes in cost-effective NIR region is a very powerful and flexible method for non-invasive *in vivo* and *in vitro* diagnostics [2-3]. NIR-spectra of biological fluids presumably contain information about the molecular changes in the normal and abnormal conditions of the cells and the patient's condition. Therefore, they can be used to predict the response to a particular treatment protocol [4]. However, NIR spectroscopy has not been yet widely used in clinical practice because of the lack of a unified strategy for spectral data analysis.
Intensive water absorption in the 700–1900 nm region usually complicates the analysis of the obtained data and reduces their informative value. Nevertheless, water absorption bands themselves contain information about different conformations of water molecules in cells. Water molecules form hydrogen bonds between each other and with their surroundings, which makes water absorption bands very sensitive to the sample composition [5]. In the present work, aquaphotomics combined with multivariate data analysis was used to study NIR spectra of plasma and serum of blood and urine, obtained from patients before and after cancer surgery. The difference in the water molecular structure in body fluids before and after surgery was investigated.

Materials and Methods

The biological body fluids (urine, plasma and serum) were collected from 14 patients before and after different cancer surgeries at the Charité—Universitätsmedizin Berlin (Germany). NIR measurements were performed in the region 900–1700 nm using a portable fibre-optic NIRQuest512 spectrometer (Ocean Optics, Inc., Orlando, FL, USA). Principal component analysis (PCA) was used to describe the basic multidimensional characteristics of the NIR data matrix. PCA-loadings were analyzed in order to find the characteristic water bands and water matrix coordinates (WAMACs), showing changes in biological fluids before and after surgery.

Results

The mean spectrum of samples before surgery was subtracted from the samples after surgery and the difference is plotted (Fig. 1) to show the highest spectral variation between them. It is clearly seen that spectral shape for all of the fluids is very similar. Subtracted peaks with assignments are presented in Table 1.

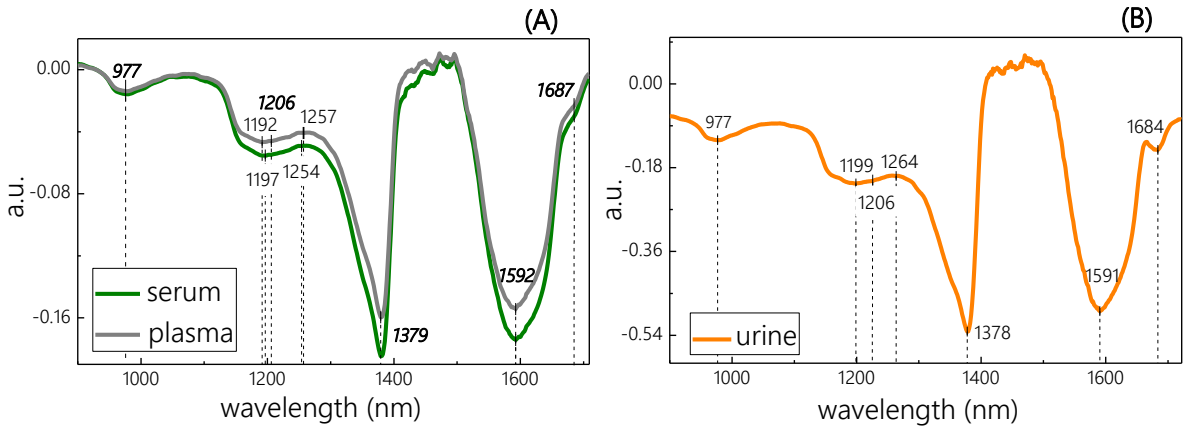

Figure 1. Subtracted average spectra of samples before and after surgery for (A) – serum, plasma, and (B) – urine.

Table 1. Assignment of the characteristic water absorbance bands.

Urine, nm	Plasma, nm	Serum, nm	Assignment
977	977	977	**976** nm - bulk water, strong correlation with water activity
1199	1192	1196	**1194.67** nm - $H^+(H_2O)_4$, 2nd overt. 2nd overtone Superoxide Tetrahydrate $O_2^-.(H_2O)_3$
1205	1206	1206	**1210.3** nm - 2nd overtone IHB stretch ($OH^-(H_2O)_3$)
1264	1257	1254	**1250.8** nm '-OH strech in fully hydrated hydronium, 2nd overt. **1268** nm - 'singlet oxygen
1378	1379	1379	**1379** nm - H_2O - $\nu_1+\nu_3$
1591	1592	1592	**1590.8** nm - aqueous proton $[H^+\cdot(H_2O)_6]$ - H_2O in $H_5O_2^+$ asymmetric stretch, 1st overt.
1684	1687	1687	**1682.9** nm - aqueous proton $[H^+\cdot(H_2O)_5]$ - H_3O^+ symmetric stretch, 1st overt.

PCA was also performed and provided further insights which will be presented.

Aknowledgment

This study was supported by the RSF project #19-79-00076.

References

1. Raja P., et al. (2019) Characterization of blood plasma of normal and cervical cancer patients using NIR Raman spectroscopy. Vibrational Spectroscopy 102: 1–7.
2. Artyushenko V., et al. (2015) Spectral fiber sensors for cancer diagnostics in vitro. Proceedings of the European Conference on Biomedical Optics. Munich, Germany, pp 21–25.
3. Dukor R.K. (2006) Vibrational spectroscopy in the detection of cancer. In: Handbook of Vibrational Spectroscopy. Hoboken, NJ, USA: John Wiley & Sons, Inc.
4. Asgari S. (2003) Intra-operative characterization of gliomas by near-infrared spectroscopy: possible association with prognosis. Acta Neurochirurgica 145: 453–460.
5. Tsenkova R., et al. (2018) Essentials of aquaphotomics and its chemometrics approaches. Frontiers in Chemistry 6:1–25.

Detection and quantification of hydrophobic pollutants in aqueous solution

Petya Stoykova [1,2*] Jelena Muncan [3], Hideyuki Inui[1] and Roumiana Tsenkova[3]

[1] Kobe University, Biosignal Research Center, Kobe, Japan;
[2] Agrobioinstitute, 1164 Sofia, Bulgaria;
[3] Kobe University, Graduate School of Agriculture, Biomeasurement Technology Lab, Kobe, Japan.

***** Presenting author and Correspondence: rtsen@kobe-u. ac.jp

Keywords: Dieldrin, NIRS aquaphotomics, Pesticides, Pyrene

Introduction

Contamination with persistent organic pollutants (POPs) is a global concern of high priority [1]. Monitoring of contamination is an important step to keep environment clean and ensure safe living.
Dieldrin is an extremely stable organochlorine insecticide, a harmful and widespread persistent pollutant. Pyrene is a representative of the polycyclic aromatic hydrocarbons, also a very harmful persistent contaminant. Aquaphotomics [2] Near infrared (NIR) spectroscopy approach is based on the analysis of information derived from the interaction between NIR light and water and evaluation of the changes in the molecular structure of water induced by a certain perturbation. Previous works have shown the feasibility of detection and quantification of different pollutants in water, such as heavy metals [3] and pesticides [4]. Further, aquaphotomics expanded the detection of contamination without relying on calibration for the specific compounds, and monitoring how the entire water spectral pattern changes over time [5] or as a consequence of purification treatment [6] instead.
The objective of this work is to explore the detection of hydrophobic pollutants, dieldrin and pyrene, in water solutions using aquaphotomics NIR spectroscopy as a novel cost-effective method. This work is a part of a larger platform for investigation of the potential of aquaphotomics for detection of hydrophobic compounds in various environments, including in vivo systems.

Materials and Methods

Samples preparation

For initial solubilization of dieldrin and pyrene as hydrophobic compounds the solvent dimethyl sulfoxide (DMSO) was used. Water solutions with final concentration from 0 to 100 ppm were prepared by direct dilution using ultra-pure Milli-Q water (Millipore, Molsheim, France).

Near infrared spectroscopy

NIR spectra of prepared solutions were acquired using RLA FOSS-XDS spectrometer (FOSS NIRSystems, Inc., Hoganas, Sweden). The spectra were acquired in the spectral range 400 – 2500 nm, with 0.5 nm step. The measurements of each sample were repeated in triplicates and randomized. During one, uninterrupted measurement of each sample, 5 consecutive spectra were recorded. The spectra of DMSO and pure water, after every 6 samples, were also acquired, giving 310 spectra in total for the analysis.

Aquaphotomics analysis

In order to explore which wavelength regions would be most informative, the spectra were split to several ranges: 400 – 700 nm, 700 – 1090 nm, 1110 – 1300 nm and 1300 – 1600 nm. Quantitative modelling of concentration was performed using Partial Least Squares Regression (PLSR) analysis on separated datasets of pyrene and dieldrin. The models were built for each of the previously defined spectral regions exploring a number of spectral pre-processing techniques. Calibration was performed using active class validation. The precision and accuracy of the PLSR models were evaluated using the following statistics: correlation coefficient

(r) of cross-validation, standard error of cross-validation (SECV) and optimum number of latent variables needed for the lowest SECV.

Results

The best quantification results of dieldrin and pyrene were achieved as follows: a) for dieldrin in the range 1110 – 1300 nm, using 1st derivative transformation, r2 = 0.93 and SECV = 8.25 ppm (Figure 1, left), and b) for pyrene, in the range 700 – 1090 nm, using smoothing, r2 = 0.99 and SECV = 0.79 ppm (Figure 1, right). Examination of the regression vectors of the respective PLSR models revealed that most influential variables include both the contribution of the contaminants themselves and of their impact on water molecular structure.

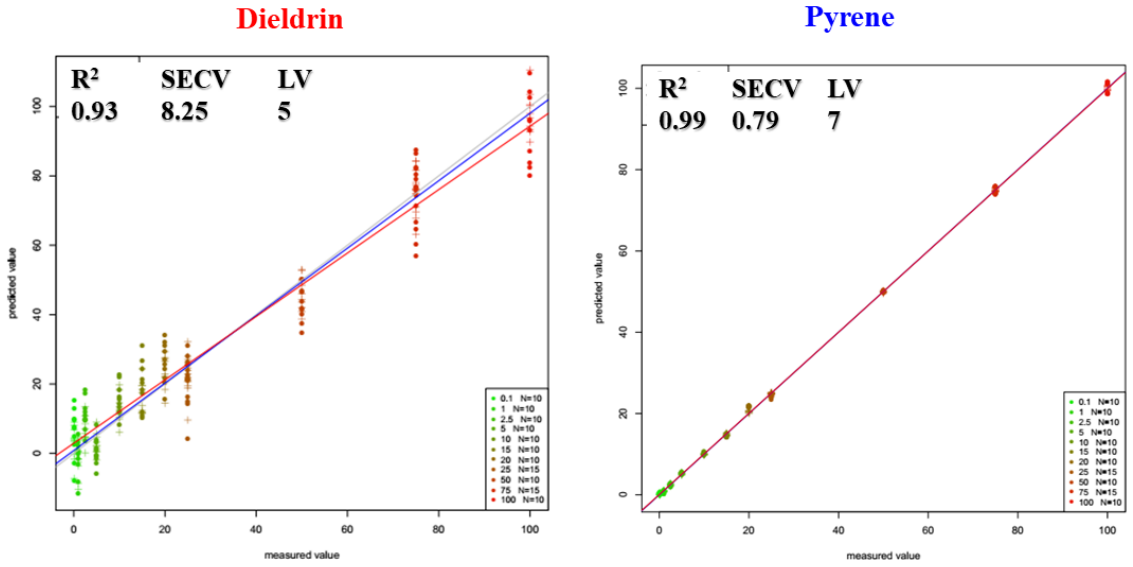

Figure 1. PLSR analysis: agreement of measured and actual concentration values for dieldrin (left) and pyrene (right)

Conclusions

The study resulted in a very good quantification of both types of POPs, in the ppm concentration range. The results indicated the high contribution of water matrix as a source of information on dissolved compounds. This work shows potential for further aquaphotomics investigation on the detection of hydrophobic compounds in other water-matrices environments, such as soil or biological systems.

References

1. Ashraf MA (2017) Persistent organic pollutants (POPs): a global issue, a global challenge. Environ Sci Pollut Res 24:4223–4227.
2. Tsenkova R (2009) Aquaphotomics: Dynamic spectroscopy of aqueous and biological systems describes peculiarities of water. J Near Infrared Spectrosc 17:303–313.
3. Putra A, Meilina H, Tsenkova R (2012) Use of near-infrared spectroscopy for determining the characterization metal ion in aqueous solution. 2nd Annu Int Conf Syiah Kuala Univ - Life Sci Eng Chapter 2:154–158.
4. Gowen AA, Tsuchisaka Y, O'Donnell C, Tsenkova R (2011) Investigation of the potential of near infrared spectroscopy for the detection and quantification of pesticides in aqueous solution. Am J Anal Chem 2:53–62.
5. Kovacs Z, Bázár G, Oshima M, et al (2015) Water spectral pattern as holistic marker for water quality monitoring. Talanta 147:598–608.
6. Muncan J, Matovic V, Nikolic S, et al (2020) Aquaphotomics approach for monitoring different steps of purification process in water treatment systems. Talanta 206:120253.

Is aquaphotomics suitable for the determination and analysis of perfluoroalkyl substances?

Jelena Munćan [1], Hideyuki Inui [2], Roumiana Tsenkova [1], Takeshi Nakano [3] and Vladimir Beškoski [4,*]

[1] Biomeasurement Technology Laboratory, Kobe University, Japan
[2] Biosignal Research Center, Kobe University, Japan
[3] Osaka University, Suita, Japan;
[4] University of Belgrade - Faculty of Chemistry, Serbia;
* Presenting author and Correspondence: vbeskoski@chem.bg.ac.rs

Keywords: perfluorooctanoic acid (PFOA), perfluorooctanesulfonic acid (PFOS), water electromagnetic spectrum

Introduction

Perfluoroalkyl and polyfluoroalkyl substances (PFASs) are chemicals that have been extensively used since the 1950s. Recently, they have been characterized as persistent, bioaccumulative and toxic, with a potential risk to the environment and humans [1]. Among PFASs, perfluoroalkyl acids (PFAAs) such as perfluorooctanoic acid (PFOA) and perfluorooctane sulfonic acid (PFOS) are the best known. Analysis of the presence of these compounds involves extraction from different matrices and the use of sophisticated, expensive instruments such as liquid chromatography (LC)–tandem mass spectrometer (MS/MS) [2]. Having in mind that Aquaphotomics is based on so called "water molecular mirror approach", where all the components of the aqueous system and surrounding energies influence the water structure, our starting hypothesis is that PFAAs dissolved in water will have influence on water electromagnetic (EM) spectrum [3]. To confirm this, near infrared spectra of water with various concentrations of PFOA and PFOS, were studied.

Materials and Methods

PFOS (>98% purity) was obtained from Tokyo Chemical Industry Co., Ltd. (Tokyo, Japan). PFOA (96% purity, 99.9% by GC area) was obtained from Sigma-Aldrich (St. Louis, MO). For the samples of PFOA and PFOS were prepared by direct dilution in ultra-pure water from 100 ppm to 10 ppb (Table 1.) The samples were prepared in duplicates.

Table 1. Final concentrations of PFAAs water solutions

	I group (ppm)				II group (ppm)				III group (ppb)				IV group (ppb)				
PFAAs	**100**	**75**	**50**	**25**	**10**	**7.5**	**5**	**2.5**	**1000**	**750**	**500**	**250**	**100**	**75**	**50**	**25**	**10**

The spectra of solutions were recorded using RLA FOSS-XDS spectrometer (NIRSystems, Inc., Hoganas, Sweden) in the spectral range 400 – 2500 nm, with the 0.5 nm step at controlled temperature T=28±1°C. For each measurement 5 consecutive spectra were recorded. The measurements of all samples were randomized. In total 425 spectra for the analysis were acquired. The data analysis was performed following the protocol [3] and aquagrams were calculated on spectra preprocessed using extended multiplicative scatter correction.

Results

The initial exploration of spectra of PFOS and PFOA water solutions, by comparing and subtracting the averaged spectra, revealed distinctive difference in water spectral pattern in the 1st overtone of water (1300-1600 nm) (Figure 1a). The quantitative analysis was performed separately for each contaminant in water, and the accuracy of developed models was compared for different ranges of concentrations (Tab.1) and for different spectral regions (700 – 1000 nm, 1300-1600 nm). The quantification model for PFOS was possible to obtain for the range 700-1000 nm, for I group range of concentrations (25 – 100 ppm), using raw spectra, resulting in the correlation coefficient r^2=0.62 and standard error of cross-validation was SECV=20.4 ppm. The

quantification of PFOA was not possible, which indicated that scattering is the phenomena behind the successful modeling of PFOS concentrations (for the range of concentrations 25 – 100 ppm).

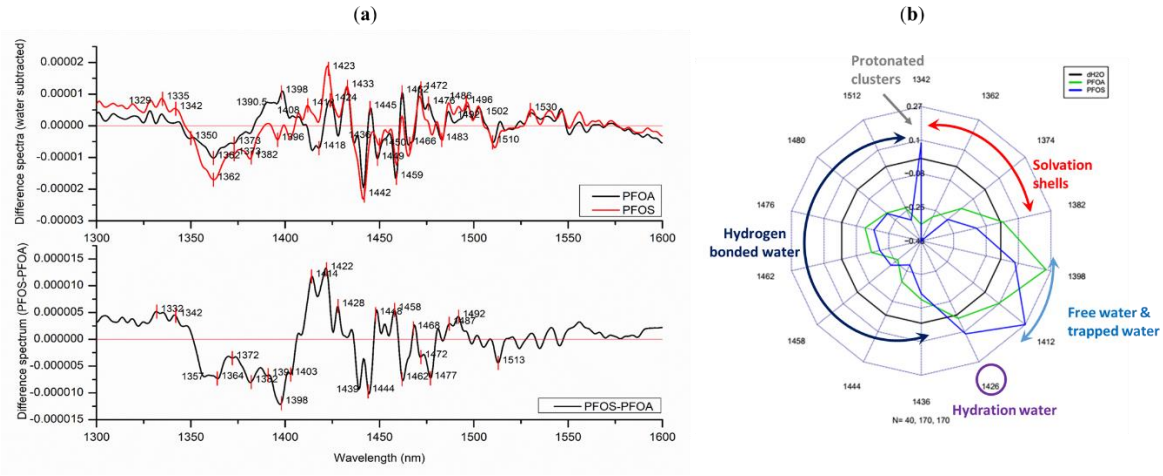

Figure 1. Aquaphotomics analysis showed distinctive difference between PFOA and PFOS water interaction: (a) Difference between averaged spectra for each contaminant solution and averaged spectra of pure water (a, above) and difference between averaged spectra of contaminant solutions (a, below); (b) Averaged aquagrams of water solutions of PFOA and PFOS normalized to pure water

This finding furthered the investigation into the differences in interaction with water of the two compounds. Comparison of water spectral patterns using aquagrams (Figure 1b) revealed that PFAAs solutions in comparison with pure water, have less hydrogen-bonded and solvation water, while more free, trapped and hydration water. High ratio of free water to hydrogen-bonded water was shown to lead to reduction of surface tension [4]. The difference between the compounds, is in different types of free water, which in the case of PFOA is confined (trapped). The largest difference, however, is in the presence of protonated and hydration water in the case of PFOS. Protonated water has a crucial role in self-assembly [5], whereas hydrated water was found to be characteristic of micelle hydration [6].

Conclusions

Aquaphotomics investigation showed differences in interaction of PFOS and PFOA with water. For the first time, spectral pattern of surfactants in water was identified, and how the differences in water molecular structure govern the self-assembly (depending on the type and concentration of compound).

References

1. Buck RC, Franklin J, Berger U, et al., (2011) Perfluoroalkyl and polyfluoroalkyl substances in the environment: terminology, classification, and origins. Integrated Environmental Assessment and Management 7:513–541.
2. Beškoski VP, Yamamoto K, Yamamoto A, et al., (2017) Distribution of perfluoroalkyl compounds in Osaka Bay and coastal waters of Western Japan, Chemosphere, 170:260–265.
3. Tsenkova R, Munćan J, Pollner B and Kovacs Z (2018) Essentials of Aquaphotomics and Its Chemometrics Approaches. Frontiers in Chemistry 6:363.
4. Takeuchi M., Sakamoto K., Martra G., et al (2005) Mechanism of photoinduced superhydrophilicity on the TiO2 photocatalyst surface. The Journal of Physical Chemistry B, 109(32):15422–15428.
5. Muncan J. Kovacs Z., Pollner B., et al., (2021) Near infrared aquaphotomics study on common dietary fatty acids in cow's liquid, thawed milk. Food Control, 122:107805.
6. Kon-no K., (1997) The Control of Morphology, Crystalline Forms and Dispersability of Colloidal Particles by Solubilized States of Water in Reversed Micellar Solutions, Journal of Japan Oil Chemists' Society, 46 (4):373–457.

Application of aquaphotomics to detect different sugar syrup adulteration of honeydew honey

Zsanett Bodor*[1], Csilla Benedek[2], Zoltan Kovacs[1]

[1] Hungarian University of Agriculture and Life Sciences, Faculty of Food Science and Technology, Department of Measurement and Process Control, 14-16 Somlói street, H-1118, Budapest, Hungary
[2] Semmelweis University, Faculty of Health Sciences, Department of Dietetics and Nutrition, 17. Vas street, H-1088, Budapest, Hungary
* Zsanett.bodor93@gmail.com

Keywords: honey, fraud, NIRS, aquaphotomics

Introduction

Honey is a well-known food and medical product worldwide, used and consumed for its rich nutritional content. Honey has a relatively high price on the market, therefore more and more fraudulent activities present related to this product. One of the most common adulteration types is the mixture of honey using different sugar syrups such as rice, beet, cane, corn and so on. The detection of adulteration of honey with sugar syrups is challenging [1]. The aim of this study was two determine the potential of aquaphotomics to detect and quantify adulteration of honey with different sugar syrups [2] at low levels. Further aim was to reveal the structural changes of water as a result of the adulteration.

Materials and Methods

In our study honeydew honey from forest region was used. Rice syrup (RS), F40 corn syrup (FS), and self-made fructose-glucose (GF) syrup (80% sugar content where ratio of glucose and fructose was 40:60, 20% distilled water) was added to honey in different concentrations: 3, 5, 10 w/w%. Control sample was kept at 37°C until all the crystals dissolved, then mixture samples were prepared, and incubated for 37°C followed by mixing to ensure homogenization. Each sample was prepared in three replicates (R1, R2, R3) including control and syrup, resulting in 39 samples. Transflectance spectra of the samples were collected using MetriNIR benchtop instrument in the spectral range of 740-1700 nm. The layer thickness of the sample in the cuvette was 0.5 mm, and the cuvette was thermo-regulated at 25°C with the help of water circulation. For statistical analysis the spectral range of 1300-1600 region was applied. All the samples were recorded using three consecutive scans resulting in nine scans per samples. Spectra was pretreated using Savitzky-Golay smoothing (2nd order polynomial, 21 sample points, no derivation) and multiplicative scatter correction was used for the baseline shift correction. Principal component analysis was applied to see discrimination patterns and detect outliers, while linear discriminant analysis using three-fold cross-validation was applied to reveal the discrimination of the samples according to their syrup concentration level. Partial least square regression was used to regress on the added concentration levels, where leave-one-sample-out cross validation was applied to validate the models. Classic Aquagrams were used to visualize the patterns of the water structural changes using the most contributing wavelengths in the PCA, LDA and PLSR models. In the case of all the statistical methods at first the models were built using the spectra of the syrups and the control honey to see the spectral pattern of the adulterants comparing honey. Then the samples adulterated using the different syrups were analyzed separately according to the type of the syrup. The 100% syrup was excluded in the case of RS and FS, but included in the case of GF adulterated honeys. Statistical analysis was performed in R-project with the help of the aquap2 package [3].

Results

Results obtained for the model containing only the spectra of the clean honey and clean syrups showed 100% classification, so all the syrups could be separated from the control sample based on the LDA models, however it should be highlighted that self-prepared GF was the most similar to the original honey ,while aquagrams also showed that the GF syrup is more similar to the honey (Figure 1. a). Analysis of the samples adulterated with

the syrups showed different results in the case of the three different syrups. Classification accuracies of LDA were various according to the syrup type, where the average correct classification of validation was between 91.1-100%. In the case of FS and RS control sample was classified correctly, while in the case of GF misclassification of the control honey sample was found belonging to 3% GF syrup adulterated samples. Determination coefficient during PLSR analysis ranged between 0.90-0.96 during validation, where honey adulterated using F40 syrup had the highest correlation between original and predicted data and the model of honey samples adulterated with GF had the lowest. Aquagrams revealed that the highest differences between control and adulterated samples can be found in the range of 1400-1420 region that can be assigned to water molecules with less hydrogen bonds and in the range of 1570-1600, that shows that that important differences can be found in the sugar content of the samples. Aquagrams also showed that RS and FS syrups are more characterized by water molecules with less hydrogen bonds while the water structure of the GF syrup is more similar to honey.

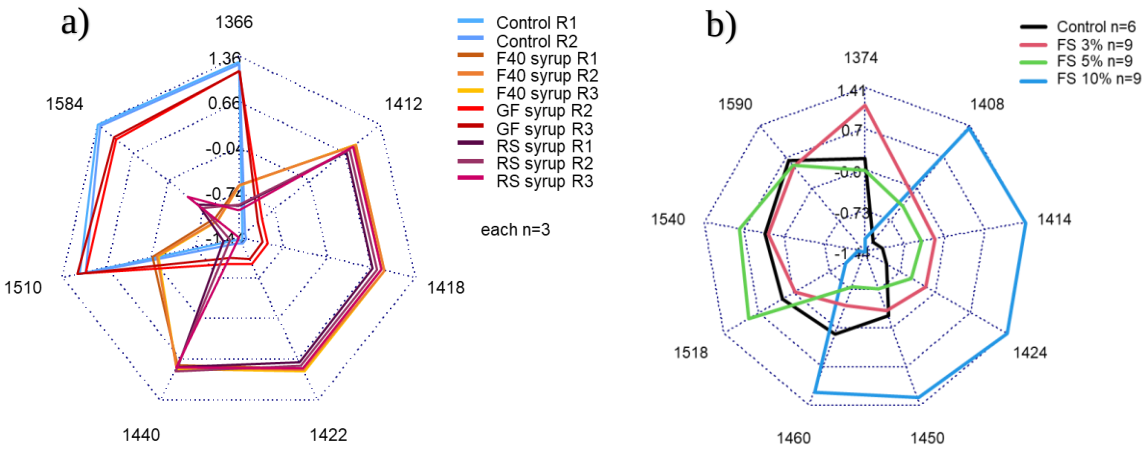

Figure 1. Aquagram after Savitzky-Golay Smooting and Multiplicative Scatter Correction (1300-1600nm) a) aquagram of the honey and syrup samples b) aquagram of the control and samples mixed with F40 syrup

Conclusions

Results of our study showed that sugar syrups from commercial origin are more characterized with free water molecules. The spectral pattern of the self-made syrup was similar to the spectral pattern of honey which is more described by strongly bonded water. Moreover, our results showed that adulteration detection and accuracy of classification is depending on the syrup type, therefore it has high importance of analyzing and build models using more type of syrup.

This paper was supported by the ÚNKP-20-3-II-SZIE-12 New National Excellence Program of the Ministry for Innovation and Technology from the source of the National Research, Development and Innovation Fund and the Doctoral School of Food Science (Hungarian University of Agriculture and Life Sciences).

References

1. European Commission (2018) Technical Round Table on Honey Authentication. Belgium
2. Bázár G, Romvári R, Szabó A, et al (2016) NIR detection of honey adulteration reveals differences in water spectral pattern. Food Chem 194:873–880. https://doi.org/10.1016/j.foodchem.2015.08.092
3. Kovacs Z, Pollner B (2016) Aquaphotomics-Software R-Package „aquap2“. In: Understanding Water in Biology 2nd International Symposium. pp 18–20

Application of NIRS and Aquaphotomics for Diluted Meat Extract Characterization

John-Lewis Zinia Zaukuu [1]*, Zoltan Gillay [1] and Zoltan Kovacs [1]

[1] Hungarian University of Agriculture and Life Science, Department of Measurements and Process Control * Presenting author and Correspondence: izaukuu@yahoo.com

Keywords: Authentication, Mincing, Absorption, Beef, Pork

Introduction

Meat is a central part of diets around the world and is considered as a primary source of protein across the globe. Its misrepresentation could have bad implications from religious and moral perspectives as people have different preferences of meat they wish to consume. According to the European Union regulations [1], even if different types of meats are mixed through processes such as mincing, their content should be fully labelled in accordance with labelling regulations. Requirements such as these have led to the exploration of rapid and advanced technologies such as the near-infrared spectroscopy (NIRS). In combination with the novel interdisciplinary scientific field known as aquaphotomics, the technique can provide information through vibrational bonding in the form of overtones and combination bands, especially in the first overtone of water, which can be interpreted with advanced statistical tools. The aim of this study was to apply NIRS and aquaphotomics to discriminate different concentrations of meat mixtures.

Materials and Methods

Fresh beef and pork thigh were purchased from reputable supermarkets (SPAR) in Budapest, Hungary and minced in the laboratory before mixing. Three repeats each of 100%, 97%, 95%, 90%, 85% and 80% w/w beef/pork mixtures, were prepared and extracted using three newly developed extraction methods: raw meat extraction, frozen extraction and cooked meat extraction. Raw meat extraction: 20g of meat mixture was transferred into a 200 mL volumetric flask and filled up to volume with distilled water then homogenized by vigorously shaking in the flask for 3 minutes then filtered. Frozen meat extraction method: 20g of raw meat mixture was stored by refrigerating at a temperature 5 °C. The samples were removed on the second day of storage, thawed by putting into a water bath of 50 °C for 20 minutes and extracted in the same way as described for the raw meat extraction method. Cooked meat extraction method: 20g of raw meat mixture was put in a cooking pot containing 200 mL distilled water at room temperature, covered with the lid and boiled for five minutes at a temperature between 150-200°C using a commercial electric hot plate (Sencor, SCP 1502SS) then filtered. Dilutions of 1% w/v aqueous dilution were prepared for each mixture using the obtained filtrates.
Spectra collection was done using the MetriNIR (MetriNIR Research, Development and Service Co., Budapest, Hungary) and a thermoregulated cuvette of 0.4 mm layer thickness. Three consecutive spectra of each minced meat mixture (without extraction) were collected at room temperature. Three consecutive transflectance spectra of each diluted meat mixture was also collected after extraction with the three different extraction methods.
Raw spectra inspection was performed and principal component analysis (PCA) was used to detect and remove outliers before classifying the different meat mixtures using linear discriminant analysis (LDA) at a wavelength range of 1300-1600 nm. Three-fold cross-validation was used to evaluate the predictive significance of the developed models. Aquagrams were also developed to visualize water spectral patterns of 80%, 90% and 100% w/w beef/pork mixtures.

Results

When the raw minced meat mixture extracts were visualized in PCA, the wavelengths 1346, 1466 and 1516 nm contributed most in the PCA loading vectors. Using LDA to classify the different meat mixtures, there was average recognition accuracy of 83.33% and average prediction of 80.99%. Only the 80% w/w and 85% beef/pork mixtures yielded 100% correct classification with cross-validation from the rest of the samples. There

were misclassifications between 90%, 95%, 97% and 99% beef/pork mixtures. When the diluted meat extracts from the raw extraction method were visualized in PCA, the wavelengths 1404, 1372, 1466 and 1516 nm contributed most in the PCA loading vectors. Using LDA to classify the different meat mixtures, there was average recognition accuracy of 89.69% and average prediction of 85.72%. Beef/pork mixtures of 90%, 95%, 99% and 100% yielded 100% classification accuracy with cross-validation. There were misclassifications between 80%, 85% and 97% beef/pork mixtures. When the diluted meat extracts from the cooked extraction method were visualized in PCA, the wavelengths 1404, 1400, 1522 and 1534 nm contributed most in the PCA loading vectors. Using LDA to classify the different meat mixtures, there was average recognition accuracy of 89.68% and average prediction of 44.49%. All the diluted meat extracts showed misclassifications. When the diluted meat extracts from the frozen extraction method were visualized in PCA, the wavelengths 1404, 1400, 1466 and 1522 nm contributed most in the PCA loading vectors. Using LDA to classify the different meat mixtures, there was average recognition accuracy of 97.62% and average prediction of 60.37%. All the diluted meat extracts showed misclassifications. The identified wavelengths in the PCA loading vectors also, proved vital for visualizing water spectral patterns in 100%, 90% and 80% w/w beef/pork mixtures (Figure 1).

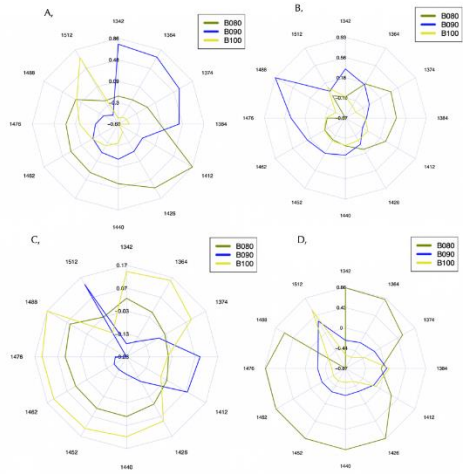

Figure 1. Aquagram plots from the analysis of minced unextracted raw meat mixtures (A), extracted minced meat using the raw meat extraction method (B), cooked meat extraction method (C) and frozen meat extraction method (D)

Conclusions

Using the aquaphotomics approach with 1%w/v dilution, NIRS could discriminate 100%, 97%, 95%, 90%, 85% and 80% w/w beef/pork mixtures. The samples extracted using the raw meat extraction gave classifications accuracies that were even better those achieved were the raw minced meat mixtures were scanned. The wavelengths 1404, 1372, 1466 and 1516 nm contributed most in the PCA loading vectors using this method and also, in aquagrams.

References

1. European Union (2011) Regulation (Eu) No 1169/2011 of the European Parliament and of the Council of 25 October 2011 on the provision of food information to consumers, amending Regulations (EC) No 1924/2006 and (EC) No 1925/2006 of the European Parliament and of the Council, an. Off J Eur Union 304:18–62. https://doi.org/10.1075/ttwia.27.04ker

Monitoring of brown rot caused by *Monilia fructigena* on plums with the aquaphotomics approach

Flora Vitalis [1,*], Juan Pablo Aguinaga Bósquez [1], Balkis Aouadi [1], Zsanett Bodor [1], John-Lewis Zinia Zaukuu [1], Zoltan Gillay [1], Zoltan Kovacs [1]

[1] Department of Measurements and Process Control, Institute of Food Science and Technology, Hungarian University of Agriculture and Life Sciences, 1118 Budapest, Hungary;
* Presenting author and Correspondence: vitalis.flora@hallgato.uni-szie.hu

Keywords: plum, storage, brown rot, aquaphotomics,

Introduction

Fruits and fruit products play a very important role in the human nutrition, they are very good sources of compounds with positive physiological effect. Plums are one of the most important stone fruits, they can be found on the market shelves, both fresh or processed. Plums are particularly sensitive and perishable fruits that ripen quickly after harvest, resulting in a short postharvest lifespan. The shelf life of these fruits is about 2-6 weeks [1]. The rapidness and quality of complex changes during ripening, harvesting, and storage are highly dependent on environmental influences such as temperature, humidity, microbiological contamination, and treatment. It is not uncommon for these changes to adversely affect the physicochemical and organoleptic properties of fruits. Monilinia species causing brown rot on fruits during fruit cultivation, harvesting, or storage can result in losses of up to 80% under favorable environmental conditions for the fungus [2]. Rapid and non-invasive near-infrared (NIR) spectroscopy-based methods are becoming widespread in the determination of physiological condition and certain quality traits of fruits in addition to empirical and/or laboratory-based, often destructive and costly techniques. Change in ambient conditions or infection on the fruit result in alterations that are initially invisible to the naked eye, but can be identified from the spectral patterns [3]. Due to the naturally high water content of fruits, thusly plums, the “water mirror” approach of aquaphotomics is presumably suitable for mapping the differences that occur [4, 5]. Our research focused on monitoring changes in plums during storage. The study aimed to apply NIRS and aquaphotomics for monitoring of quality change of fruits stored under different conditions and early detection of Monilia fructigena infection.

Materials and Methods

The plums were divided into two groups for refrigerated and room temperature storage, and their surface was disinfected. About 1 cm of cut was applied to the surface of one-third of the plums with a sterile knife and was infected with Monilia fructigena fungal mycelium. The second third of the plums were infected on the fruit surface without injury. The remaining third was left intact, these formed the control group. Five parallel sample preparations were performed per sample group. The resulting 30 plum samples (i. e. 2 × 3 × 5) were subjected to NIR-based analysis. The spectral data were collected with a NIR-S-G1 (InnoSpectra Co., Hsinchu, Taiwan) hand-held reflectance spectrometer in the wavelength range of 900-1700 nm. Spectra were recorded along the vertical axis of the fruits (from stalk to apex) at five measurement points. Three consecutive scans were recorded at each measurement point. The measurements were performed twice daily for eight days. A total of 450 sample spectra (i. e. 30 × 5 × 3) were collected per measurement occasion. The data were evaluated in the wavelength range of 1300-1600 nm after combined spectral pretreatments. Exploratory principal component analysis (PCA) was used to map the patterns and to identify outliers in the data. Soft independent modeling of class analogies (SIMCA) was applied as supervised methods to discriminate and classify samples. Aquagrams were constructed to illustrate the trends hidden in the data.

Results

Visible signs of Monilia infection were observed after two days only on plums with injured surfaces and stored at room temperature. The results showed high variability, therefore the constructed models had to be optimized

in each case using different spectrum pretreatment methods. It was confirmed by PCA that the location of the spectrum acquisition on the plums was also influential, so it was worth examining them separately. In this way, it was possible to determine which measuring points on the surface of the fruits were the most suitable to discriminate storage time or sample groups. The SIMCA interclass distances indicated demonstrably large differences between infected plums stored under different conditions. Of all sample groups, the largest interclass distances were detected in the results of injured plums. However, there was no incontrovertible distinguishability within sample groups. The spectral patterns of plums showed a dynamic change over the storage time. The similarity in the patterns was that the plums initially showed markedly low absorbance around 1512 nm, which can be attributed to the absorption band of strongly bound water molecules. In the range of 1411 to 1489 nm, the absorption gradually decreased. The absorbance of plums stored under refrigerated conditions increased between 1365 and 1384 nm (Fig. 1a), while samples stored at room temperature behaved oppositely (Fig. 1b).

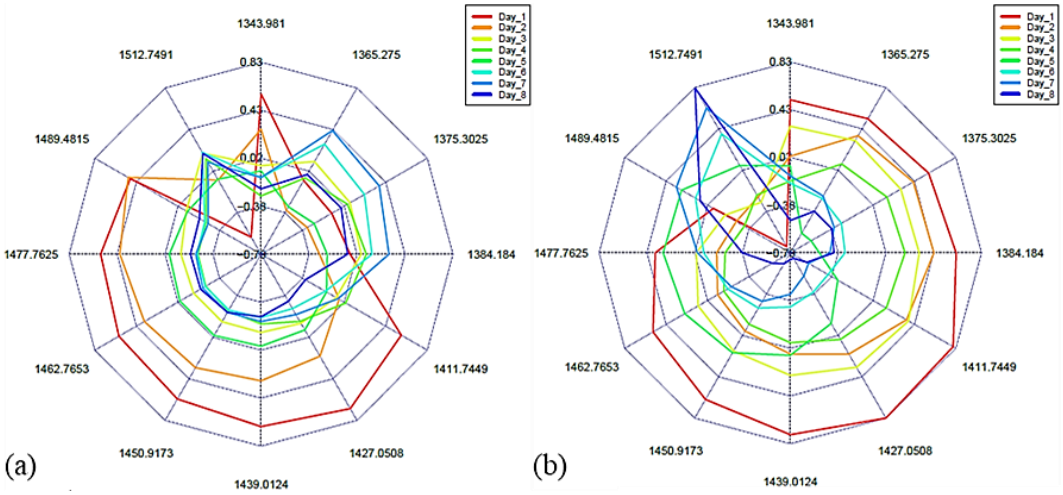

Figure 2. Aquagrams of plums infected with Monilia through injury stored at refrigerated (a) and room temperature (b)

Conclusions

In the present study, the alterations caused by Monilia fructigena fungal infection were monitored in plums. The research results are of both economic and scientific significance, as postharvest technologies and Monilia infection can cause large losses and there are few scientific sources on the use of rapid analytical methods in this area, especially for plums. There were detectable changes in plums during storage. Due to the natural variability of the fruits, it would be worthwhile to conduct further experiments with larger sample size.

References

1. Manganaris GA, Crisosto CH (2020) Stone fruits: Peaches, nectarines, plums, apricots. In: Controlled and Modified Atmospheres for Fresh and Fresh-Cut Produce. Elsevier, pp 311–322
2. Aiello D, Restuccia C, Stefani E, et al (2019) Postharvest biocontrol ability of Pseudomonas synxantha against Monilinia fructicola and Monilinia fructigena on stone fruit. Postharvest Biol Technol 149:83–89
3. Jinendra B, Tamaki K, Kuroki S, et al (2010) Near infrared spectroscopy and aquaphotomics: Novel approach for rapid in vivo diagnosis of virus infected soybean. Biochem Biophys Res Commun 397:685–690
4. Tsenkova R (2010) Aquaphotomics: Water in the biological and aqueous world scrutinised with invisible light. Spectrosc Eur 22:6
5. Kaur H (2020) Investigating aquaphotomics for fruit quality assessment. The University of Waikato

Poster Session II

Can carbohydrates change the shape of water?

Vladimir Beškoski [1], Jelena Munćan [2,*], Branka Lončarević [3], Gordana Gojgić-Cvijović [3], Dragica Jakovljević [3], Hideyuki Inui [4] and Roumiana Tsenkova [2]

[1] University of Belgrade - Faculty of Chemistry, Serbia;
[2] Biomeasurement Technology Laboratory, Kobe University, Japan
[3] University of Belgrade – Institute of Chemistry, Technology and Metallurgy, Serbia;
[4] Biosignal Research Center, Kobe University, Japan;
***** Presenting author and Correspondence: jln.muncan@gmail.com

Keywords: D-Glucose, D-Fructose, Sucrose, GOS, FOS, Inulin, Pullulan, Levan

Introduction

Aquaphotomics is a relatively novel scientific discipline which can be used for elucidation of structural and related functional properties of aqueous systems [1]. The aim of this study was to analyse water solutions of carbohydrates of different size from monosaccharides (glucose and fructose) via, disaccharides (sucrose), gluco and fructo-oligosaccharides and various selected polisaccharides (based on glucose and fructose, respectively) using Aquaphotomics [2,3]. Knowing that main functions of carbohydrates within our body are various: providing energy and regulation of blood glucose; sparing the use of proteins for energy; breakdown of fatty acids and preventing ketosis; biological recognition processes; flavor and sweeteners and dietary fibers who can promote digestive health, knowledge about their interaction with water molecules can have strong influence on our understanding of some basic but also complex metabolic processes.

Materials and Methods

The following carbohydrates were prepared for near infrared spectroscopy measurements by direct dilution: monosaccharides (D-glucose and D-fructose), disaccharide (sucrose which is composed of two monosaccharides: glucose and fructose), GOS – gluco-oligosaccharide (oligosaccharide based on glucose), FOS – fructo-oligosaccharide (oligosaccharide based on fructose), and polisaccharides (pullulan - polysaccharide based on glucose units; inulin - polysaccharide based on fructose units; levan - polysaccharide based on fructose units). Solutions of carbohydrates were prepared in ultra-pure water in concentrations 2, 4, 8, 6 and 10 g/L**.**

The spectra of solutions were recorded using RLA FOSS-XDS spectrometer (NIRSystems, Inc., Hoganas, Sweden) in the spectral range 400 – 2500 nm, with the 0.5 nm step at controlled temperature T=28±1°C. For each measurement 5 consecutive spectra were recorded. The measurements of all samples were randomized. In total 615 spectra for the analysis were acquired. The data analysis was performed following the aquaphotomics protocol [4] which included spectral exploration using subtracted spectra and principal component analysis (PCA), while supervised classification analysis Soft independent modelling of class analogies was used to inquire about the differences between different types of sugar at each concentration level.

Results

The averaged spectra for each sugar separately (calculated by averaging of all spectral replicates, spectral consecutives and concentrations) from which the average spectrum of pure water was subtracted are presented in Fig.1. These difference spectra show distinct features for each of the examined sugars, but compared to pure water have in general less free water (~1410 nm), and more hydrogen bonded water (~ 1580 nm), meaning that all the sugars are acting like structure-making agents. The peak at 1410 nm shows - increase in the negative value in the order of the polysaccharide – oligosaccharide – disaccharide – monosaccharide, and also a red shift – shift of the peak towards the longer wavelengths which shows differences in water organization depending

on the sugar type – from free water to water involved with hydration (~1416 nm). The differences are most pronounced in the regions indicated with red squares on Fig.1.

The results of SIMCA analysis for each concentration level showed 100% accuracy of discrimination even for the lowest concentrations spectral dataset, for which the interclass distances were the lowest, however still large, in the range 2.49 to 21.57 (the average being 6.91), which shows reliable separation of classes. The exploration of discriminative powers from each SIMCA model showed the most important wavelengths in the spectra of sugar solutions for discrimination between sugars, at each concentration level (Fig. 2). With the increasing concentration of sugars, the discriminating powers showed larger values, particularly large in the region 1610-1760 nm, at the same, particular bands, traditionally associated with the vibrations of carbohydrates [5].

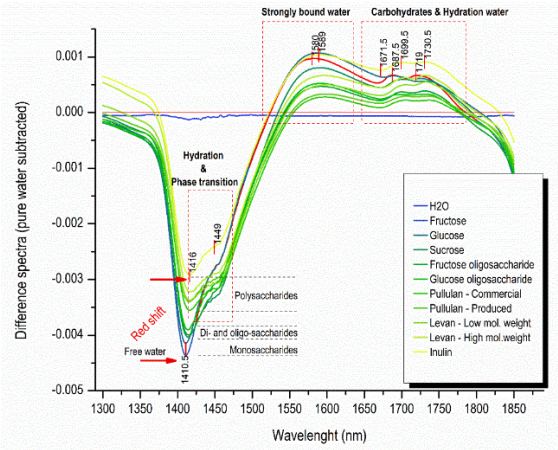

Figure 1. Structural changes of water induced by different sugars – difference spectra.

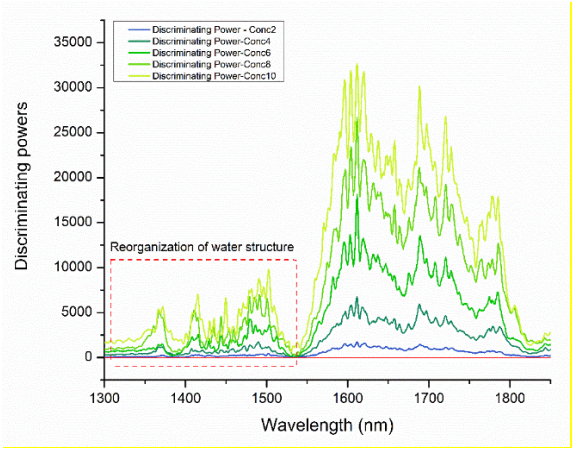

Figure 2. SIMCA analysis – discriminative powers of SIMCA models built for classification of sugars at each concentration level separately.

However, the region 1310 – 1530 nm, associated with the water molecular vibrations showed subtle shifts of the absorbance bands and the changes in the ratios of the sub-bands indicating that water molecular structure rearranges specifically depending on the sugar and concentration together, and that this spectral region shows the cooperative effect as reported in a recent literature [5].

Conclusions

Bacterial exopolysaccharides, such as levan can acts as an antiviral, antioxidant, antitumor and anti-inflammatory agent. Fungal exopolysaccharides including pullulan, has shown unique structural and physicochemical properties, providing high water solubility, low biodegradability and good fiber and film forming capacity. Near infrared spectroscopy study of these molecules can lead to a better understanding of the hydration of carbohydrates and the related functionality in many areas of applications: food industry, medicine, cosmetics, pharmacy, agriculture, environmental protection, etc. It should be emphasized that for example, it is known that the plants accumulate some of these sugars as a part of the stress response to cold or dehydration. Heaving in mind climate changes and growing demands for food on our planet, studies in the field of interaction of carbohydrates and water using aquaphotomics can help us in the field of biotechnology for the production of novel more resilient plant species.

References

1. Tsenkova R, Munćan J, Pollner B and Kovacs Z (2018), Front Chem 6:363.
2. G.D. Gojgic-Cvijovic GD, Jakovljevic DM, et al (2019), Int J Biol Macromol, 121:142–151.
3. B. Lončarević B, Lješević M, Marković M, et al (2019), Ecotoxicol Environ Saf 181:187–193.
4. Tsenkova, R., Munćan, J., Pollner, B., & Kovacs, Z. (2018), Front Chem, *6*, 363.
5. Beganović, A., Beć, K. B., et al. (2020), Spectrochim. Acta A Mol. Biomol. Spectrosc, 237, 118359.

Spectral study on low frequency Raman of hydrogen-bonded substances on the surface of icy moons

Yasuhiro Miwa[1,*], Hanae Ozaki[1] , and Atsushi Tani[1]

[1] Graduate School of Human Development and Environment, Kobe University, Kobe, 657-8501, Japan;
***** Presenting author and Correspondence: 186d415d@stu.kobe-u.ac.jp

Keywords: Icy moons, Salt hydrate, Terahertz

Introduction

The surface environment of icy moons is governed by ice, salt, and hydrogen-bonded materials consisting of water ice and various salts. Europa, a Jupiter's moon, has a relatively young surface with many complex cracks and ridges, indicating that the geological surface is active. On Saturn's moon Enceladus, cracked terrain is also observed. As several explorations and observations have revealed candidate constituents on the icy moon surface [1], the main constituent salts are a combination of four different ions (Na+, Mg2+, Cl-, SO42-): for example, magnesium sulfate hydrates (epsomite MgSO4·7H2O and meridianiite MgSO4·11H2O), magnesium chloride hydrates, and sodium sulfate hydrate (mirabilite Na2SO4·10H2O). In contrast to the knowledge of the constituent materials, the interaction between water and salts in the constituent materials, such as the crystal states that reflect the actual surface environment conditions in detail, has not been considered well. In fact, the surface environment is expected to be locally diverse due to heat transport in the inner ocean, effects from material circulation, and reactions caused by radiation from space to the surface [2]. The hydration number of magnesium sulfates and chlorides may be changed, and the hydration state may differ from the stable phase.

In this case, it is significant to focus on the hydrogen-bonded materials that constitute such diverse surface environments because the surface environment assumed by the known parameters of surface temperature and constituent materials is not sufficient to understand the geological activities occurring on the surface. The molecular interactions observed by terahertz spectroscopy, which can identify salt crystal polymorphs and reveal their ordered structures [3], can reveal how the solid surface materials are assembled and what kind of aggregates they form. In this study, we focused on the salt hydrates that are the basis of the solid materials that compose the surface environment of icy moons like Europa and Enceladus, and investigated the possibility of their evaluation by terahertz spectroscopy using sulfate and chloride salts for systematic comparison.

Materials and Methods

$MgSO_4 \cdot 7H_2O$ and $MgCl_2 \cdot 6H_2O$ were purchased commercially. The anhydrate sample of $MgSO_4$ was prepared by heating $MgSO_4 \cdot 7H_2O$ at 260°C for 30 minutes under vacuum. The sample of $MgCl_2 \cdot 2H_2O$ was prepared by heating $MgCl_2 \cdot 6H_2O$ at 140°C for 20 minutes under vacuum.

The powdered samples were packed into carousel cells, and the carousel was placed in the Raman measurement holder. Low frequency Raman experiments were performed at room temperature in the range of 50-1500 cm^{-1} by DXR Smart (Thermo Fisher Scientific Inc.). The spectral resolution was 5 cm^{-1} and the wavelength and power of the laser was 780 nm and 150 mW, respectively. Scan times was 5 times and exposure time in each scan was 60 s. After the measurement, reduced Raman process [4] was applied to the obtained spectra especially in the low frequency region by reducing the effect of thermal excitation. The hydration number of epsomite, anhydrous salt, and hydrated $MgCl_2$ samples was confirmed because the peaks corresponding to the anionic mode were good agreement with those in previous studies [5, 6].

Results

In Epsomite, two peaks were mainly detected around 65 and 255 cm^{-1}, while in $MgSO_4$ anhydrous salt, no clear peak around 65 cm^{-1} was detected. In $MgCl_2 \cdot 6H_2O$, there was a broad peak around 200 cm^{-1} and a clear peak

at 64 cm^{-1}. In contrast, in $MgCl_2 \cdot 2H_2O$, there were two peaks with different widths and intensities from those of hexahydrate and an additional peak at 130 cm^{-1} were identified.

For the region of 100-300 cm-1, the observed peaks are related to cations and anions. In epsomite, broad peak around 255 cm-1 is attributed to O-H···O of sulfate ion [7]. On the other hand, the peak around 200 cm-1 of MgCl2•6H2O is considered to be due to the low wavenumber shift caused by the difference in anions in comparison with the results in sulfates. Furthermore, below 100 cm-1, the peak at 64 cm-1 of MgCl2•6H2O was shifted to lower wavenumber and was sharper than that of epsomite. The differences between MgSO4 and MgCl2 can be attributed to the charge density and size of the anions. In the case of SO42-, the high charge density anion affects the ion-water electrostatic interaction, which includes ion-dipole interactions and ion-water molecular interactions. In the case of Cl-, which is a low charge density anion, hydrogen bonding between water and anion is considered to be the main interaction [8]. At the peak position, MgSO4 became high wavenumber due to the effect of high charge density. In MgCl2, since Cl- has a small ionic radius and spherical symmetry, its motion is simple and the peak is sharp.

In addition, a strong peak around 65 cm-1 was observed only for those with a large hydration number, indicating that water molecules are involved in this mode. In terms of the hydration number of MgCl2, the peak intensity ratio of around 65/200 cm-1 changes according to the hydration number. As the hydration number increases, the peak of Cl- ion around 200 cm-1 becomes weaker and the peak around 65 cm-1 becomes stronger. This reinforces the fact that the peak near 65 cm-1 is related to water. These results suggest that the hydration state can be estimated from observations in the low wavenumber region, especially for Mg salts. This finding is expected to be useful for understanding the complex hydration conditions on the surface of ice moons.

Conclusions

The Mg salt hydrates showed a relatively strong peak around 65 cm-1, and the intensity ratio of peaks around 65 to 200 cm-1 depends on the number of hydrations. This indicates that the discrimination and quantitative evaluation of multiple types of salts can be done simultaneously. By using them to develop measurements of other salts and frozen brines, we can provide constraints from laboratory-based spectroscopic experiments on a number of chemical reactions that are likely to occur in the surface environment of actual icy moons prior to future exploration.

References

1. Dalton JB (2010) Spectroscopy of icy moon surface materials. Space Sci Rev 153:219–247.
2. Hibbitts CA, Stockstill-Cahill K, Wing B, Paranicas C (2019) Color centers in salts - Evidence for the presence of sulfates on Europa. Icarus 326:37–47.
3. Grishina S, Koděra P, Uriarte LM, et al (2018) Identification of anhydrous $CaCl_2$ and $KCaCl_3$ in natural inclusions by Raman spectroscopy. Chem Geol 493:532–543.
4. Iwata K, Okajima H, Saha S, Hamaguchi HO (2007) Local structure formation in alkyl-imidazolium-based ionic liquids as revealed by linear and nonlinear raman spectroscopy. Acc Chem Res 40:1174–1181.
5. Wang A, Freeman JJ, Jolliff BL, Chou IM (2006) Sulfates on Mars: A systematic Raman spectroscopic study of hydration states of magnesium sulfates. Geochim Cosmochim Acta 70:6118–6135.
6. Shi E, Wang A, Ling Z (2020) MIR, VNIR, NIR, and Raman spectra of magnesium chlorides with six hydration degrees: Implication for Mars and Europa. J Raman Spectrosc 51:1589–1602.
7. Genceli FE, Lutz M, Spek AL, Witkamp GJ (2007) Crystallization and characterization of a new magnesium sulfate hydrate $MgSO_4$ $11H_2O$. Cryst Growth Des 7:2460–2466.
8. Ahmed M, Namboodiri V, Singh AK, Mondal JA (2014) On the intermolecular vibrational coupling, hydrogen bonding, and librational freedom of water in the hydration shell of mono- and bivalent anions. J Chem Phys 141:160748.

The investigation of water spectra and water activity using Aquaphotomics approach.

Sukritta Anantawittayanon[1*], Jelena Muncan[1] and Roumiana Tsenkova[1]

[1] Biomeasurement Technology Laboratory, Graduate School of Agricultural Sciences, Kobe University, Japan
***** Presenting author and Correspondence: rtsen@kobe-u.ac.jp

Water activity is a standard parameter used in food studies to describe the water properties in the food matrix, traditionally defined as the amount of free water in the system. The analysis results reveals that other water species also potentially affect the water activity value. As particular water species provide different features, only measuring water activity is not enough to investigate water interaction in foodstuffs specifically. Using the Aquaphotomics approach to explore the water interaction in food could further explain the relationship between water and food degradation.

Keywords: Water activity, Food preservation, Food degradation, Near-infrared spectroscopy, Aquaphotomics

Introduction

Water is the essential molecule, providing significant relationship to the change in food substance. While, water activity is a widely used parameter to describe the properties of water in food. The aims of this study are to investigate the relationship between water activity and the water in foodstuffs through Aquaphotomic approach to better understand about water activity and the properties of different water species.

Materials and Methods

This study includes spectral data collection and water activity measurement from various type of systems, including coffee powder, grain, cracker, butter, bread and grape. NIR spectra were collected using MicroNIR spectrometer (Viavi Solutions, formerly JDSU, USA) (900 – 1700 nm) with 5 consecutive measurements per one measurement point. The water activity value of the samples was measured with the water activity meter Aqualab 4TE (Decagon Devices, Inc., Pullman, WA, USA) at the room temperature, set at 25ºC.

Results

The average SNV spectra presented the blue-shift, the absorbance shift to the shorter wavelength region, as the water activity increase. Higher water activity system has more energy in the water matrix in general.

The PLSR results reveal that water spectra change in 1421 – 1430 nm, water hydration band (C6), and water solvation shell in 1448 – 1454 nm (C8) showed a negative correlation with water activity in all cases. While the water spectral change in 1472 – 1482 nm and 1482 – 1495 nm, water molecules with 3 and 4 hydrogen bonds, respectively, showed a positive correlation with water activity in all cases.

The water spectral change in 1398 – 1418 nm, the free water region, was generally positively correlated to water activity, and always opposite to the protonated water in the C3. The protonated water in C3 mostly showed a negative correlation with water activity, except in the coffee powder data set, representing the change at a low water activity level.

Table 1. The trend of correlation between each defined water bands, C1 to C12, to the measured water activity data. The results were acquired from the water activity regression vector using PLSR analysis with raw spectra in the water 1st overtone region, 1300 – 1

WAMACS	C1	C2	C3	C4	C5	C6	C7	C8	C9	C10	C11	C12	
Range, nm	1336-1348nm	1360-1366nm	1370-1376nm	1380-1388nm	1398-1418nm	1421-1430nm	1432-1444nm	1448-1454nm	1458-1468nm	1472-1482nm	1482-1495nm	1506-1516nm	Aw range
All samples	+	-	-	+	+	-	+	-	-	+	+	-	0.09 - 0.96
Coffee powder	-	+	+	+	-	-	-	-	+	+	+	-	0.15 - 0.32
Cracker	+	-	-	+	+	-	-	-	+	+	+	+	0.09 - 0.64
Grain	+	+	-	-	+	-	+	-	+	+	+	+	0.48 - 0.66
Butter	+	-	-	-	+	-	-	-	-	+	+	+	0.90 - 0.96
Bread	+	-	-	+	+	-	-	-	+	+	+	+	0.93 - 0.96

Conclusions

Water activity is a parameter describing the water matrix, just like pH that describe protons in the system. According to the analysis, as the water activity getting higher, the water spectra shift to the higher energy region. The water hydration, C6, showed negative correlation with water activity. While, C10 and C11 always provided positive correlation.

In general, free water showed positive correlation to the water activity, but it was not the case for very low water activity level. However, it was found that the change trend of free water and protonated water in C3 was in the opposite.

References

1. Troller, J. Water Activity and Food. (Academic Press Inc, 1978).
2. Barden, L. M. Understanding Lipid Oxidation in Low-Moisture Food Submitted to the Graduate School of the. (2014).
3. Labuza, T. P., Kaannane, A. & Chen, J. Y. Effect of Temperature on the Moisture Sorption Isotherms and Water Activity Shift of Two Dehydrated Foods. J. Food Sci. 50, 385–392 (1985).
4. Scott, W. J. Water Relations of Food Spoilage Microorganisms. Adv. Food Res. 7, 83–127 (1957).
5. Hahn-Hägerdal, B. Water activity: a possible external regulator in biotechnical processes. Enzyme and Microbial Technology vol. 8 322–327 (1986).
6. Tsenkova, R. Aquaphotomics: Water in the biological and aqueous world scrutinised with invisible light. Spectrosc. Eur. 22, 6–10 (2010).
7. Tsenkova, R. Introduction aquaphotomics: Dynamic spectroscopy of aqueous and biological systems describes peculiarities of water. J. Near Infrared Spectrosc. 17, 303–314 (2009).
8. Sandak, J., Sandak, A. & Meder, R. Assessing trees, wood and derived products with near infrared spectroscopy: Hints and tips. in Journal of Near Infrared Spectroscopy vol. 24 485–505 (IM Publications LLP, 2016).
9. Sun, Q., Senecal, A., Chinachoti, P. & Faustman, C. Effect of Water Activity on Lipid Oxidation and Protein Solubility in Freeze-dried Beef during Storage. J. Food Sci. 67, 2512–2516 (2002).

Characterization of moisture absorption process of rebaudioside using near infrared spectroscopy and aquaphotomics

Lele Gao [1], Hengchang Zang [1] and Lian Li [1,*]

[1] School of Pharmaceutical Sciences, Cheeloo College of Medicine, Shandong University, Jinan, 250012, Shandong, China;

***** Presenting author and Correspondence: lilian@sdu.edu.cn

Keywords: Near infrared spectroscopy, aquaphotomics, PCA, 2D-COS

Introduction

Rebaudioside (RA) as the main component of stevia rebaudiana is a new sugar with wide application in the pharmaceutical and food industry. However, it is easy to adsorb water which would increase the viscosity, making it difficult in formulating the right formulation. Therefore, it is necessary to understand the state of water which is absorbed by RA. In order to reveal the adsorption mode and bonding of water, near-infrared spectroscopy diffuse reflectance analysis technology combined with aquaphotomics[1] were used to analyze the moisture absorption process of RA.

Materials and Methods

A RA sample was dried at 105 ºC for 6 h. Then it was transferred into a constant temperature (26±1℃) and humidity (40±1%) environment for 4 h. The sample was taken out to collect spectra at different time points in the moisture absorption process. The spectra were analyzed by aquaphotomics methods, second derivative, principal component analysis [2] and two-dimensional correlation spectrum (2D-COS) analysis[3] to clarify the way of water molecule adsorption.

Results

Figure 1a showed that score 1 represented the whole adsorption process. Surface water molecules (1921 nm in the loading plot figure 1b) quickly adsorbed on the surface of RA powder to form a monomolecular layer at the beginning. When the surface adsorption sites are about to be saturated, the rate of moisture absorption slowed down. Figure 1c showed that as the time went by the bond water begin to increase from 2 h later, which could be find in the loading plot in Figure 1d (1944 nm).

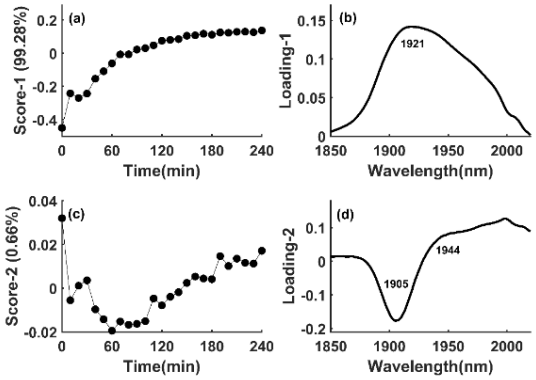

Figure 1. Scores and loadings of the first two principal components in the combination bands of OH. (a) and (c) Scores plot of PCA analysis; (b) and (d) Loading plots of PCA analysis.

In order to investigate the sequence of structure changes in detail during the adsorption process, 2D-COS was introduced to find the rules different water changed during the process. From Figure a1 and b1, it could be found that redshift occurred at the auto peak from 1911 nm to 1936 nm at the 1st h and the 3rd h, respectively. It meant that more hydration bonds were formed, and bonded water played important role gradually. In Figure c1, the auto peak position was 1936 nm which demonstrated that the adsorption was saturated.

According to Noda rules[4], it could be concluded that during the first hour the changes at 1991 nm was faster than that at 1890 nm, which indicated that surface water was formed easily compared to free water. During the next two hours, the structural change at 1944 nm was slower than 1905 which still proved that surface water played the major role. And at the finally stage, no relative peaks were identified which indicated that no structural changes occurred and it could be the saturated point for RA.

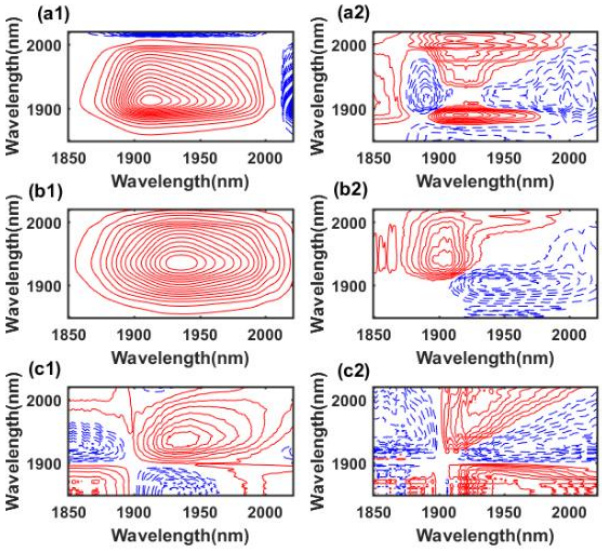

Figure 7. Synchronous (1) and asynchronous (2) 2D correlation spectra of the first hour (a) the middle two hours (b) and the last hour (c) of the RA moisture absorption process. The red solid line represents the positive sign, and the blue dotted line represents the negative sign.

Conclusions

In this study, near infrared spectroscopy was used for the first time to characterize the water changes during the moisture absorption of RA in order to help us to understand the RA adsorption process. It could be useful for take some measures to avoid moisture absorption in the future.

References

1. Tsenkova, R.; Kovacs, Z.; Kubota, Y., Aquaphotomics: near infrared spectroscopy and water states in biological systems. Sub-cellular biochemistry 2015, 71, 189-211.
2. Wehrens, R., Principal component analysis. In Chemometrics with R, Springer Berlin Heidelberg: 2011; 43-66.
3. Sun, Y.; Ma, L.; Cai, W.; Shao, X., Interaction between tau and water during the induced aggregation revealed by near-infrared spectroscopy. Spectrochimica Acta Part A: Molecular and Biomolecular Spectroscopy 2020, 230, 118046.
4. Noda, I., Generalized two-dimensional correlation method applicable to infrared, Raman, and other types of spectroscopy. Applied Spectroscopy 1993, 47 (9), 1329-1336.

Understanding of Yogurt Bio-Functional Water

Aleksandar Stoilov [1] and Roumiana Tsenkova [2]

[1] Yunosato Aquaphotomics Lab;
[2] Kobe University;
***** Presenting author and Correspondence: alex.boikov@abv.com

Keywords: Yunosato Spa, yogurt, bio-functional water, cosmetics, microorganisms

Introduction

Water is everywhere, in living cells and around them. It carries with it the information of its soluble particles and its environment in the form of molecular conformations. Yunosato Spa Center has already established production of yogurts and cosmetics, using these molecular conformations. That is why we at Yunosato Aquaphotomics Lab began researching ways of preserving and extracting that vital information of water by vacuum heating and blending methods, for the purpose of developing new food and skin products. As a quick and non-invasive evaluation and understanding, NIRS and Aquaphotomics have been applied.

Materials and Methods

In this study 3kg of Yunosato yogurt was placed inside FEC. Vacuum drying unit at 1000C with vapor reaching up to 400C. After extracting the water, it was then blended with Bulgarian rose water and Yunosato's TsukinoShizuku mineral water. After choosing from many blended ratios, the most prominent ones were cultivated on Obbi's FC bio-checker tubes, each one with 4 types of media designated for total count of bacterial, Escherichia coli, Staphylococcus Aureus and mold / yeast. Subsequent to incubating the bio-checkers for 5 days at 300C, their spectra, together with the spectra of the water samples at 360C, were measured using MicroNIR 1700ES spectrometer, while applying temperature control with a water bath. Also results from reference data, such as pH levels, electrical conductivity, total dissolved solids and salinity were monitored.

Results

On aquagram the spectral patterns of the 2 types of Yunosato yogurts were observed, distinguishing their probiotic content, where Yogurt N.2 having only Bacillus bulgaricus displayed more hydrogen bonded water, with more hydronium ions and free water molecules, while Yogurt N.7 consisting of both Japanese and Bulgarian probiotics displayed higher probiotic activity.

By also examining the spectral patterns of the water samples, it was possible to observe yogurt BFW (bio-functional water) sharing partly the characteristics of its original yogurt product, with main differences at 1300-1600nm seen as higher absorbance of bands related to free water molecules, hydronium ions and small water clusters.

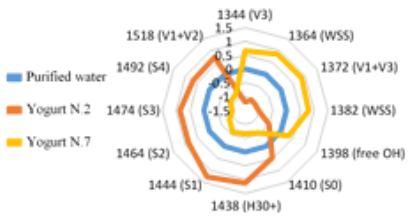

Figure 1. Aquagram of Yunosato yogurts

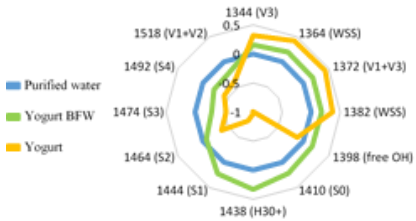

Figure 2. Aquagram of yogurt and its BFW

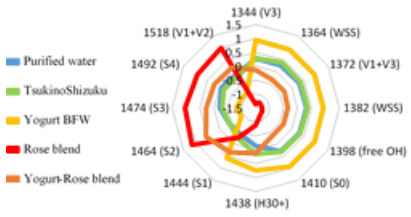

Figure 3. Aquagram of water samples at 36^{0}C

Figure 4. Bacterial growth of:
(**a**) Yogurt BFW; (**b**) Yogurt-Rose blend

When looking at the 360C samples, simulating as if at body temperature, yogurt BFW was seen with most water activity, while Rose blend had most strongly bounded water. Between them was the chosen Yogurt-Rose blend with a rich spectral pattern, including high absorption at 1438nm (H3O+), 1444nm (S1) and 1464nm (protein synthesis).

Visible cultures were observed only on the media designated for total bacteria count with yogurt BFW, suggesting that the preserved yogurt characteristics offer a good environment for microbial metabolism, while no cultures developed on the Yogurt-Rose blend media, showing inhibition of bacterial growth (Figure 4).

The above findings, together with the already known effects of rose water and its antiseptic, anti-inflammatory, anti-bacterial, antioxidant and anti-aging properties, proposed that our blend, when applied on skin, should provide a rich and balanced functionality, suitable for various skin types and situations, while leaving a pleasant smell that in several studies has shown to relax the central nervous system in mice.

Conclusions

By successfully preserving some of the characteristics of Yunosato yogurt in its extracted water and blending it with a chosen Yunosato and rose waters ratio, while monitoring their spectral patterns via Near-Infrared Aquaphotomics, a possible new natural cosmetic product with many beneficial effects was developed.

References

1. Tsenkova, R. 2009. “Aquaphotomics: dynamic spectroscopy of aqueous and biological systems describes peculiarities of water”, Journal of Near Infrared Spectroscopy 17 (6):303-313.
2. Slavchev, A., “Monitoring of Water Spectral Pattern Reveals Differences in Probiotics Growth When Used for Rapid Bacteria Selection”, PloS One, vol. 10 (7), 2015
3. Boskabady M., Iran J Basic Med Sci. “Pharmacological Effects of Rosa Damascena”, 14 (4): 295–307

Understanding the interaction between water and polymer in thermo-sensitive hydrogel phase transition system by near-infrared spectroscopy

Chongwen Xiong[1], Biao Ma [2] , Xueguang Shao [2] and Longhai Guo[2,*]

[1] State Key Laboratory of Organic-Inorganic Composites, Beijing University of Chemical Technology, Beijing 100029, PR China;
[2] Research Center for Analytical Sciences, College of Chemistry, Nankai University. Tianjin 300071, R. P. China.;
***** Corresponding authors at: State Key Laboratory of Organic-Inorganic Composites, Beijing University of Chemical Technology, Beijing 100029, PR China. E-mail addresses: guolh@mial.buct.edu.cn

For understanding the role of water in the temperature-sensitive hydrogel phase transition system, aqueous solution of poly (N,N- dimethylacrylamide)40-b-poly(diacetone acrylamide)50-poly(N,N-dimethylacrylamide) 40 (PDMAA40-b-PDAAM50-b-PDMAA40) amphiphilic triblock copolymer with different concentrations were synthesized and prepared. Sol-gel transition will happen upon heat. Temperature-dependent near-infrared spectra were got from 30 to 68 ℃. The spectra were processed by continuous wavelet transform (CWT) to confirm different peaks. Principal component analysis (PCA) was used to study the structural changes of polymer and water with temperature. The Second principal component of PCA results show that the water species with one hydrogen bonds (S1) changes near lower critical solution temperature (LCST) at the concentration of 15 wt%, 20 wt%. The turning point in PCA analysis was earlier at the concentration of 30 wt%. Through the analysis of PCA, it was found that there was a weak interaction between water and polymer and the S1 water was the main component. Concentration effects were also observed that as the concentration increased, the turning point of S1 water changed earlier, which corresponded to the LCST of polymer.

Keywords: Thermo-sensitive hydrogel Continuous wavelet transform Principal component analysis

Introduction

In recent years, the temperature induced phase transition of water gel system has attracted widespread attention. In this work, we explored the interaction between water and polymer in this system by using near-infrared spectroscopy of temperature change, and found that there is weak binding between water and polymer, which is dominated by water S1.

Materials and Methods

According to the method in the literature [2], the polymers were synthesized and different concentrations of solutions were configured. The structural formula is shown in Figure 1(a).

All near-infrared spectra are measured on a Vertex 70 multi-band near-infrared spectrometer (Bruker, Germany). The NIR spectra of $PDMAA_{20}$-$PDAAM_{50}$-$PDMAA_{20}$ polymer aqueous solutions with three concentrations (15wt%, 20wt%, 30wt%) at 30 ~ 68°C (2°C interval) were measured, as shown in Figure 1b.

CWT and PCA will be all carried on MATLAB.

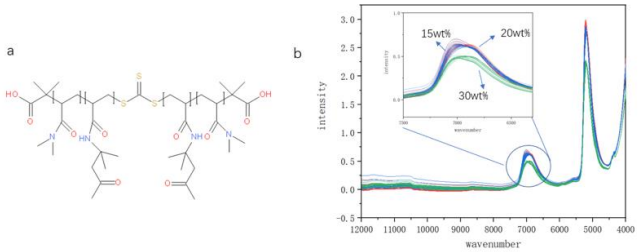

Figure 1. (a): structural formula of $PDMAA_{20}$-$PDAAM_{50}$-$PDMAA_{20}$. (b): Measured raw spectrum.

Results

The CWT results were shown in figure 2. And Second principal component of the PCA in range of 7400-6200cm-1 results were shown in figure 3.

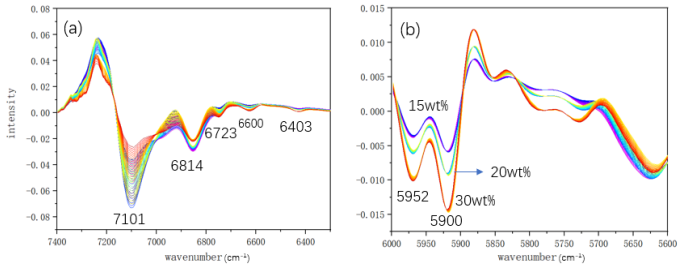

Figure 2. Transformed spectra of different concentrations in the range of (a):7400-6200cm^{-1}. (b):6000-5600cm^{-1}.

In Figure 2(a), two negative peaks at 7101 and 6814 cm-1 correspond to water S0 and water S2. In Figure 2(b), two negative peaks at 5952 and 5900 cm-1 correspond to the absorption 2 ν 3 of the C–H bond in CH3 and CH2, respectively.

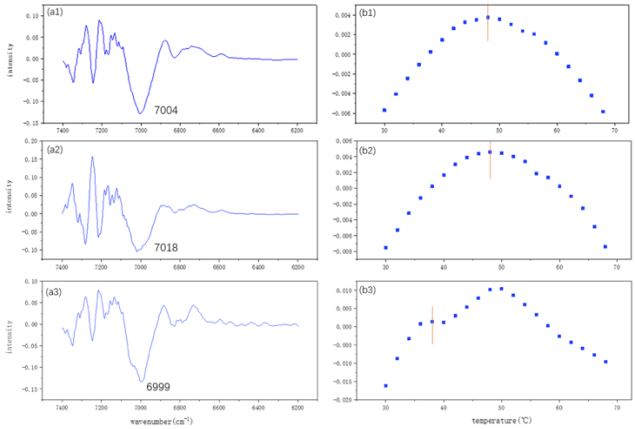

Figure 3. The Second principal component of the transformed spectra with different concentrations of (a1)15wt%, (a2)20wt%, (c) 30wt% and their scores (b1-b3).

As shown in figure 3, the negative peak at around 7000 cm^{-1} corresponds to water S_1 according to the literature[1].

Conclusions

Temperature-dependent NIR spectra were used for analyzing the structural variation of water and polymer. CWT processed spectra were used to confirm the attribution of peak position. The weak interaction was found in the second principal of PCA. The turning point appears at a higher temperature at low concentrations and get a lower temperature at a high concentration. Meanwhile, the loading show water S1 was the main component in weak interaction. Therefore, Water may be an effective probe for research thermo-sensitive hydrogel phase transition system.

References

1. Cui X, Cai W, Shao X (2016) Glucose induced variation of water structure from temperature dependent near infrared spectra. RSC Advances 6:105729-105736
2. Shi H, Qiu T, Ou-Yang HD et al. (2019) ABA-type triblock copolymer micellar system with lower critical solution temperature-type sol-gel transition. J Colloid Interface Sci 545:220-230

Temperature-dependent variable selection in near-infrared spectra for aquaphotomics

Xiaoyu Cui,[1,2] Wensheng Cai,[2] Xueguang Shao[2*]

[1] State Key Joint Laboratory of Environmental Simulation and Pollution Control; College of Environmental Sciences and Engineering, Peking University, Beijing 100871, China
[2] Research Center for Analytical Sciences, College of Chemistry, Nankai University. Tianjin 300071, China
***** Correspondence: e-mail xshao@nankai.edu.cn

Temperature-dependent near-infrared (NIR) spectroscopy has been developed to analyze water structures in aqueous systems. However, it is difficult to obtain information from the spectrum to understand the temperature dependence due to the overlapping of the spectra. This paper presents a method to select the temperature - dependent variable (wavenumber) from the NIR spectra at different temperatures.

Keywords: Near-infrared spectroscopy; Aquaphotomics; Temperature; Variable selection;

Introduction

Temperature-dependent near-infrared (NIR) spectroscopy has been developed and taken as a new technique for aquaphotomic studies to analyze water structures in aqueous systems [1]. It has been found that the interaction mode of water and ethanol can be effectively studied by temperature-controlled near-infrared spectroscopy [2]. It is revealed that glucose promotes the formation of regular water structure [3,4].To elucidate the gelation process of proteins and the role of water structure [5]. However, due to the complexity of water characteristic spectrum in temperature-controlled near-infrared spectroscopy, it is difficult to obtain information from the spectrum to understand the effect of temperature on water structure. In order to investigate the temperature dependency, particular attention is paid on selecting temperature-related variables (wavenumbers) in temperature-dependent NIR spectra in this study [6]. A method was proposed by combining continuous wavelet transform (CWT) with uninformative variable elimination with Monte Carlo re-sampling (MC-UVE). CWT is adopted to calculate the spectral components with different frequency to expand the variables into multi-fold. Then the importance of the variables in these spectral components was evaluated by MC-UVE in the quantitative model of temperature. Therefore, the temperature-dependent spectral variables can be obtained by the proposed method, which can be used to study the structural changes of water for understanding the characteristics of the aqueous solutions.

Materials and Methods

Glucose, NaCl and human serum albumin (HSA) are of analytical grade and purchased from Concord Technology Co., Ltd. Tianjin, China. Double distilled water was used for preparation of the solutions. The concentrations of NaCl and HAS aqueous solution are 5.8 and 5 g L^{-1}, respectively, and the concentrations of a series of glucose solutions are 20, 40, 60, 80 and 100 g L^{-1}. The temperature in the experiment was controlled by a model 2216e temperature controller (Bruker Optics Inc., Ettlingen, Germany). The temperature changed from 30 to 60 ºC with a step of 5 ºC. All NIR spectra were measured from 4000 to 12000 cm^{-1} (833-2500 nm) by a Vertex 70 spectrometer (Bruker Optics Inc., Ettlingen, Germany), using a cuvette of 1 mm. A tungsten–halogen light source and InGaAs detector were used. The spectra are digitalized with ca. 4 cm-1 interval in Fourier transform. To increase signal to noise ratio, both air reference and the spectra were measured with scan number 64. Simulated datasets were designed to validate the proposed method. Gaussian functions were used to generate the peaks in the simulated spectra.

Results

Fig. 1 (a) and (b) show the simulated spectra of one peak varying with temperature, and its CWT calculation with different scales. With the decrease of the scale parameter, a positive peak corresponding to the simulated spectral peak emerges with the sidelobes. With the transformed spectra of different temperature, the stability,

as shown in Fig. 1 (d), can be obtained by MC-UVE, which indicates the significance of the spectral change with temperature. Compared with the standard deviation of the simulated spectra shown in Fig. 1 (c), which also shows the variation of the spectra with temperature, the position of the largest stability is consistent with that of the peak in the profile of the standard deviation. Furthermore, there are also areas with larger stability in the figure, which is clearly consistent with the position of the negative sidelobes in Fig. 1 (b). Therefore, the variables in the transformed spectra that have a strong temperature dependency can be found by the method. Consist result was obtained for more peaks in the simulation. It should be noticed that the figure looks like a fountain, spreading the overlapping peaks in the spectra, thus it is named as fountain graph in the following discussions.

In a fountain graph for aqueous solutions, the dependency of all the variables in the transformed spectra of all the CWT scales was shown. In order to select less variables, the variables with larger stability in one scale can be used as a representative. Fig. 2 shows the transformed spectra of water by CWT with scale 30 and the location of the variables with largest stability in each "water stream" for water and the solutions. Comparing the wavenumbers of the selected variables, it can be found that they are located at similar but not identical positions for different solutions. The results can be used for discrimination of the solutions. Moreover, it can be seen that, compared with the variables of water, those of NaCl, glucose and HSA are at larger, similar and smaller wavenumbers, respectively. The result may be accounted for by that NaCl is capable to promote the formation of hydrogen bonds in the solution, HSA destroys the hydrogen bond network of water, and glucose is mild to the water structure [5,7,8]. Therefore, the selected variables can be used to reflect the effect of the solutes on water structure and distinguish these solutions.

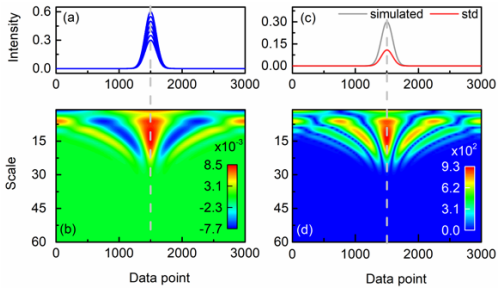

Figure 1. Result of (a) simulated spectra, (b) CWT-transformed spectra, (c) spectrum of the first temperature (grey) and the standard deviation (red) of the spectra, and (d) fountain graph.

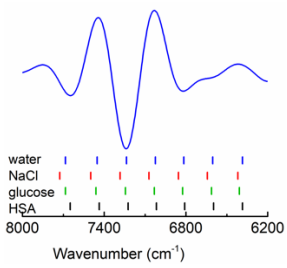

Figure 2. CWT-transformed spectrum with scale = 30 and the selected variables for the samples of water, NaCl, glucose (20 g L^{-1}) and HSA.

Conclusions

A method for selecting the temperature-dependent variables from the temperature-dependent NIR spectra was developed, combining CWT and MC-UVE. The selected variables reflected the water structure in aqueous solutions, and thus the variables are informative to discriminate the samples. The method may provide a tool to identify the characteristic variables in NIR spectra for understanding the function of water in aqueous systems.

References

1. Cui, X. Y.; et al. Sci. China Chem. 2019, 62:583.
2. Cui, X. Y.; et al. Chemom. Intell. Lab. Syst. 2017, 170:109.
3. Cui, X. Y.; et al. RSC Advances 2016, 6:105729.
4. Cui, X.Y.; et al. Anal. Chim. Acta 2017, 957:47.
5. Liu, X.W.; et al. Chin. Chem. Lett. 2017, 28:1447.
6. Cui, X. Y.; et al. Chemom. Intell. Lab. Syst. 2018, 183:23.
7. Gowen, A.A.; et al. Anal. Chim. Acta 2013, 759: 8.
8. Mason, P.E.; J. Phys. Chem. B 2005, 109:13104

Spectrophotometric simultaneous determination of trace Cu^{2+} and Co^{2+} in aqueous solution by membrane preconcentration coupled with chemometrics

Xihui Bian*, Qian Liu, Xiaona Zhan, Peng Liu and Yugao Guo

State Key Laboratory of Separation Membranes and Membrane Processes, School of Chemical Engineering and Technology, Tiangong University, Tianjin 300387, China
* Correspondence author: bianxihui@163.com

Heavy metal ions have been an increasing serious pollutants as the development of industries. Developing rapid and simple detection methods for the heavy metal ions in water environment became special issues. Membrane enrichment technology combined with ultraviolet visible (UV-Vis) diffuse reflectance spectroscopy were used to measure the trace Cu2+ and Co2+. Different preprocessing and variable selection methods were investigated and then partial least squares (PLS) model were built. The results show that UV-Vis spectroscopy combined with membrane enrichment can simultaneously determinate of trace amounts of Cu2+ and Co2+ in aqueous solution.

Keywords: UV-visible diffuse reflectance spectroscopy; heavy metal ions; membrane enrichment; simultaneous detection; partial least squares

Introduction

Heavy metal is one of the serious water pollution sources. It is of great significance to develop efficient, rapid and simple detection technology of heavy metal ions. Due to the rapid detection, simple operation and low cost, UV-Vis is a good selection for heavy metal ions detection [1,2]. However, it is difficult to determine trace heavy metals by UV-Vis because of its the lower sensitivity and overlapped peaks. Membrane technology [3], as a new separation and enrichment technology with high efficiency, energy saving and environmental friendliness, has been widely used in many fields. This research combine the advantages of membrane enrichment technology and UV-Vis diffuse reflection. The samples after enrichment are directly scanned by UV-Vis without elution. Chemometric methods were employed for preprocessing the spectra, selecting the related variables and simultaneous determination of different heavy metal ions.

Materials and Methods

A total of 29 samples include Cu2+ ranged in 2-12μg/L and Co2+ ranged in 3-10μg/L were prepared. Then 1 -(2-pyridylazo)-2-naphthol as a complexing agent was added to the solution to form a metal complex. Secondly, the metal complex was enriched on the membrane and the UV-Vis diffuse reflectance spectra of the membrane surface were measured. The 29 samples were split into a calibration set with 19 samples and a prediction set with 10 samples. The effects of SG smoothing, MSC, SNV, MSC, 1st Der, 2nd Der, CWT and their combinations were studied. Based on the optimal preprocessing method, UVE, MC-UVE and RT were further investigated to select the useful variables. Partial least squares regression model was finally established to predict the content of heavy metal ions for unknown samples.

Results

Seven preprocessing methods and their combinations are compared and the results shown in Figure 1. SG smoothing and MSC was selected as the best preprocessing method for Cu2+ and Co2+, respectively. Then UVE, MC-UVE and RT were compared based on the pretreatment spectra. MCUVE uses less variables and get best prediction for both ions. Finally, PLS model was built and predicted for the samples in the prediction set. Figure 2 displays the relationship between the prepared value and predicted values. For Cu2+, the RMSEP, R and recovery was 1.3904, 0.9568 and 72.3%-96.6%. For Co2+, PMSEP, R and recovery was 0.4257, 0.9808

and 90%-108.8%, respectively. The results indicates that good fitness and prediction can be achieved for the two ions by SG-MCUVE-PLS and MSC-MCUVE-PLS.

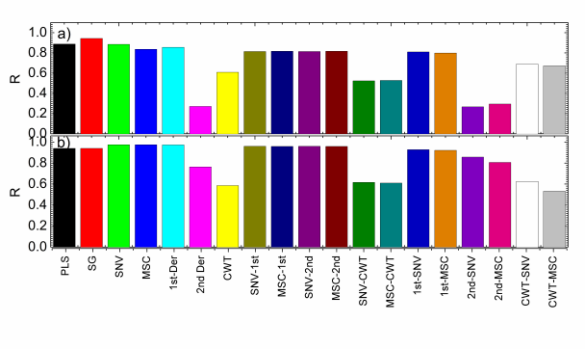

Figure 1. The R of different preprocessing methods and their combinations for (**a**) Cu^{2+} and (**b**) Co^{2+}.

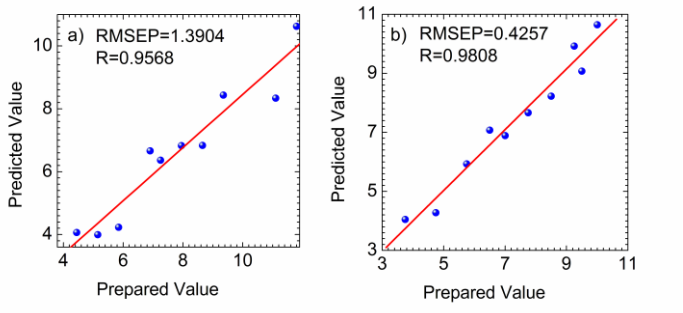

Figure 2. The relationship between the prepared value and predicted value for the prediction set for (a) Cu2+ by SG-MCUVE-PLS and (b) Co2+ by MSC-MCUVE-PLS.

Conclusions

Membrane enrichment coupled with UV-Vis diffuse reflectance spectroscopy and chemometrics is a promising method for simultaneously determination of trace heavy metal ions in aqueous solution.

References

1. Guo Y, Teng C, Liu J, et al (2020) Spectrophotometric determination of trace heavy metal ions in water with the assistance of electrospun nanofiber membrane extraction and chemometrics calculation. J Appl Spectrosc 87(1): 174–179.

2. Hejazi L, Mohammadi Diako E, Yamini Y, et al (2004) Solid-phase extraction and simultaneous spectrophotometric determination of trace amounts of Co, Ni and Cu using partial least squares regression. Talanta 62(1): 185–191.

3. Yin CH, Hu HL, Du YP, et al (2012) Sensitive determination of trace mercury by UV–visible diffuse reflectance spectroscopy after complexation and membrane filtration-enrichment. J Hazard Mater 233: 207–212.

Investigation of different types of water using Aquaphotomics

Makoto Sakai [1*], Jelena Muncan [2], Roumiana Tsenkova [2]

[1] Isol Technica Co., Ltd., Kyoto, Japan;
[2] Kobe University, Graduate School of Agriculture, Biomeasurement Technology Lab, Kobe, Japan;
***** Presenting author and Correspondence: m-sakai@isol-technica.co.jp

Keywords: Water, Aquaphotomics, Aquagram

Introduction

Investigate the differences between different types of water using aquaphotomics.

Materials and Methods

Ten types of water were used as experimental samples (Figure 1). NIR spectra were acquired using the XDS Rapid Liquid Analyzer (FOSS NIRSystems Inc., Hoganas, Sweden). The spectra was acquired in the region 400-2500 nm and the steps at 0.5 nm. The measurement order is performed randomly. As Environmental Control (EnvC), MQ was measured at the beginning and end of the experiment and every 5 samples. 3 samples were replicated each, and each sample was measured 5 times in consecutive to obtain a total of 170 NIR spectra. After measuring with XDS, Measure pH, Dissolved Oxygen (DO), Electric conductivity (COND), Oxidation-reduction Potential (ORP).

Name	Description
MQ (EnvC)	Ultra-pure water (Direct-Q UV3, Merck Millipore, Billerica, Massachusetts)
Tko	Tap water (Kobe University, Kobe)
Tos	Tap water (Osaka City University, Osaka)
Tky	Tap water (Ohara, Kyoto)
G	Gold Water (Yunosato spa water, Wakayama)
S	Silver Water (Yunosato spa water, Wakayama)
TS	Tsukino-Shizuku Water (G+S mixed)
RP	Reverse Osmosis water +Pressure treatment (About 500 atm pressure)
MA	Multivalent amine added water

Figure 1. 9 types of water

Results

The Aquagrams[1] of 9 types of water are shown (Figure2). Tko is significantly different in tap water. In Spa water, G is different. Tos, Tky, RP, S, TS and MA have strong hydrogen bonds. G has a lot of Free Water. The Assignment table[1] is shown (Table1).

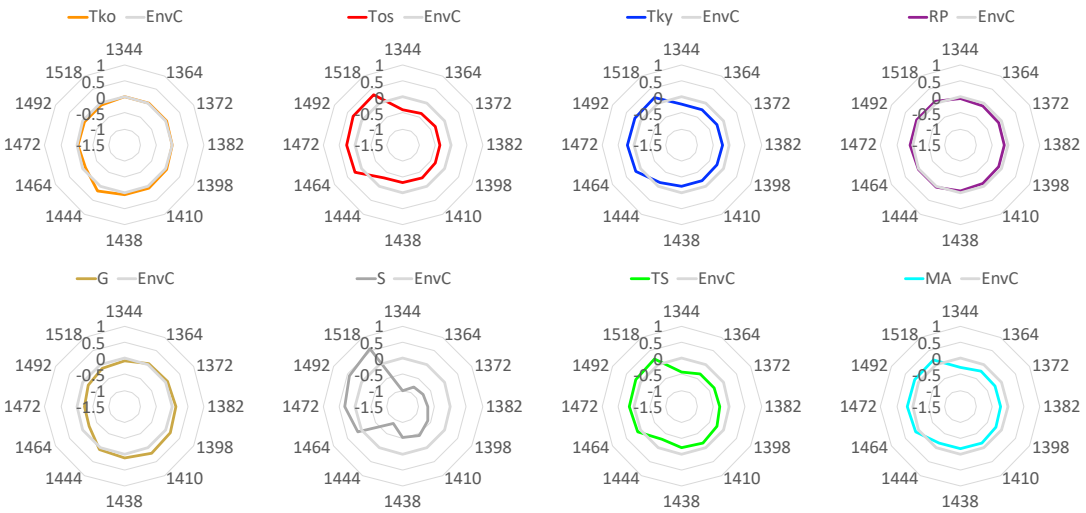

Figure 2. Aquagrams

Assignment		References
1336-1348	Protonated water clusters, $2\nu_3$: H_2O asymmetric stretching vibration	C1 WAMACS
1360-1366	Hydroxylated water clusters, $OH^-\cdot(H_2O)_{1,2,4}$: Water solvation shell	C2 WAMACS
1370-1376	$\nu_1+\nu_3$: H_2O symmetrical and asymmetric stretching vibration	C3 WAMACS
1380-1388	$O_2^-\cdot(H_2O)_4$: Hydrated superoxide clusters, $OH^-\cdot(H_2O)_{1,4}$: Water solvation shell, $2\nu_1$: H_2O symmetrical stretching vibration	C4 WAMACS
1398-1418	Trapped water (Water confined in a local field of ions), S_0: Free water, Water with free OH^-	C5 WAMACS
1421-1430	Water hydration, $H^-\cdot OH$ bend, $O^-\cdot H\cdots O$	C6 WAMACS
1432-1444	S_1: Water molecules with 1 hydrogen bond (dimer), H_3O (Hydronium)	C7 WAMACS
1448-1454	OH-·(H2O)4,5: Water solvation shell, Protein transfer mode in acidic aqueous solutions	C8 WAMACS
1458-1468	S_2: Water molecules with 2 hydrogen bonds (trimer), $2\nu_2+\nu_3$: H_2O bending and asymmetrical stretching vibration	C9 WAMACS
1472-1482	S_3: Water molecules with 3 hydrogen bonds (tetramer), $H3O2^-$, $H5O2^+$	C10 WAMACS
1482-1495	S_4: Water molecules with 4 hydrogen bonds (pentamer)	C11 WAMACS
1506-1516	Strongly bound water, $\nu_1+\nu_2$: H_2O Symmetrical and Bending vibration	C12 WAMACS

Table 1. Assignments

Conclusions

Even if the same tap water or hot spring water is collected at different sampling locations, the structure of the water will change significantly, and some water in completely different environments will show similar properties. These subtle changes can be captured by using the aquaphotomics method.

References

1. Tsenkova R (2009) Aquaphotomics: Dynamic spectroscopy of aqueous and biological systems describes peculiarities of water. J Near Infrared Spectrosc 17:303–3

Platinum Sponsors

Spa Yunosato, Shigeoka Co., Ltd. (株式会社 重岡)

PROACTIVE (株式会社プロ・アクティブ)

Gold Sponsors

DHC（株式会社ディーエイチシー）

Isol Technica (株式会社アイゾールテクニカ)

Silver Sponsors

Nichiei Intec (日栄インテック株式会社)

MDPI

Suntory Global Innovation Center
(サントリーグローバルイノベーションセンター株式会社)

Foundations & Support

Hyogo Prefectural Government
(兵庫県)

Tsuki no Shizuku Foundation
(一般財団法人　月のしずく)

The Naito Foundation
(公益財団法人　内藤記念科学振興財団)

The Tojuro Iijima Foundation for Food Science and Technology
(公益財団法人　飯島藤十郎記念食品科学振興財団)